Enclosure 3

Westinghouse Topical Report WCAP-18546-NP, "Westinghouse AXIOM® Cladding for Use in Pressurized Water Reactor Fuel."

(Non-Proprietary)

(174 pages attached)

March 2021

Westinghouse Electric Company
1000 Westinghouse Drive
Cranberry Township, PA 16066

WCAP-18546-NP
Revision 0

March 2021

Westinghouse AXIOM® Cladding for Use in Pressurized Water Reactor Fuel

WCAP-18546-NP
Revision 0

Westinghouse AXIOM® Cladding for Use in Pressurized Water Reactor Fuel

Guirong Pan
Materials and Fuel Rod Design

Andrew J. Mueller
Materials and Fuel Rod Design

Andrew R. Atwood
Materials and Fuel Rod Design

Glenn H. Heberle
Transient Analysis

Yun Long
PWR Core Methods

Kevin J. Barber
LOCA Integrated Services I

Robert M. Jakub
LOCA and Containment Analysis

David B. Mitchell
PWR Fuel Technology

Andrew B. Bowman
Licensing Engineering

Gregory A. Jewett
LOCA and Containment Analysis

Jonna M. Partezana
Materials and Fuel Rod Design

Ann Marie DiLullo
LOCA and Containment Analysis

Jane Xiaoyan Jiang
Thermal-Hydraulic and Seismic Engineering

David T. Rumschlag
PWR Core Methods

Jesse S. Fisher
Fuel Rod and Thermal-Hydraulic Design

Michael A. Krammen
PWR Fuel Technology

Adam M. Smith
Business Process, Design, and Additive Support

Douglas R. Hake
Nuclear Design A

Shine-Zen Kuhn
Fuel Rod and Thermal-Hydraulic Design

Yixing Sung
PWR Core Methods

Luther H. Hallman Jr.
Materials and Fuel Rod Design

Otto Linsuain
PWR Core Methods

T. Adam Wilson
Nuclear Design A

March 2021

Prepared: Guirong Pan*, Materials and Fuel Rod Design

Reviewed: Andrew B. Bowman*, Licensing Engineering

Approved: Andrew R. Atwood*, Manager, Materials and Fuel Rod Design

*Electronically approved records are authenticated in the electronic document management system.

Westinghouse Electric Company LLC
1000 Westinghouse Drive
Cranberry Township, PA 16066, USA

ACKNOWLEDGEMENTS

This topical report could not have been completed without the collaboration and support of many Westinghouse employees across several technical disciplines. Special thanks to the following key contributors and their management for their dedication and support of the **AXIOM** cladding program:

Bedirhan Akdeniz
PWR Core Methods

LeJohnny Anthony
Thermal-Hydraulic and Seismic Engineering

Jeffery A. Brown
Core Engineering and Software Development

Tim M. Crede
Fuel Rod and Thermal-Hydraulic Design

Osama Elkadim
Materials and Fuel Rod Design

Justin T. Figley
LOCA and Containment Analysis

Kyle R. Drennon
Product Engineering Lab

Francis X. Gradich
Technical Operations

Peter A. Hilton
PWR Core Methods

Brian P. Ising
LOCA Integrated Services I

Jayashri N. Iyer
Materials and Fuel Rod Design

Brent S. Jeffcoat
Structures, Fuel Assembly Design & Test

Zeses E. Karoutas
Chief Engineer - Innovation

Paul J. Kersting
Fuel Rod and Thermal-Hydraulic Design

Jeffery R. Kobelak
LOCA Integrated Services

Ho Q. Lam
PWR Core Methods

Serhat Lider
Transient Analysis

Jin Liu
Thermal-Hydraulic and Seismic Engineering

Roger Lu
PWR Fuel Technology

Calvin J. Lyles
Product Engineering Lab

Charles C. Macierowski
Product Engineering Lab

Gregg Max
LOCA and Containment Analysis

David W. McDevitt
LOCA and Containment Analysis

Charles J. Metz
Technical Operations

Edward M. Monahan
Transient Analysis

John H. Nelson
Technical Operations

Rosemary T. Null
LOCA and Containment Analysis

Michael R. Orner
Fuel Rod and Thermal-Hydraulic Design

Brian D. Ottinger
Churchill Lab Services

Balakrishna Palanki
Materials and Fuel Rod Design

Nikolay P. Petkov
LOCA Integrated Services I

Brian D. Ricketts
Technical Operations

Theodore E. Rodack
Transient Analysis

Javier E. Romero
Fuel Hardware Solutions

Michael D. Ruffner
Technical Operations

Eric C. Savage
Nuclear Design A

Andrew J. Sheaffer
Nuclear Design A

Sylena E. Smith
Radiation Engineering and Analysis

Scott A. Snider
Transient Analysis

Dustin E. Staub
Thermal-Hydraulic and Seismic Engineering

Joseph G. Thorne
Technical Operations

Steve K. Usouski
Fuel Rod and Thermal-Hydraulic Design

Michael T. Wenner
Nuclear Design A

Derek S. Wenzel
Hardware

EXECUTIVE SUMMARY

This document is the licensing topical report for the application of **AXIOM**® fuel cladding material in pressurized water reactor (PWR) nuclear fuel. **AXIOM** cladding was developed based on the successes of **Optimized ZIRLO™** cladding to target increasingly challenging fuel management practices and to provide margin for more restrictive regulatory criteria. More specifically, **AXIOM** cladding is designed to exhibit improved corrosion resistance, lower hydrogen pickup, and lower creep and growth compared to current Westinghouse products.

AXIOM cladding is a niobium-bearing zirconium alloy like the **ZIRLO**® alloy, with reduced tin content to increase corrosion resistance like the **Optimized ZIRLO** alloy, and with the addition of other alloying elements including vanadium and copper to improve specific properties like hydrogen pickup. The **AXIOM** alloy has been processed to be in the partially recrystallized annealed (pRXA) condition similar to the **Optimized ZIRLO** cladding to compensate for the creep strength loss caused by the reduced tin content.

Material research and optimization for **AXIOM** cladding development began in 2000 with four major variants identified for further in-reactor testing. Following the introduction of **AXIOM** alloys in a commercial reactor test program in 2002, irradiation programs have included the use of **AXIOM** alloys in various fuel designs, and multiple commercial PWR plants and test reactor programs in U.S. and Europe, with burnup reaching 75 GWd/MTU. In all the irradiation programs, post-irradiation examination (PIE) included **AXIOM** cladding together with either **ZIRLO** cladding, **Optimized ZIRLO** cladding, or both for side-by-side performance comparisons. Irradiated **AXIOM** rods with various burnup levels have been examined and are available for further PIE in a hotcell. Currently, eight full lead use assemblies (LUAs) of **AXIOM** cladding are being irradiated for production demonstration, to gather additional operating experience, and to provide additional support for licensing and commercial introduction of the **AXIOM** alloy as a new cladding material.

The **AXIOM** alloy has demonstrated better in-reactor corrosion performance compared to the **Optimized ZIRLO** alloy, especially in high duty operating environments. Thus far, the **AXIOM** alloy has shown excellent in-reactor dimensional stability. Less irradiation growth in the axial direction and less creep strain in the diametral direction than **ZIRLO** cladding have been observed. The topical report discusses the operating experience and the characterization of the **AXIOM** clad fuel properties and performance based on both in-reactor and out of reactor testing.

The final chosen **AXIOM** alloy has shown the best overall performance based on the extensive PIE database of poolside and hot-cell results from various irradiation programs as well as out-of-reactor testing. All operating requirements were considered, including corrosion and hydrogen pickup, creep and growth behavior, compatibility with fuel rod design criteria, tolerance for coolant chemistry variability, strength properties, research findings that serve as the basis for the proposed 10 CFR (Code of Federal Regulations) 50.46c rulemaking, manufacturability, microstructure stability at high burnup, etc. The final chosen **AXIOM** composition is zirconium with **[**

][a,c]

The **AXIOM** alloy is planned to be used as a fuel rod cladding material in all typical Westinghouse and Combustion Engineering PWR production fuel assemblies. Only the cladding material is being changed; and will be used with existing NRC-approved cladding dimensions, fuel structures, fuel assembly

components, and fuel materials. For this topical report, the **AXIOM** fuel rod cladding material will be pursuing a license to **[**

][d,e]

The topical report describes in detail how the properties and performance of **AXIOM** cladding are incorporated into existing NRC-approved analytical methods for use in plant-specific safety analyses. The topical report contains a regulatory roadmap to describe where specific regulatory criteria and requirements are discussed within the topical report. Additionally, any necessary changes to existing topical reports relative to effect of material properties are defined or identified in this topical report.

This topical report provides a description and justification of new fuel performance models for **AXIOM** cladding in the areas of **[** **]**[a,c]. The models are documented including their uncertainty treatment. The databases used to develop the models are described along with the procedure used to create the models and a comparison of the models to the data. The most important models for the use of **AXIOM** cladding are **[**

][a,c]. Also provided are **[**

][a,c]. The models reflect the trends observed from experience that the corrosion/HPU benefit with **AXIOM** cladding becomes apparent in higher duty operation at higher burnups. In low duty conditions, **AXIOM** and **Optimized ZIRLO** claddings exhibit similar corrosion behavior.

The cumulative description of **AXIOM** cladding documented in the topical report will demonstrate to the NRC staff that **AXIOM** cladding may be implemented in operating commercial PWRs while ensuring regulatory compliance and safety.

[1] Note that this text has been updated from that shown in the executive summary submitted on December 16, 2020 (ML20352A297).

TABLE OF CONTENTS

LIST OF FIGURES

LIST OF TABLES

ACRONYMS, ABBREVIATIONS, AND TRADEMARKS

Acronyms and Abbreviations:

3-D	three dimensional
ADOPT	advanced doped pellet technology
AOO	anticipated operational occurrence
AOR	analysis of record
ASME	American Society of Mechanical Engineers
ASTM	American Society for Testing and Materials
ATT	axial tensile test
BE	best estimate
BOL	beginning of life
BPVC	Boiler and Pressure Vessel Code
CEA	Commissariat à l'Energie Atomique, or control element assembly
CE	Combustion Engineering
CFFF	Columbia Fuel Fabrication Facility
CFR	Code of Federal Regulations
CHF	critical heat flux
CLB	current licensing basis
COLR	core operating limits report
C-P	Cathcart-Pawel
CP-ECR	Cathcart-Pawel ECR
CSR	contractile strain ratio
DBT	ductile-to-brittle transition
DNB	departure from nucleate boiling
DNBR	DNB Ratio
DSC	differential scanning calorimetry
EC	eddy current
ECCS	emergency core cooling system
ECR	equivalent cladding reacted
EDS	energy dispersive spectroscopy
EM	evaluation model
EOL	end of life
FA	fuel assembly
FCEP	fuel criteria evaluation process
FEA	Finite Element Analysis
FR	fuel rod
FRD	fuel rod design
FSAR	Final Safety Analysis Report
FSLOCA™	FULL SPECTRUM™ loss-of-coolant accident
GDC	general design criteria
GTRF	grid to rod fretting
H/T	Heat treatment
HT	high temperature

HVE	hot vacuum extraction
HPU	hydrogen pickup
ID	inner diameter
IFBA	integral fuel burnable absorber
IN	information notice
ISO	International Organization for Standardization
LB	lower bound
LBLOCA	large break loss-of-coolant accident
LOCA	loss-of-coolant accident
LTA	lead test assembly
LTR	lead test rod
LUA	lead use assembly
LWR	light water reactor
MLO	maximum local oxidation
M-P	measured – predicted
M/P	measured / predicted
NRC	Nuclear Regulatory Commission
OBE	Operation Basis Earthquake
OD	outer diameter
O/M	oxygen-to-metal ratio
PAD	performance analysis and design
PCI	pellet-clad interaction
PCMI	pellet-clad mechanical interaction
PCT	peak cladding temperature
PIE	post-irradiation examination
PIRT	phenomenon identification and ranking table
PQD	post quench ductility
pRXA	partial recrystallization anneal
PWR	pressurized water reactor
PWROG	Pressurized Water Reactor Owners Group
RAI	requests for additional information
RCCA	rod cluster control assembly
RCS	reactor coolant system
RCT	ring compression test
REA	rod ejection accident
RG	Regulatory Guide
RIA	reactivity-initiated accident
RIP	rod internal pressure
RT	room temperature
RTDP	revised thermal design procedure
RTT	ring tensile test
RXA	recrystallization anneal
SBLOCA	small break loss-of-coolant accident
SE	Safety Evaluation
SEM	scanning electron microscope
SLB	steam line break

SPP	second phase particle
SRA	stress relief anneal
SRP	Standard Review Plan
SRSS	square root sum of the squares
STS	Standard Technical Specifications
T/H	thermal hydraulic
TRD	accumulated thermal reactive duty
TRE	thermal reaction energy
TREX	tube reduced extrusion
TSSD	terminal solid solubility for dissolution
UB	upper bound
UFSAR	updated final safety analysis report
UTS	ultimate tensile stress or ultimate tensile strength
WC/T	WCOBRA/TRAC
WMTR	Westmoreland Mechanical Testing and Research
YS	yield stress or yield strength

Trademark Notes:

AXIOM, ADOPT, FULL SPECTRUM, FSLOCA, ZIRLO, Low Tin ZIRLO and Optimized ZIRLO are trademarks or registered trademarks of Westinghouse Electric Company LLC, its affiliates and/or its subsidiaries in the United States and may be registered in other countries throughout the world. All rights reserved. Unauthorized use is strictly prohibited. Other names may be trademarks of their respective owners.

ANSYS and all **ANSYS**, Inc. brand, product, service and feature names, logos and slogans are trademarks or registered trademarks of **ANSYS**, Inc. or its subsidiaries located in the United States or other countries.

1 INTRODUCTION

Westinghouse Electric Company has developed **AXIOM**® advanced fuel rod cladding material to provide enhanced corrosion resistance when compared to current zirconium-based fuel cladding materials. The **AXIOM** alloy is the next generation of robust alloys targeting very high fuel duties. **AXIOM** cladding is designed to exhibit improved corrosion resistance, lower hydrogen pick-up, and lower creep and growth compared to current Westinghouse fuel cladding products.

1.1 BACKGROUND

In support of industry demands for higher performance cladding materials, Westinghouse developed the **Optimized ZIRLO™** alloy as an improved version of the **ZIRLO**® alloy. The development approach was to obtain improvements in corrosion performance while maintaining the overall robust performance of **ZIRLO** alloy by slightly reducing the tin (Sn) content. Building on the successes of **Optimized ZIRLO** cladding, and in recognition of increasingly challenging fuel management practices, **AXIOM** cladding further reduces the tin content to gain additional improvements in corrosion resistance. However, it is known that tin has beneficial effects on the mechanical strength, especially creep strength. To compensate for the creep strength loss caused by the reduced tin content, instead of a stress-relief annealed (SRA) condition as in the case of **ZIRLO** cladding, the **AXIOM** alloy has been processed to be in the partially-recrystallized annealed (pRXA) condition similar to **Optimized ZIRLO** cladding. In addition to the major alloying elements of niobium and tin, other alloying elements including copper and vanadium were added to improve specific properties, like hydrogen pickup. Material research and optimization for **AXIOM** cladding development began in 2000 followed by initial alloy testing. In 2005, lead test rod (LTR) irradiation programs began at a variety of research and commercial power reactors worldwide with four major variants. **AXIOM** candidate alloy LTRs have been successfully irradiated to burnups over 70 gigawatt-days per metric ton of uranium (GWd/MTU) in several reactors. Pool side and hotcell post irradiation examinations have been conducted on these irradiated rods. The development of **AXIOM** cladding has also been documented in several publications.

The final **AXIOM** composition was selected in 2015 after a comprehensive evaluation among the candidate alloys. All operating requirements were considered, including corrosion and hydrogen, creep and growth behavior, compatibility with fuel rod design criteria, tolerance for coolant chemistry variability, strength properties, research findings that serve as the basis for the proposed 10 CFR (Code of Federal Regulations) 50.46c rulemaking, manufacturability, microstructure stability at high burnup, etc. Compared to other candidate alloys, the final **AXIOM** composition was trailing in areas including **[ ]**[a,c], but leading in all other areas especially hydrogen pick up, strength, dimensional stability, etc. The final **AXIOM** composition was selected based on the overall best performance supporting high burnup applications. A full-size production ingot of the final **AXIOM** composition has been melted and the fabrication processes including tube manufacturing and finished fuel assembly loading have been qualified. The Westinghouse Quality Assurance Program ensures that **AXIOM** cladding is manufactured as defined in this topical report. Eight lead test assemblies from the final production ingot are currently in operation at Plant W starting their third cycle.

Out-of-pile testing results are presented in Section 3, together with the irradiation experience presented in Section 4 and Section 5, demonstrating the properties and performance of **AXIOM** cladding.

1.2 AXIOM CLADDING DEFINITION

AXIOM cladding is a niobium-bearing zirconium alloy like **ZIRLO** alloy, with reduced tin content to increase corrosion resistance and the addition of other alloying elements including vanadium and copper to improve specific properties. To compensate for the creep strength loss caused by the reduced tin content, **AXIOM** alloy has been processed to be in the partially recrystallized annealed (pRXA) condition instead of a stress-relief annealed (SRA) condition as in the case of **ZIRLO** cladding. The final heat treatments yield a partially recrystallized microstructure which is approximately **[ ]**[a,c] recrystallized. Table 1.2-1 provides a comparison of the chemical compositions of **AXIOM**, **ZIRLO**, and **Optimized ZIRLO** alloys.

Table 1.2-1 Chemical Composition (%) of AXIOM, ZIRLO and Optimized ZIRLO Cladding

Alloy	Microstructure
ZIRLO	SRA
Optimized ZIRLO	pRXA
AXIOM	pRXA

a,c

1.3 PURPOSE AND CONSTRAINTS

This licensing topical report contains information supporting the application of **AXIOM** cladding as fuel cladding in PWR nuclear fuel. Results of extensive testing reported in this document are used to describe and establish the properties of **AXIOM** cladding. These tests and properties identify how **AXIOM** cladding will be incorporated into analytical codes and methods. The purpose of this document is to provide the necessary information to obtain Nuclear Regulatory Commission (NRC) approval for the application of **AXIOM** alloy as fuel cladding material. **AXIOM** cladding is intended for use within the following constraints.

Reactor and Fuel Assembly Design

- For use with NRC-approved PWR reactor designs
- For use with NRC-approved Westinghouse and CE fuel designs with corresponding rod dimensions
- For use with NRC-approved fuel materials and pellet coatings or additives (e.g., integral fuel burnable absorber (IFBA), gadolinium)

Operating Domain

- **[**

][d,e]

- For fuel being irradiated up to and including 62 GWd/MTU, the existing NRC-approved fuel assembly design and methodology limits for fuel up to 62 GWd/MTU will be applied.
- Best Estimate Oxide Thickness ≤ 100 μm (Section 5.3)
- Best Estimate Hydrogen Pickup ≤ **[ ]**[a,c] (Section 5.3)

Accident Criteria

- Upper bound (UB) loss-of-coolant accident (LOCA) – equivalent cladding reacted (ECR)%: **[ ]**[a,c]
- UB LOCA – peak cladding temperature (PCT) ≤ 2200°F (Section 6.2.1.4)
- UB Locked Rotor PCT ≤ 2375°F (Section 6.2.2.2)
- Rod Ejection Accident (REA) – Clad Failure pellet-clad mechanical interaction (PCMI) Enthalpy Addition ≤ **[ ]**[a,c]

2 TOPICAL REPORT OVERVIEW AND REGULATORY ROADMAP

This report will demonstrate that **AXIOM** fuel cladding material may be used in commercial nuclear reactors in compliance with all applicable regulations. This section provides a regulatory roadmap of the topical report. Section 2.1 maps the content of the topical report to applicable regulatory guidance. Section 2.2 provides a list of current NRC-approved topical reports for which applicability will be extended to include the fuel material described herein. Section 2.3 discusses some anticipated licensee implementation activities associated with **AXIOM** cladding.

2.1 ROADMAP TO APPLICABLE REGULATORY GUIDANCE

General Design Criteria (GDC) 10, "Reactor Design" in Appendix A of Title 10 of the CFR Part 50 (Reference 2.1) states the following:

> *"The reactor core and associated coolant, control, and protection systems shall be designed with appropriate margin to assure that specified acceptable fuel design limits are not exceeded during any condition of normal operation, including the effects of anticipated operational occurrences."*

This GDC broadly establishes the need for design limits for critical reactor components. One critical reactor component is the fuel rod cladding, which is one of the primary barriers to fission product release. In addition to GDC 10, GDC 2 applies as it relates to the seismic design of structures, systems, and components; GDCs 25, 26, 27 and 28 apply as they relate to reactivity control systems to ensure fuel design limits are met; and GDC 35 applies as it relates to emergency core cooling system design to ensure that fuel and clad damage would not interfere with cooling the reactor and that the cladding metal-water reaction is limited to negligible amounts. To effectively comply with the requirements of these GDCs, this topical report will seek to establish the associated safety limits applicable to the **AXIOM** cladding material.

To ensure all pertinent safety limits are defined, the guidance provided in NUREG-0800, "Standard Review Plan for the Review of Safety Analysis Reports for Nuclear Power Plants" (Reference 2.2) is used as a guide. Standard Review Plan (SRP) Section 4.2 "Fuel System Design," Section 4.3 "Nuclear Design," and Section 4.4 "Thermal and Hydraulic Design" are the sections most pertinent to the performance of fuel rods. However, analyses that are performed in accordance with the guidance in SRP Section 6.2.1 and SRP Chapter 15 may also be indirectly impacted by the properties of **AXIOM** cladding. The following subsections provide additional information about how **AXIOM** cladding will demonstrate compliance with the criteria of these guidance documents.

Additionally, it is recognized that **AXIOM** cladding is not listed with the acceptable fuel cladding materials defined in 10 CFR 50.46. However, consistent with the introduction of similar cladding materials such as **Optimized ZIRLO** cladding, this topical report considers the 10 CFR 50.46 regulation. It is further recognized that the proposed 10 CFR 50.46c regulation significantly restructures how compliance must be demonstrated. This topical report addresses the research findings underlying 10 CFR 50.46c. The data for **AXIOM** cladding that is specific to the research findings for 10 CFR 50.46c are presented in Sections 3.11 and 3.12, and the discussion of **AXIOM** cladding considering the research findings is provided in Section 6.2.1.4.

RG 1.236 (Reference 2.14) provides guidance on acceptable analytical methods, assumptions, and limits for evaluating the nuclear reactor's initial response to a postulated PWR reactivity insertion accident (RIA) (i.e., a control rod ejection accident or REA), based on empirical data from in-pile, prompt power pulse test programs and analyses from several international publications on fuel rod performance under prompt power excursion conditions. In accordance with the guidance, the fuel cladding limits applicable to **AXIOM** cladding are described in several sections of the report including Sections 3.10.1, 5.1.3, and 5.2.1.

2.1.1 SRP Section 4.2

The guidance of SRP Section 4.2 is established to provide assurance of the following:

(1) the fuel system is not damaged as a result of normal operation and anticipated operational occurrences (AOOs)
(2) fuel system damage during postulated accidents is never so severe as to prevent full control and shutdown rod insertion within the assumed rod drop time when it is required
(3) the number of fuel rod failures is not underestimated for postulated accidents
(4) core coolability is always maintained

The following sections in this topical report address the acceptance criteria delineated in SRP Section 4.2.

II.1.A (Fuel System Damage) – See Sections 6.1, 6.2 and 6.4 of this topical report.
II.1.B (Fuel Rod Failure) – See Sections 6.1, 6.2 and 6.4 of this topical report.
II.1.C (Fuel Coolability) – See Sections 6.1, 6.2 and 6.4 of this topical report.
II.2 (Description and Design Drawings) – See Sections 1 and 3 of this topical report.
II.3.A/B (Operating Experience / Prototype Testing) – See Section 3 through 5 of this topical report.
II.3.C (Analytical Predictions) – See Sections 6.1 through 6.4 of this topical report.
II.4 (Testing Inspection and Surveillance Plans) – No difference than other zirconium cladding.

2.1.2 SRP Section 4.3

Discussions specific to the impact of **AXIOM** cladding on the area of nuclear design are presented in Section 6.3.

2.1.3 SRP Section 4.4

Discussion related to the area of thermal and hydraulic design is presented in Section 6.4.

2.1.4 SRP Section 6.2.1

Section 6.2.1 presents information related to containment integrity following postulated LOCA, steam line break, or feedline break accidents; and is included here for completeness. Containment integrity and compartment mass and energy release analyses are not sensitive to the specific fuel rod cladding. The existing SRP guidance remains applicable to **AXIOM** cladding. The impact of **AXIOM** cladding on the analytical methods used to demonstrate compliance with SRP Section 6.2.1 is discussed in Section 6.2.3 of this report.

2.1.5 SRP Chapter 15

SRP Section 15.0 identifies high-level acceptance criteria applicable to AOOs and postulated accidents. The remainder of SRP Chapter 15 is split into individual event sections that include more detailed acceptance criteria for each AOO or postulated accident. The impact of **AXIOM** cladding on the acceptance criteria throughout SRP Chapter 15 is addressed in Section 6.2 of this report.

2.2 APPLICATION TO EXISTING NRC-APPROVED TOPICAL REPORTS

The most commonly used Westinghouse zirconium-based cladding alloys are **ZIRLO** and **Optimized ZIRLO** cladding as described in NRC-approved topical reports WCAP-12610-P-A (Reference 2.3) and WCAP-12610-P-A, Addendum 1-A (Reference 2.4) respectively. Once approved, **AXIOM** cladding will be considered appropriate for use in place of all existing zirconium-based Westinghouse alloys as a fuel rod cladding for use in PWRs.

This topical report will also address and expand the limits of applicability of other existing NRC-approved topical reports to incorporate **AXIOM** cladding and associated limitations defined herein. In many cases, no changes are needed to the existing topical reports to ensure compatibility with the **AXIOM** alloy. In cases where some modification is necessary to incorporate **AXIOM** cladding, this topical report describes the updates necessary to model **AXIOM** cladding and demonstrates why it may be safely utilized in place of other zirconium-based cladding materials. In all cases, no revisions will be made to the existing NRC-approved topical reports to specifically list **AXIOM** cladding as an approved fuel material. This approach is appropriate, since any operating plant that seeks to implement **AXIOM** cladding would need to incorporate this topical report into their licensing basis using an appropriate licensing change process and the following subsections define the applicability of **AXIOM** cladding to existing NRC-approved topical reports.

2.2.1 Reload Methodology

WCAP-9272-P-A (Reference 2.5) defines the methodology that is used for plants that have contractual arrangements with Westinghouse for reload designs. WCAP-16500-P-A (Reference 2.6) discusses the reload methodology used for most CE-designed PWR plants. The reload safety evaluation methodology is a systematic process to confirm that pertinent reload parameters are bounded by the corresponding value used in the reference safety analyses and to perform an evaluation of the effects on the reference safety analysis if a reload parameter is not bounded. Reference safety analyses have been performed using NRC-approved analytical methodologies for NRC-approved fuel materials and designs. The reload methodologies do not include conditions or limitations associated with specific fuel materials. Upon NRC approval of this topical report, these reload methodologies may be used to evaluate reloads containing **AXIOM** cladding using analytical methodologies approved by the NRC for that purpose.

2.2.2 Westinghouse Fuel Criteria Evaluation Process

WCAP-12488-A and WCAP-12488-A, Addendum 1-A (Reference 2.7) defines the NRC-approved fuel criteria evaluation process (FCEP) for Westinghouse designed PWR plants. FCEP defines a systematic approach for assessing fuel design changes to determine if prior NRC review and approval is needed before implementing the design change. The NRC approval of the FCEP process notes that it cannot be used to extend applicability of fuel performance models to new materials that have not been previously reviewed

and approved by the NRC. This topical report defines updates to fuel performance and safety analysis analytical modeling for **AXIOM** cladding. Once this topical report is approved for use by the NRC, the updated fuel performance modeling applicable to **AXIOM** cladding will comply with this limitation and may be used with the NRC-approved FCEP process. The NRC-approved FCEP process does not include restrictions on the applicable cladding materials that may be assessed with the process. Based on the similarities between **AXIOM** cladding and the existing NRC-approved Westinghouse zirconium-based fuel cladding materials, the assessment process defined in the FCEP topical report and addendum remains appropriate for assessing design changes when material-specific properties for **AXIOM** alloy as defined in this topical report are incorporated. Therefore, upon approval of this topical report, WCAP-12488-A and WCAP-12488-A, Addendum 1-A will be applicable to fuel designs containing **AXIOM** cladding.

2.2.3 Fuel Assembly Designs and Cladding Materials

The current Westinghouse and CE fuel designs use NRC-approved fuel rod cladding materials as reflected in References 2.3, 2.4, and 2.6. In this way, it is consistent with past practice for the fuel assembly design to utilize a cladding material that has been reviewed and approved by the NRC in a stand-alone topical report. Supported by the material properties and modeling discussion in this topical report, Westinghouse can adequately analyze the use of **AXIOM** cladding with all its existing fuel designs. Upon NRC approval of this topical report, all Westinghouse and CE fuel designs approved prior to the submittal date of this topical report will be extended to include **AXIOM** cladding as an approved cladding material.

2.2.4 Nuclear Design Methods

Implementation of **AXIOM** cladding does not require modification or update to any previously NRC-approved topical reports assessing neutronics and nuclear design, since the applicable codes already include the pertinent alloying materials within the cross-section libraries for modeling of **AXIOM** cladding. The existing nuclear design method topical reports support inclusion of **AXIOM** cladding into the analytical methods without updates to the NRC approval. Additional discussion of the nuclear design methods is provided in Section 6.3. Upon approval of this topical report, the existing Westinghouse and CE nuclear design methods will include **AXIOM** cladding as an acceptable cladding material.

2.2.5 Fuel Performance Methods

Implementation of **AXIOM** cladding will be performed using the most recent NRC-approved, Westinghouse fuel performance and design model as documented in WCAP-17642-P-A, Revision 1 (Reference 2.8). In the Safety Evaluation (SE) for the PAD5 topical report, the NRC included limitations and conditions restricting the use of PAD5 to Zircaloy-4, **ZIRLO**, and **Optimized ZIRLO** cladding materials with a maximum rod average burnup of 62 GWd/MTU. Upon approval of this topical report, this will be expanded to include the **AXIOM** cladding material defined in Sections 1.2 and 3, and irradiation experience in Section 4.

As indicated previously, it is not necessary to revise the PAD5 (Reference 2.8) topical report to incorporate the revised limitations and conditions since they will only be applicable for analyses performed on **AXIOM** cladding and are reflected in this topical report, which will be incorporated into the plant's licensing basis with the implementation of **AXIOM** cladding. Additional details of updates to the fuel performance and design model (PAD5) are discussed in further detail in Sections 5 and 6.1.1 as well as the fuel performance criteria in Section 6.1.2 that provides an update for **AXIOM** cladding to the beginning of life clad stress

criterion described in Reference 2.8. This discussion does not impose a limitation or restriction on the use of future NRC-approved fuel performance methods to perform analyses of **AXIOM** cladding when approved for that purpose.

2.2.6 Thermal-Hydraulic Methods

Implementation of **AXIOM** cladding does not require modification or update to any previously NRC-approved topical reports assessing margins to thermal-hydraulic design criteria such as the departure from nucleate boiling ratio (DNBR) limit. The similarities between current NRC-approved cladding materials and **AXIOM** cladding will support inclusion of **AXIOM** cladding into those analytical methods without updates to any content in the NRC-approved topical reports and the Safety Evaluation reports. Upon approval of this topical report, the thermal hydraulic methods will be considered approved to analyze the **AXIOM** cladding material. Additional discussion of applicability of the existing thermal-hydraulic methods is provided in Section 6.4.

2.2.7 Safety Analysis Methods

Westinghouse maintains many different NRC-approved methods for performing safety analyses in support of Chapter 15 (typically) of a plant's updated Final Safety Analysis Report (FSAR). These methodologies are separated into different categories as presented below.

2.2.7.1 LOCA Analyses

As discussed previously, implementation of **AXIOM** cladding will be contingent on the use of the PAD5 fuel performance model. Therefore, LOCA analyses are expected to be performed using the **FULL SPECTRUM™** LOCA (**FSLOCA™**) methodology approved by the NRC in Reference 2.9 or the NOTRUMP evaluation model approved in References 2.10 and 2.11. Aspects of the LOCA methodologies that could be affected by **AXIOM** cladding are discussed in Section 6.2.1.

In addition, the research findings that serve as the basis for the proposed 10 CFR 50.46c rulemaking are considered to determine applicable emergency core cooling system (ECCS) acceptance criteria for **AXIOM** cladding as discussed in Sections 3.11, 3.12, and 6.2.1.4.

2.2.7.2 Non-LOCA Transient Analyses

The similarities between **AXIOM** cladding and existing zirconium based cladding materials will allow incorporation of **AXIOM** cladding into the non-LOCA transient analysis methods without making updates to the NRC Safety Evaluations or content of those approved topical reports. Upon approval of this topical report, the non-LOCA transient analysis methods will be considered approved to analyze the **AXIOM** cladding material. Additional details of the non-LOCA transient analysis methods are discussed in Section 6.2.2.

2.2.7.3 Containment Integrity Analyses

In general, the applied methodologies used to analyze LOCA and steamline break mass and energy releases and containment response are insensitive to the fuel cladding materials. The similarities between **AXIOM** cladding and existing zirconium based cladding materials will allow incorporation of **AXIOM** cladding

into the methods without making updates to the NRC safety evaluations or content of those approved topical reports. Upon approval of this topical report, the existing Westinghouse containment integrity analysis methods will include **AXIOM** cladding as an acceptable cladding material. Additional discussion of the containment integrity analysis methods is provided in Section 6.2.3.

2.2.7.4 Radiological Consequences Analyses

Westinghouse does not maintain any NRC-approved methodologies for performing radiological consequences analyses as the analyses are performed in accordance with published regulatory guidance. Implementation of **AXIOM** cladding does not impact the models and methods used in performing offsite and control room dose consequences accident analyses. Applicability of **AXIOM** cladding to the assumptions identified in NRC regulatory guidance is discussed further in Section 6.2.4.

2.2.7.5 Fuel Assembly Seismic LOCA Dynamic Analyses

The similarities between **AXIOM** cladding and existing zirconium based cladding materials will allow incorporation of **AXIOM** cladding into the seismic LOCA dynamic analysis methods without making updates to the NRC Safety Evaluations or content of those approved topical reports. Upon approval of this topical report, the seismic LOCA dynamic analysis methods will be considered approved to analyze the **AXIOM** cladding material. Additional details of the analysis methods are discussed in Section 6.2.5.

2.3 POTENTIAL LICENSEE IMPLEMENTATION ACTIONS

This section is not intended to prescribe a required licensing approach that a licensee must follow when implementing **AXIOM** cladding, but rather presents pertinent licensing considerations associated with implementing **AXIOM** cladding as well as the most likely licensing approach. The following list applies to plants that have converted to Improved Technical Specifications based on the Standard Technical Specifications (STS) of NUREG-1431 (Reference 2.12) and NUREG-1432 (Reference 2.13):

- The specific cladding material applicable to the plant has classically been included in the fuel description included in Design Features of the Technical Specifications (STS 4.2.1). If the plant-specific Design Features section includes details of the cladding alloys applicable to the fuel, then updates will be required to incorporate **AXIOM** cladding into this portion of the Technical Specifications.
- Fuel performance modeling associated with **AXIOM** cladding has been defined herein with the PAD5 fuel performance methodology (Reference 2.8). If a plant has not previously implemented PAD5, implementation may require a change to the burnup-dependent Safety Limit on peak fuel centerline temperature (STS 2.1.1.2), which shall be maintained less than 5080°F, decreasing by 9°F per 10,000 MWd/kgU of burnup. If this burnup dependency is discussed in the plant Technical Specification Bases for Safety Limit 2.1.1, corresponding Bases changes will also be required. Markups to the Updated Final Safety Analysis Report (UFSAR) Reactor chapter will be required under the plant process for updates pursuant to 10 CFR 50.71(e).
- Aspects of the LOCA methodologies that could be affected by **AXIOM** cladding and applicable ECCS acceptance criteria for **AXIOM** cladding are discussed herein. Implementation of a new LOCA analysis of record that addresses these aspects and acceptance criteria requires that the

appropriate methodology(ies) be included in the COLR (Core Operating Limits Report**)** list of references (STS 5.6.3.b). Technical Specification Bases changes and UFSAR updates may also be required.

- In cases where the cladding specific fuel failure thresholds based on RG 1.236 (Reference 2.14) are required to be addressed as part of implementation of **AXIOM** cladding, it may be necessary for a plant to implement the Westinghouse three-dimensional (3-D) rod ejection analysis methodology (Reference 2.15).
- Since this topical report is a stand-alone document that defines analytical modeling and approaches to demonstrate that the material-specific limits for **AXIOM** cladding are met, it may be necessary to include this topical report in the COLR list of references.
- Spent and new fuel criticality analyses are not addressed in this topical report, but may require licensee implementation action, as applicable, based on their current licensing basis (CLB).

The exact nature of the required Technical Specification changes will depend upon the CLB of the plant. Based on the discussion above, a license amendment request will likely be required to implement **AXIOM** cladding. However, the licensee remains responsible for choosing the appropriate licensing approach for implementing **AXIOM** cladding in compliance with their operating license and regulations.

2.4 CHAPTER 2 REFERENCES

2.1. U.S. NRC 10 CFR Part 50: Appendix A. “General Design Criteria for Nuclear Power Plants.”

2.2. U.S. NRC NUREG-0800, “Standard Review Plan for the Review of Safety Analysis Reports for Nuclear Power Plants: LWR Edition” (Formerly Issued as NUREG-75/087).

2.3. WCAP-12610-P-A, “VANTAGE+ Fuel Assembly Reference Core Report,” April 1995.

2.4. WCAP-12610-P-A & CENPD-404-P-A, Addendum 1-A (Proprietary), “Optimized ZIRLO™,” July 2006.

2.5. WCAP-9272-P-A, “Westinghouse Reload Safety Evaluation Methodology,” July 1985.

2.6. WCAP-16500-P-A, “CE 16×16 Next Generation Fuel Core Reference Report,” August 2007.

2.7. WCAP-12488-A, “Westinghouse Fuel Criteria Evaluation Process,” October 1994, and Addendum 1-A, Revision 1, January 2002.

2.8. WCAP-17642-P-A, Revision 1, “Westinghouse Performance Analysis and Design Model (PAD5),” November 2017.

2.9. WCAP-16996-P-A, Revision 1, “Realistic LOCA Evaluation Methodology Applied to the Full Spectrum of Break Sizes (FULL SPECTRUM LOCA Methodology),” November 2016.

2.10. WCAP-10054-P-A, “Westinghouse Small Break ECCS Evaluation Model Using the NOTRUMP Code,” August 1985.

2.11. WCAP-10079-P-A, “NOTRUMP A Nodal Transient Small Break and General Network Code,” August 1985.

2.12. U.S. NRC NUREG-1431, Revision 4, "Standard Technical Specifications – Westinghouse Plants," April 2012.

2.13. U.S. NRC NUREG-1432, Revision 4, "Standard Technical Specifications – Combustion Engineering Plants," April 2012.

2.14. U.S. NRC Regulatory Guide 1.236, "Pressurized-Water Reactor Control Rod Ejection and Boiling-Water Reactor Control Rod Drop Accidents," June 2020.

2.15. WCAP-15806-P-A, "Westinghouse Control Rod Ejection Accident Analysis Methodology Using Multi-Dimensional Kinetics," November 2003.

3 CHARACTERIZATION OF AXIOM MATERIALS PROPERTIES

3.1 MICROSTRUCTURE

3.1.1 Density

The room temperature density of **AXIOM** cladding was measured geometrically on bulk material. The geometric density measured at 22°C (72°F) was **[ ]**[a,c]. An identical geometrical density was measured at 25°C (77°F) but with a higher uncertainty (1%). For comparison, the density for **Optimized ZIRLO** cladding and **ZIRLO** cladding are **[ ]**[a,c], respectively. The immersion density method was used to experimentally determine the densities of the **Optimized ZIRLO** and **ZIRLO** cladding (Reference 3.1).

3.1.2 Microstructure

The microstructure of **AXIOM** cladding consists of second phase particles (SPP) **[ ]**[a,c] homogeneously distributed throughout the zirconium matrix. Typically, these precipitates are present in a range of sizes up to **[ ]**[a,c] with an average particle size in the **[ ]**[a,c] range. The final heat treatments yield a partially recrystallized microstructure which is **[ ]**[a,c] .

3.2 THERMAL PROPERTIES

The thermal properties of **AXIOM** cladding were fully characterized, including specific heat, thermal diffusivity, thermal conductivity, thermal expansion, and phase transition temperatures. The tests were performed in the NETZSCH Instrument North America, LLC Applications Laboratory in Burlington MA. Thermal properties testing including differential scanning calorimetry (DSC), dilatometry and thermal diffusivity were conducted in accordance with American Society for Testing and Materials (ASTM) E1269, E228 and E1461 procedures, respectively, in an argon environment. NETZSCH is ISO 17025 accredited for these tests.

[

][a,c]

3.2.1 Specific Heat

The specific heat was determined using DSC measurements, which measures the difference in heat input into a sample and a reference material, as a function of temperature, following ASTM E1269. The tests were performed with flowing 99.999% pure argon and a temperature ramp rate of 18°F/min (10°C/min), from room temperature to 2192°F (1200°C); measurements were taken on both heating and cooling.

The specific heat, on heating and cooling, of four **AXIOM** samples are plotted in Figure 3.2-1 and Figure 3.2-2. The estimated measurement uncertainty is 3%. The four **AXIOM** data plots are within the measurement uncertainty, so the data is repeatable. For comparison, the specific heat data for **ZIRLO** and **Optimized ZIRLO** cladding are provided. **[**

][a,c]

Accounting for measurement uncertainty, the **AXIOM** alloy specific heat data matches reasonably well with **ZIRLO** and **Optimized ZIRLO** alloys; there is no appreciable difference.

*Figure 3.2-1 Specific heat capacity measurements for **AXIOM** alloy and reference **ZIRLO** and **Optimized ZIRLO** cladding on heating*

[a,c

] a,c

*Figure 3.2-2 Specific heat capacity measurements of **AXIOM** alloy along with **ZIRLO**, **Optimized ZIRLO** cladding on cooling.*

3.2.2 Thermal Expansion

The thermal expansion was determined using a differential dilatometer. The tests were performed under a continuous flow of 99.999% argon gas. Data was collected over a temperature range from room temperature to 1832°F (1000°C) with a heating rate of 5.4°F/min (3°C/min), with exception of 1022°F (550°C) where it was held for 1 hour. The average coefficient of thermal expansion (the slope of the linear fit line) is provided in Table 3.2-1. The **AXIOM** alloy axial thermal expansion during heat up to 1112°F (600°C) is plotted in Figure 3.2-3; **ZIRLO** and **Optimized ZIRLO** alloy data is provided for comparison. The estimated measurement uncertainty is 4%.

[

] a,c

For T in °F:

[a,c

] a,c

(Equation 3.2-1)

(Equation 3.2-2)

For T in °C:

[ ] a,c

(Equation 3.2-3)

(Equation 3.2-4)

Table 3.2-1 Summary of the Coefficient of Thermal Expansion in the Axial Direction

Alloy	Form of Materials	Temperature Range (°C)	Heating (/°C)	Cooling (/°C)
[ ] a,c				
[ ] a,c				

*Figure 3.2-3 Comparison of the axial thermal expansion (heating) for **AXIOM**, **ZIRLO**, and **Optimized ZIRLO** alloys*

3.2.3 Phase Transition Temperatures

The phase transition temperatures are summarized in Table 3.2-2 as determined by DSC and in Table 3.2-3 as determined by the dilatometry method. The phase transition temperature from $\alpha \leftrightarrow \alpha + \beta$ from the DSC is the onset temperature based on the tallest peak. The $\alpha + \beta \leftrightarrow \beta$ phase transition temperature is determined visually from the plot, where the peak ends.

The thermal expansion plots are generally linear to temperatures of 1112 to 1202°F (600 to 650°C) before the $\alpha \leftrightarrow \alpha + \beta$ phase transition. Deviations from linearity at temperatures above 1202°F (650°C) were indicative of phase transitions. The linear regression fit is performed on data in the range of 1112 to 1202°F (600 to 650°C) and is extrapolated to temperature higher than 1202°F (650°C) to identify the phase transition temperature visually, i.e., the initial deviation from linearity. After the $\alpha + \beta \leftrightarrow \beta$ phase transition, the thermal expansion plots are back to linearity. Refer to Figure 3.2-4 for an example of the phase transition temperature as determined by the axial thermal expansion. **[**

][a,c]

*Figure 3.2-4 The determination of the phase transition temperatures from the axial thermal expansion for **AXIOM** alloy*

Table 3.2-2 Phase Transition Temperature from DSC

Alloy	Form of Materials	Transition Temperature (Heating)		Transition Temperature (Heating)		
		α ↔ α +β [°C]	α + β ↔ β [°C]	α ↔ α +β [°F]	α + β ↔ β [°F]	
						a,c

Table 3.2-3 Phase Transition Temperature from Thermal Expansion

Alloy	Form of Materials	Transition Temperature (Heating)		Transition Temperature (Heating)		
		α ↔ α + β [°C]	α + β ↔ β [°C]	α ↔ α +β [°F]	α + β ↔ α [°F]	
						a,c

3.2.4 Thermal Diffusivity and Thermal Conductivity

The thermal diffusivity was measured with a NETZSCH LFA 467 HyperFlash™ instrument, using the methods of ASTM E1461; the measurement is carried out by rapidly heating one side of a sample and measuring the temperature rise curve on the opposite side. The samples are disk-shaped with approximately 12.7 mm in diameter and 2 mm thick. Prior to testing, the samples were spray coated with approximately 5 μm of graphite to increase the energy absorbed on the flashed side and increase the temperature signal on the back side of the sample. The estimated uncertainty is 5%. The results are plotted in Figure 3.2-5 with error bars showing the uncertainty.

The thermal conductivity is calculated from the thermal diffusivity by the following equation:

$$\lambda = D \times \rho \times C_p \qquad \text{(Equation 3.2-5)}$$

where: λ is thermal conductivity, D is thermal diffusivity, ρ is density, and C_p is specific heat. The estimated uncertainty for the calculated thermal conductivity is 7%.

The thermal conductivity data is plotted in Figure 3.2-6 with **ZIRLO** and **Optimized ZIRLO** alloy data for comparison. The thermal conductivity of **AXIOM** cladding is slightly different from **ZIRLO** and **Optimized ZIRLO** cladding. The thermal conductivity **[ ]**[a,c]

[ ]^{a,c} For modeling purposes, the thermal conductivity is represented by the following two-part equations:

[ ]^{a,c}

(Equation 3.2-6)

(Equation 3.2-7)

The raw data for thermal diffusivity and thermal conductivity are provided in Table 8.1-1 in Appendix 8.1.

[ ]^{a,c}

*Figure 3.2-5 Thermal diffusivity of **AXIOM** alloy along with **ZIRLO** and **Optimized ZIRLO** alloys. The error bars indicate the 5% uncertainty.*

*Figure 3.2-6 Thermal conductivity of **AXIOM** alloy along with **ZIRLO** and **Optimized ZIRLO** alloys. The error bars indicate the 7% uncertainty.*

3.3 MECHANICAL PROPERTIES

3.3.1 Young's Modulus

Young's modulus is determined by the interatomic forces that are difficult to change significantly without changing the basic crystal structure of the materials. The presence of less than 3% alloying elements in zirconium alloys will not affect the basic crystal structure and the interatomic bonding of the zirconium atoms. Therefore, the Young's modulus of **AXIOM** cladding is indistinguishable from Zircaloy-4, **ZIRLO** and **Optimized ZIRLO** High Performance Cladding Materials within experimental error. The following equations (Reference 3.4) for axial and circumferential elastic constants for fuel cladding for temperatures from 0 to 1200°F (-20 to 650°C) apply to **AXIOM** cladding:

The axial elastic modulus is:

[ ] **a,c** (Equation 3.3-1)

The circumferential elastic modulus is:

[ ] **a,c** (Equation 3.3-2)

3.3.2 Poisson's Ratio

Poisson's Ratio is related to the elastic and shear modulus as shown in the (Equation 3.3-3) below. However, this equation is valid only for isotropic materials. **AXIOM** cladding is highly textured by design. **[**

][a,c]

$$\nu = (E / 2G) - 1 \qquad \text{(Equation 3.3-3)}$$

where:

ν = Poisson's ratio,
E = Young's (elastic) modulus, and
G = shear modulus.

The Poisson's ratio (circumferential strain/imposed longitudinal strain) is:

[ ]a,c (Equation 3.3-4)

The Poisson's ratio (radial strain/imposed longitudinal strain) is:

[ ]a,c (Equation 3.3-5)

3.3.3 Microhardness

Vickers microhardness tests were performed by pressing an indenter of standardized shape into the specimen with a known force and measuring the size of the indentation to ASTM E384 requirements in accordance with Westinghouse internal procedures. The data reported in Table 3.3-1 were measured on surfaces perpendicular to the axial direction ("transverse"). The transverse microhardness for **AXIOM** cladding is in the **[ ]**[a,c] range.

Table 3.3-1 Microhardness of AXIOM Cladding

[ ]b,c

3.3.4 Texture and Contractile Strain Ratio (CSR)

Direct x-ray pole measurements were made at mid-wall, inner and outer diameter locations of **AXIOM** cladding. The measurements were made at Lambda Research, Inc. to ASTM E81 requirements. Lambda Research is ISO 17025 accredited for ASTM E81.

The Kearns' basal pole texture parameters were calculated from the x-ray pole measurements and are listed in Table 3.3-2. The average texture parameters of **ZIRLO** and **Optimized ZIRLO** cladding samples are also included for comparison (Reference 3.1). Representative pole figures are also included in Figure 8.2-1 in the Appendix 8.2. **[**

][a,c]

Contractile strain ratio (CSR) measurements were made on **AXIOM** cladding. The measurements were made in accordance with Westinghouse internal procedures which meet ASTM B811 requirements. The CSR values ranged from **[** **]**[a,c] The CSR measurements of **AXIOM** cladding are included in Table 8.1-2 in Appendix 8.1.

Table 3.3-2 Texture Parameters of Basal Poles [0002] Factors for AXIOM, ZIRLO and Optimized ZIRLO Cladding

Alloy	Location	Sample Size	Axial	Circum.	Radial
AXIOM					
Optimized ZIRLO					
ZIRLO					

[ ]b,c

3.3.5 Tensile Properties

The axial tensile test data for unirradiated **AXIOM** cladding is available from various lead test assembly (LTA) programs and testing as a function of temperature performed for design purposes. Testing was performed to ASTM E8/E8M and ASTM E21 at room and elevated temperature, respectively both internally and at Westmoreland Mechanical Testing and Research (WMTR). WMTR is ISO 17025 accredited for these tests. The stress versus test temperature data for **AXIOM** cladding were evaluated to define the best estimate, upper bound and lower bound (95% confidence) models. The 95/95 upper and lower bound models were obtained by fitting the statistical analysis at each test temperature.

3.3.5.1 Unirradiated Yield Strength

Figure 3.3-1 shows the yield strength data analysis for unirradiated **AXIOM** cladding. **[**

][a,c] Based on this analysis the following curves are determined:

Best estimate model (T in °F):

[ ]a,c (Equation 3.3-6)

Upper bound model (T in °F):

[ ]a,c (Equation 3.3-7)

Lower bound model (T in °F):

[ ]a,c (Equation 3.3-8)

3.3.5.2 Unirradiated Ultimate Tensile Strength

Figure 3.3-2 shows the ultimate tensile strength data analysis for unirradiated **AXIOM** cladding. **[**

]

Based on this analysis, the following curves are determined:

Best estimate model (T in °F):

[ ]a,c (Equation 3.3-9)

Upper bound model (T in °F):

[ ]a,c (Equation 3.3-10)

Lower bound model (T in °F):

[ ]a,c (Equation 3.3-11)

[ ]a,c

*Figure 3.3-1 Yield strength data analysis for unirradiated **AXIOM** cladding*

*Figure 3.3-2 Ultimate tensile strength data analysis for unirradiated **AXIOM** cladding*

3.3.6 Thermal Creep

Thermal creep tests were performed at **[**

][a,c] The test was conducted in accordance with Westinghouse internal procedures. Outer diameter measurements were made at regular intervals to determine the creep strain. The relevant **AXIOM** cladding data are listed in Table 8.1-3 in Appendix 8.1 and plotted in Figure 3.3-3 along with reference **ZIRLO** cladding data from the same tests. **[**

][a,c] Calibration of the creep model is based on irradiated data and discussed in Section 5.5.

*Figure 3.3-3 Creep properties of **AXIOM** and **ZIRLO** cladding at 725°F (385°C) and 15.6 ksi (107.6 MPa) effective stress*

3.4 FATIGUE

Fatigue testing was performed on **AXIOM** and **Optimized ZIRLO** cladding samples at room temperature by Dirats Laboratories. Dirats Laboratories are ISO 17025 accredited for fatigue testing. **[**

][a,c]

The results, along with historical **ZIRLO** cladding data, are plotted on Figure 3.4-1. The design fatigue limit curve is consistent with **ZIRLO** and **Optimized ZIRLO** cladding materials and is based on the Langer-O'Donnell model (References 3.1 and 3.4) and modified by the two criteria:

- The calculated pseudo stress amplitude (Sa) has to be multiplied by a factor of two to obtain the allowable number of cycles (Nf).
- The allowable cycles for a given Sa is five percent of Nf or a safety factor of 20 on the number of cycles.

Figure 3.4-1 Plot showing the fatigue data, Langer-O'Donnell model, and fatigue design limit

3.5 AUTOCLAVE CORROSION

AXIOM cladding was corrosion tested in 800°F – 1500 psi (427°C – 10.3 MPa) steam and 680°F – 2700 psi (360°C – 18.6 MPa) pure water environments. The water tests were conducted in accordance with the ASTM G2/G2M while the 800°F (427°C) steam tests were performed in accordance with Westinghouse internal procedures consistent with ASTM G2/G2M steam tests. The weight gain of **AXIOM** cladding as a function of exposure time out to 180 days in 800°F (427°C) steam is listed in Table 8.1-4 and plotted in Figure 3.5-1. The weight gain of **AXIOM** cladding as a function of exposure time out to 674 days in 680°F (360°C) water is listed in Table 8.1-5 and plotted in Figure 3.5-2. In both static tests, **AXIOM** cladding corrosion was significantly lower than the reference **ZIRLO** cladding samples.

*Figure 3.5-1 Corrosion results for multiple lots of **AXIOM** cladding in 800°F (427°C) steam at 1500 psi (10.3 MPa) as a function of exposure*

*Figure 3.5-2 Corrosion results of multiple lots of **AXIOM** cladding in 680°F (360°C) pure water at 2700 psi (18.6 MPa) as a function of exposure*

3.6 HIGH TEMPERATURE CLADDING BURST TESTING

Burst testing was conducted in the LOCA burst facility in the laboratory at the Columbia Fuel Fabrication Facility (CFFF) in accordance with Westinghouse internal procedures. **[**

]a,c

The maximum circumferential burst strain vs. the burst temperature data is plotted in Figure 3.6-1, showing the comparison of the **ZIRLO**, **Optimized ZIRLO**, and **AXIOM** cladding results. **[**

]a,c

a,c

*Figure 3.6-1 Comparison of all **AXIOM** cladding data with the **ZIRLO** and **Optimized ZIRLO** cladding database*

*Figure 3.6-2 Burst temperature vs. burst pressure for **ZIRLO**, **Optimized ZIRLO**, and **AXIOM** cladding samples. The "burst temperature" for these samples are plotted as the highest average temperature of TC1 and TC2.*

3.7 HIGH TEMPERATURE CREEP

[

][a,c]

Several comparison high temperature biaxial creep tests were performed **[**

][a,c] in accordance with Westinghouse internal procedures. In these tests, **AXIOM** and **Optimized ZIRLO** cladding were tested side by side. **[**

][a,c] to determine the OD strain. **[**

][a,c] The measured strain rates are shown in Table 3.7-1.

Since these tests were performed at a constant internal pressure, the mid-wall hoop stress is increasing as the sample diameter is expanding and the wall thickness is getting thinner during the test as shown by the thin-wall pressure vessel equation below:

$$\sigma_{Hoop} = \mathrm{P}_i \frac{d}{2\mathrm{t}} \qquad \text{(Equation 3.7-1)}$$

Where σ_{Hoop} = mid-wall hoop stress
$\mathrm{P_i}$ = internal pressure
d = average mid-wall diameter, and
t = average wall thickness.

In constant volume plastic deformation with no axial strain, the cross-sectional area is constant. Therefore, for a tube the post-test inner diameter (ID) can be calculated from the initial sample measurement and the post-test OD using the following equation:

$$a = \sqrt{b^2 - b_o^2 + a_o^2} \qquad \text{(Equation 3.7-2)}$$

where a = post-test ID,
$\mathrm{a_o}$ = pre-test ID,
b = post-test OD, and
$\mathrm{b_o}$ = pre-test OD.

[

]^{a,c}

The **AXIOM** and **Optimized ZIRLO** cladding strain rates measured in these tests are plotted with the **ZIRLO** and **Optimized ZIRLO** cladding results obtained previously in Figure 3.7-1 (Reference 3.1). The solid lines are the current cladding model based on the vacuum testing results of **ZIRLO** cladding and the individual data points represent the French Commissariat a l'Energie Atomique (CEA) steam environment testing of **Optimized ZIRLO** cladding. [

]^{a,c}

Table 3.7-1 High temperature creep results for AXIOM and Optimized ZIRLO cladding

Test Temperature (°C / K)	Sample #	Cladding Alloy	Avg Midwall Hoop Stress (MPa)	Total Time (sec)	OD Strain (%)	OD Strain Rate (sec^{-1})

b,c

a,c

*Figure 3.7-1 High temperature strain (creep) rates of **AXIOM** (red circles) and **Optimized ZIRLO** (blue diamonds) cladding plotted with the average hoop stress compared to previous **Optimized ZIRLO** (diamonds) and **ZIRLO** cladding (lines) test results*

3.8 HIGH TEMPERATURE METAL WATER REACTION

AXIOM cladding samples were cleaned, dimensionally characterized and weighed to obtain the pre-oxidized masses. Each sample was then exposed to steam at temperatures of **[**

][a,c] for varying periods of time using Westinghouse internal procedures. The oxidized mass of each **AXIOM** cladding sample, exposure temperature, and the exposure time were recorded for each sample.

[

][a,c] The parabolic oxidation rates of **AXIOM** cladding as a function of the temperature are listed in Table 3.8-2 and plotted as a function of reciprocal temperature in Figure 3.8-2. The Baker-Just and Cathcart-Pawel correlations and previously reported **ZIRLO** and **Optimized ZIRLO** cladding oxidation rates are shown for comparison (Reference 3.1).

[

][a,c]

Table 3.8-1 High Temperature Steam Oxidation Results for AXIOM Cladding

Sample ID	Oxidation Run #	Temperature (°C)	Time (sec)	Weight Gain (mg/dm²)	Weight Gain² (g/cm²)²

b,c

Table 3.8-2 Parabolic Metal-Water Reaction Rates for AXIOM, ZIRLO and Optimized ZIRLO Cladding

Alloy	Temperature (°C)	Reaction Rate $(g/cm^2)^2/s$
[		] b,c

[ ] a,c

*Figure 3.8-1 High temperature steam oxidation rates of **AXIOM** cladding*

*Figure 3.8-2 High temperature metal-water reaction rates for **AXIOM**, **ZIRLO** and **Optimized ZIRLO** cladding*

3.9 EMISSIVITY

Emissivity depends strongly on the surface condition and the presence of any oxide. **[**

][a,c]

Given that all Westinghouse cladding alloys have identical surface finish, the emissivity of oxidized fuel cladding is dominated by the zirconium oxide formed which is unaffected by the minor differences in alloying elements. **AXIOM** cladding is processed identically to the other alloys tested and has an identical surface finishing. Therefore, within the measurement uncertainty, the emissivity of oxidized **AXIOM** cladding is judged to be identical to **ZIRLO** and **Optimized ZIRLO** cladding. Existing licensed emissivity values for **ZIRLO** and **Optimized ZIRLO** cladding are valid for **AXIOM** cladding.

3.10 HYDRIDE REORIENTATION

Investigations of **ZIRLO** cladding have found that the critical stress for hydride reorientation is about **[ ]**[a,c] in both the unirradiated and irradiated condition (Reference 3.4) The hydride reorientation of **AXIOM** cladding in relation to the standard stress-relieved **ZIRLO** cladding and fully recrystallized **Low Tin ZIRLO™** tubing (identical chemistry as **Optimized ZIRLO** cladding) above the reported threshold was evaluated in accordance with Westinghouse internal procedures. Characterization of hydrided **AXIOM** tubing containing approximately **[ ]**[a,c] hydrogen was performed before and after a hydride reorientation heat treatment. The heat treatment consisted of heating the cladding to 752°F (400°C), pressurizing the cladding with 11.6 ksi (80 MPa) internal hoop stress and furnace cooling to room temperature while maintaining pressure.

Image analysis was performed on the metallographically prepared cross-sections. The fraction of radial hydrides (±30° of vertical) and circumferential hydrides (±30° of horizontal) before and after this heat treatment were measured and compared. A summary of the average measured radial hydrides for each material is shown in Table 3.10-1.

In the as-hydrided condition, **ZIRLO** cladding showed **[ ]**[a,c] of the hydrides were radial on average. The radial hydride content increased approximately **[ ]**[a,c] with an average radial percentage of **[ ]**[a,c], as a result of the pressurized heat treatment. By comparison, in the as-hydrided condition, **AXIOM** cladding showed **[ ]**[a,c] of the hydrides were radial. The radial hydride percentage increased to **[ ]**[a,c] as a result of the pressurized heat treatment. A graphical representation of the hydride orientations measured for one of the **AXIOM** cladding samples tested is shown in Figure 3.10-1.

Table 3.10-1 Summary of Hydride Reorientation Results

Cladding Alloy	Heat Treatment Condition	Location	Average % Radial

b,c

a,c

*Figure 3.10-1 Montages of **AXIOM** cladding with color overlay of hydride orientation as-hydrided and following pressurized reorientation heat treatment. Red = ± 30° of circumferential; Blue = ± 30° of radial; Green = in-between orientations*

3.10.1 Impact on Rod Ejection Accident (REA) Limits

For REA the PCMI limit for **AXIOM** cladding will be based on **[**

][a,c]

Reg Guide 1.236 (Reference 3.3) provides the following PCMI cladding failure thresholds (Peak Radial Average Fuel Enthalpy Rise (Δcal/g) versus Excess Cladding Hydrogen (wppm)) at PWR temperatures (at or above 500°F / 260°C):

SRA Cladding at PWR temperatures (at or above 500°F / 260°C)

$$\Delta\, {}^{cal}/_{g} = Min\left(150, \left(1.80E + 05 * H_{EX}^{-1.5} + 60\right)\right) \quad \text{(Equation 3.10-1)}$$

RXA Cladding (Unlined) at PWR Temperatures (at or above 500°F / 260°C)

$$\Delta\, {}^{cal}/_{g} = Min\left(150, (5.50E + 05 * H_{EX}^{-2} + 50)\right) \quad \text{(Equation 3.10-2)}$$

Where H_{EX} is the hydrogen above the TSSD (terminal solid solubility for dissolution) limit.

Measurement of radial hydride fraction before and after reorientation treatment from Section 3.10 are used as input. **[**

][a,c] The following ratio was determined:

[ ]a,c (Equation 3.10-3)

This was done for the as-hydrided and reoriented conditions. This results in two values for factors, **[**

][a,c] respectively. **[**

][a,c]

The pRXA **AXIOM** cladding failure criteria is then **[**

][a,c]

[ ]a,c (Equation 3.10-4)

H_{EX}: Hydrogen > TSSD levels (Excess Cladding Hydrogen)

[

][a,c]

The resulting PCMI Failure enthalpy increase is plotted in Figure 3.10-2 for SRA cladding, RXA cladding and pRXA **AXIOM** cladding (**[ ]**[a,c]) as a function of excess hydrogen.

Details on the calculation of the cladding hydrogen are presented in Section 5.3

*Figure 3.10-2 Enthalpy increase limit vs. excess cladding hydrogen for SRA cladding, pRXA **AXIOM** cladding and RXA cladding*

3.11 POST QUENCH DUCTILITY

In accordance with draft Regulatory Guide (RG) 1.223 (Reference 3.5) and Westinghouse internal procedures, post quench ductility (PQD) testing of **AXIOM** cladding was performed. Tubing samples were oxidized in flowing steam at 2200°F (~1200°C) to various equivalent clad reacted (ECR) levels using as-fabricated and pre-hydrided samples. Ring compression testing (RCT) of three specimens from each oxidation sample were performed at 275°F (135°C) to determine the PQD (offset strain). The protocols for oxidation and RCT testing met all the guidelines recommended in the draft RG 1.223 (with three minor exceptions:

[ ]a,c

Plots of the offset strain as a function of Cathcart-Pawel ECR (CP-ECR) for the different hydrogen levels are shown in Figure 3.11-1. These plots were used to determine the ductile-to-brittle transition (DBT) as a function of hydrogen using the curve fit method prescribed in draft RG 1.223 Section A-12.4. Note that only the red symbols in each plot were used for the curve fit (≤ 7% offset strain). Based on the intersection of each curve with the ductility criterion, the DBT as a function of hydrogen was determined, Table 3.11-1.

An overall plot of the test results is shown in Figure 3.11-2 where each oxidation condition is shown by an open symbol when all 3 RCT tests were ductile, gray filled symbols when there was a mix of both ductile and brittle RCT results (transitional) and solid symbols when all 3 RCT tests were brittle. **[**

][a,c] Using the methodology permitted by the draft regulatory guides, sufficient hydrogen levels were tested **[** **]**[a,c] for **AXIOM** cladding through the projected end of life.

[

][a,c]

[

]a,c

Table 3.11-1 Summary of DBT Calculations Made from RCT Data of AXIOM Cladding

[ ]^b,c

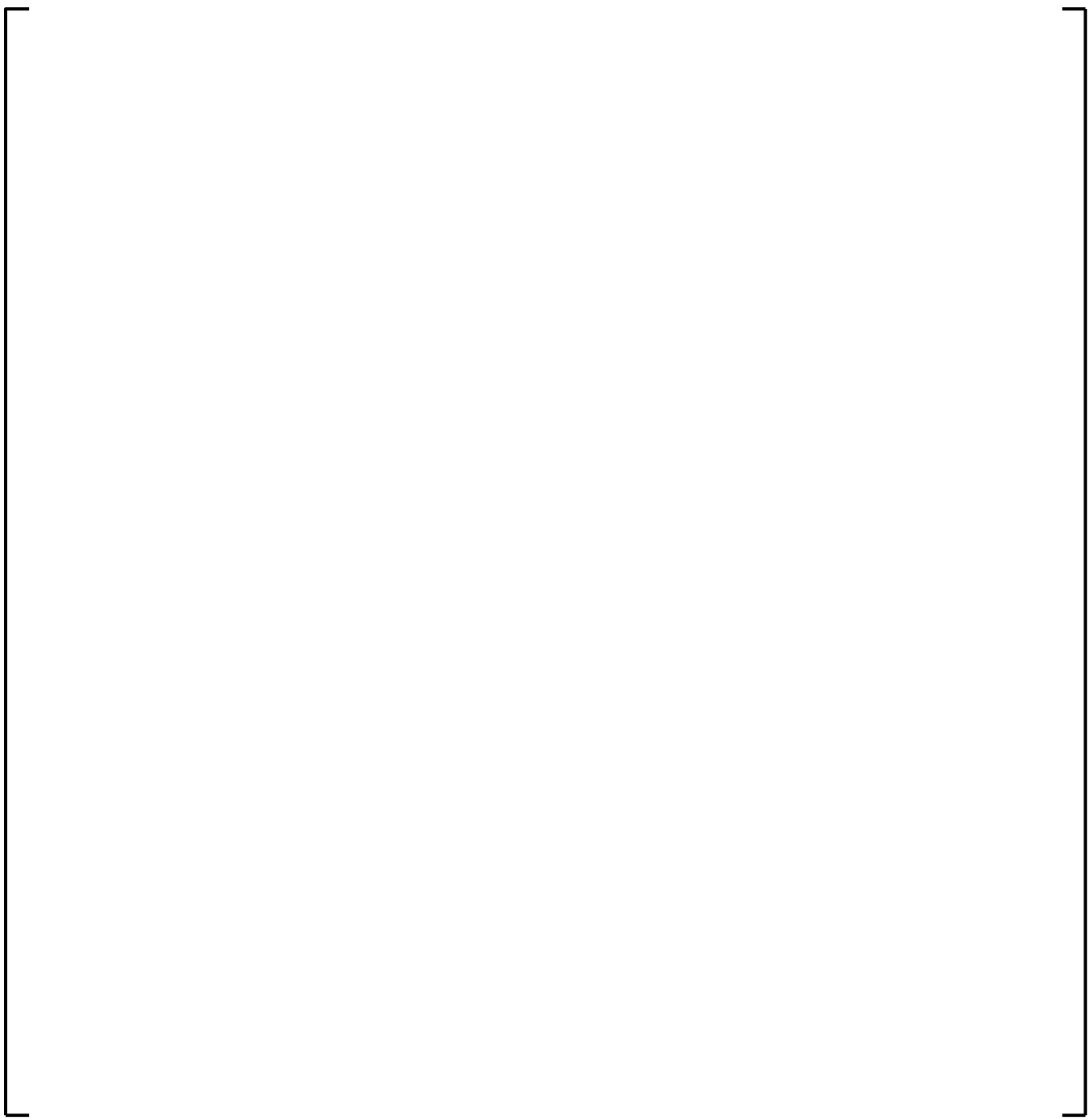

a,c

*Figure 3.11-1 Post quench offset strain as a function of CP-ECR for **AXIOM** cladding oxidized at 2200°F (~1200°C) with [*

]^{a,c}

a,c

Figure 3.11-2 Individual sample post quench ductility following a 2200°F (~1200°C) oxidation as a function of hydrogen and CP-ECR

a,c

*Figure 3.11-3 Cross-sectional light optical micrographs of **Optimized ZIRLO** and **AXIOM** cladding following 2200°F (~1200°C) steam oxidation to 18% CP-ECR and water quenching*

Figure 3.11-4 Summary of microhardness measurements for as-fabricated cladding following 2200°F (~1200°C) steam oxidation to 18% CP-ECR and water quenching

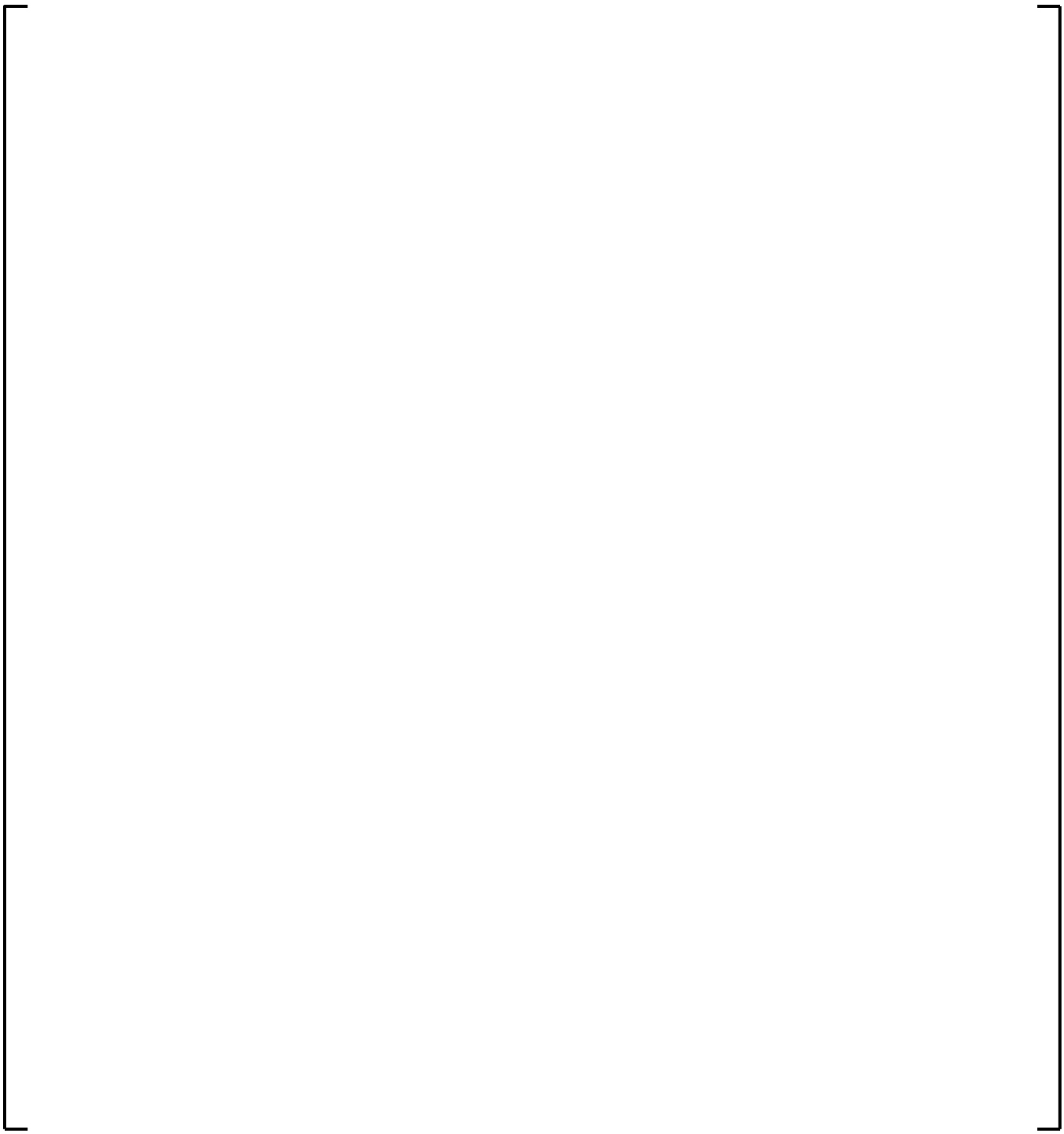

a,c

*Figure 3.11-5 [ ]**a,c** of as-fabricated **AXIOM** cladding sample following 2200°F (~1200°C) steam oxidation to 18% CP-ECR and water quenching*

[ ]a,c

Figure 3.11-6 [ ]a,c

[**a,c**

] **a,c**

Figure 3.11-7 **[**

]a,c

3.11.1 Low Temperature Post Quench Ductility

Post quench ductility testing results at lower peak oxidation temperatures have shown improvements in the DBT of Westinghouse cladding materials. To potentially obtain this additional margin in the future, proof of concept testing on **AXIOM** cladding was performed. The testing was performed using the procedures outlined in draft RG 1.223 (Reference 3.5), as described in Section 3.11. A peak oxidation temperature of **[ ]**[a,c] for hydrogen levels from 100 to 200 ppm were tested.

Comparisons of the lower peak oxidation temperature results to those discussed in Section 3.11 are shown in plots of the offset strain as a function of CP-ECR for the different hydrogen levels in Figure 3.11-8. By comparing the **[**

][a,c]. These proof of concept tests suggest that if additional margin is needed in the future, an alloy specific lower peak oxidation temperature DBT limit may be established.

a,c

*Figure 3.11-8 Post quench offset strain as a function of CP-ECR for **AXIOM** cladding oxidized at 2200°F (~1200°C) and a lower peak oxidation temperature with **[***

***]**[a,c]*

3.12 BREAKAWAY OXIDATION

In accordance with draft RG 1.222 (Reference 3.7) and Westinghouse internal procedures, breakaway oxidation testing of tubing was performed on **AXIOM** cladding samples. A summary of the tests is shown in Table 3.12-1. The tests met all the guidelines recommended in the RG **[**

][a,c]

In accordance with draft RG 1.222, **AXIOM** test lots were tested at temperatures from 1472 to 1922°F (800 to 1050°C) and at times of 5,000 seconds or the time to reach 18% CP-ECR at that temperature (whichever was less). **[**

][a,c]

Following draft RG 1.222 recommendations, two confirmatory tests with as-fabricated samples at the critical temperature and time **[** **]**[a,c] were performed. These tests did not result in breakaway oxidation (Table 3.12-1). This confirms the minimum time for breakaway oxidation to occur at **[** **]**[a,c] Three tests performed at **[** **]**[a,c] on samples with grid scratches representative of the surface condition of actual fuel rods loaded into fuel assemblies did not show hydrogen levels greater than 200 ppm (Table 3.12-1). Based on these results, it is concluded that scratches have an insignificant effect on breakaway oxidation times for this alloy.

Therefore, the critical temperature and time identified for **AXIOM** cladding is **[** **]**[a,c] , which corresponds to a CP-ECR greater than 18%. Based on the post quench ductility testing of **AXIOM** cladding (Section 3.11), the presence of hydrogen in the cladding, which promotes the absorption and diffusion of oxygen into the base metal under high-temperature LOCA conditions causing beta-layer embrittlement, is a more limiting embrittlement mechanism than breakaway oxidation for the **AXIOM** alloy. That is, the cladding would become brittle based on the ductile-to-brittle transition shown in Figure 3.11-2 (from Section 3.11) prior to experiencing breakaway oxidation.

Further, a survey of LOCA results for plants licensed with Westinghouse LOCA methodologies indicates that no plant has a time above 1472°F (800°C) for longer than **[** **]**[a,c] Therefore, not only is breakaway oxidation protected by the more restrictive embrittlement criterion shown in Figure 3.11-2 (from Section 3.11) for **AXIOM** cladding, but existing analytical results show substantial margin to the time above 1472°F (800°C) at which breakaway oxidation could occur.

Table 3.12-1 Summary of Breakaway Oxidation Tests

b,c

3.13 CHAPTER 3 REFERENCES

3.1 WCAP-12610-P-A and CENPD-404-P-A, Addendum 1-A, "**Optimized ZIRLO™**," July 2006.

3.2 U. S. NRC NUREG/CR-0497: MATPRO v11, "A Handbook of Materials Properties for Use in the Analysis of Light Water Reactor Fuel Rod Behavior," February 1979.

3.3 U. S. NRC Regulatory Guide 1.236, Revision 0, "Pressurized-Water Reactor Control Rod Ejection and Boiling-Water Reactor Control Rod Drop Accidents," June 2020 (ADAMS ML20055F490).

3.4 WCAP-17642-P-A, Revision 1, "Westinghouse Performance Analysis and Design Model (PAD5)," November 2017.

3.5 U. S. NRC Regulatory Guide 1.223, "Determining Post Quench Ductility," (Draft), 2016 (ADAMS ML16005A134).

3.6 U. S. NRC Regulatory Guide 1.224, "Establishing Analytical Limits for Zirconium-Alloy Cladding Material." (Draft), 2016 (ADAMS ML16005A133).

3.7 U. S. NRC Regulatory Guide 1.222, "Measuring Breakaway Oxidation Behavior," (Draft), 2016 (ADAMS ML16005A135).

3.8 Neumann G. and Tuijin C., "Self-diffusion and Impurity Diffusion in Pure Metals," Pergamon, 2008.

4 IRRADIATION PROGRAMS AND EXPERIENCE

4.1 IRRADIATION EXPERIENCE

In this section, the extensive irradiation experience of **AXIOM** cladding in different applications is presented. The purpose is to demonstrate that the in-reactor performance of **AXIOM** cladding is superior or equivalent to that of **ZIRLO** and/or **Optimized ZIRLO** cladding.

Since the introduction of **AXIOM** alloys in Plant R in 2002, irradiation programs have included the use of **AXIOM** alloys in different forms and in multiple reactors. The various irradiation programs are summarized in Table 4.1-1 and described in the sections below. Following an overview of the irradiation programs, the post irradiation examination (PIE) results of the irradiation programs are listed. In all the irradiation programs, PIE included **AXIOM** with either **ZIRLO** or **Optimized ZIRLO** cladding or both for side-by-side performance comparison. Currently, **AXIOM** cladding is under full lead use assemblies (LUA) irradiation to gather additional operating experience and poolside data, to provide additional support for licensing and commercial introduction of **AXIOM** alloy as a new cladding material. The total number of **AXIOM** fuel rods under irradiation or irradiated as of December 2020 is shown in Figure 4.1-1. The burnups for rods currently being irradiated are estimated values. The reactor coolant system (RCS) chemistry for commercial nuclear plants with **AXIOM** clad fuels are summarized in Table 4.1-2. **AXIOM** clad fuel has operated in one commercial reactor (Plant D Unit 2) with zinc injection into the RCS. Full **AXIOM** lead test assemblies (LTAs) are starting the third cycle irradiation in Plant W Unit 3 with RCS elevated lithium environment to 4.5 ppm. Fuel assembly (F/A) visual examinations were performed on the **AXIOM** LTAs after two cycles of irradiation showing excellent integrity.

Table 4.1-1 Summary of Irradiation Experience of AXIOM Cladding

[a,c]

*Figure 4.1-1 **AXIOM** rods irradiated as of December 2020*

Table 4.1-2 Summary of RCS Chemistry at Plants with AXIOM Cladding Fuel

4.2 OVERVIEW OF IRRADIATION PROGRAMS

4.2.1 Plant R Creep and Growth Program

For the Plant R creep and growth program, the non-fueled tubular cladding sections were pressurized to specific levels and positioned in the thimble tubes of assemblies operating at relatively high power. The pressure differentials provided variations in hoop stresses to allow measurements of diametrical creep under controlled levels of hoop stresses. The free irradiation growth was also measured on some samples, which were open to the coolant on the ID and had no pressure differential across the wall. The specimens were irradiated either in the unstressed or stressed state. The cladding materials included **ZIRLO** cladding, **Optimized ZIRLO** cladding and **AXIOM** cladding. The Plant R tests provide unique and valuable data for product development and updates of creep and growth models. These tests allow creep measurements to be made after multiple operating cycles and are not affected by the effects of pellet-clad touch down.

There were several assemblies involved. **AXIOM** alloy was included in the assemblies starting in spring 2004. The last assembly was discharged in spring 2010. The information and irradiation schedule of the multiple assemblies with **AXIOM** cladding included are summarized in Table 4.2-1. Hotcell post-irradiation examinations (PIEs) were conducted on each discharged assembly.

Table 4.2-1 Plant R Creep and Growth Program

Assembly	Completion Date	Cycles (BOC-EOC)	# of AXIOM Datapoints	Description

a,c

4.2.2 Plant B AXIOM Cladding LTA Program

The Plant B **AXIOM** cladding LTA program is made up of [

]a,c

The LTAs were inserted in the core in spring 2005. At the end of the second cycle in spring 2008, PIEs were performed on one of the assemblies, and [

]a,c Pool-side PIEs including high resolution visual, oxide thickness and rod growth were performed on the rods after 3 cycles of operation with burnup reaching over 70 GWd/MTU. [

]a,c were shipped to Studsvik (Sweden) for comprehensive hotcell examinations. The non-destructive examinations included rod internal pressure and fission gas release (FGR), profilometry, as well as all those tests that had been performed at pool side including visual, oxide thickness and rod growth. The destructive tests included light optical microscopy of cladding, mechanical testing, hydrogen analysis, and scanning electron microscopy (SEM).

In summary, oxide data and fuel rod growth data of **AXIOM** cladding fuel rods after Cycles 2 and 3 from the Plant B reactor are included in the database for **AXIOM** cladding corrosion and growth model. **[**

][a,c]. Hydrogen pickup and mechanical properties after irradiation for **AXIOM** cladding are from the Plant B high burnup rods examined in hotcell.

4.2.3 Plant D AXIOM Cladding LTA Program

The Plant D **AXIOM** cladding LTA program is made up of **[**

][a,c]

The irradiation started in fall 2006 in Plant D Unit 1. After one cycle of operation, some assemblies were returned to core for a second cycle in Plant D Unit 1. Some assemblies stayed in the spent fuel pool for PIE inspection before returning to core in Plant D Unit 2 in fall 2008. The pool-side PIE on once burned assemblies included clad corrosion rod growth as well as profilometry. Some assemblies were discharged after two cycles of operation in Plant D Unit 1 Cycle 16.

During the PIE campaign of the twice-burned assemblies, some rods were inspected and extracted from these assemblies and inserted into an all-**AXIOM**- alloys fresh assembly X89Y. **[**

][a,c]. This reconstituted assembly was inserted into Plant D Unit 2 in April 2010 and was irradiated for one cycle for the twice-burned rods to reach close to 75 GWd/MTU burnup at the end of the cycle. A PIE was performed in January 2012 to inspect assemblies including the reconstituted LTA X89Y and some twice-burned LTAs. Assembly visuals, assembly length, fuel rod visuals, rod length, clad corrosion, and profilometry examinations were performed. Assembly X89Y held thrice-burned fuel rods with burnups ranging from **[** **]**[a,c]. The remaining rods in X89Y are once burned with burnups ranging from 21.8 to 25.2 GWd/MTU. D59H and D61H have been operated for two cycles with burnups ranging from 46.5 to 54.6 GWd/MTU.

In summary, oxide data and fuel rod growth data of **AXIOM** clad fuel rods after Cycles 1, 2, and 3 from the Plant D Units 1 and 2 reactors are included in the database for **AXIOM** cladding corrosion and growth model. **[**

][a,c]

4.2.4 Plant M AXIOM Cladding LTA Program

The Plant M LTAs include **[**

][a,c]

The irradiation began in April 2006 in Plant M Unit 2. The LTAs were unloaded for PIE at the end of the first cycle for oxide and rod growth measurements. One LTA was discharged after the second cycle for PIE including oxide and rod growth measurement in spring 2009. One LTA remained in irradiation for 3 cycles. PIE campaign of the thrice-burned and twice-burned assemblies were performed in October 2011. The PIE again included peripheral rod oxide as well as rod growth. **AXIOM** alloy rods were subjected to extended pool side inspection, including single rod visual inspection and oxide measurement in February 2012. **AXIOM** alloy rods were extracted from twice-burned LTA together with some **Optimized ZIRLO** alloy rods and inserted into a fresh assembly in September 2010. The reconstituted assembly were irradiated for one cycle and discharged in December 2012. Pool side PIE was conducted on the reconstituted assembly in June/July 2013 with the focus on the oxide, rod length and visual inspection of the high burnup rods (~ 70 GWd/MTU).

In summary, oxide data and fuel rod growth data of **AXIOM** clad fuel rods after Cycles 1, 2, and 3 from the Plant M reactor are included in the database for the **AXIOM** cladding corrosion and growth model. The third cycle data included reconstituted rods with burnup close to 70 GWd/MTU.

4.2.5 Plant T LTA Project

The Plant T LTA project was designed to evaluate the Pellet Cladding Interaction (PCI) and corrosion resistance of advanced cladding and pellet materials and to collect in-reactor data necessary to qualify these materials. **[**

][a,c]

The **AXIOM** cladding-containing LTAs were inserted in Plant T in mid-2008. Inspection campaigns were conducted on one LTA after the first and second cycles of irradiation. The assembly growth data, the fuel rod growth and oxide of peripheral rods in this assembly are included in the database. In Summer 2013, inspections and rod extractions were conducted on third burned (~ 37 GWd/MTU) and twice burned (~ 27 GWd/MTU) assemblies. The inspection results (Fuel rod growth, fuel assembly growth and oxide thickness) are included in the database. In December 2014, FR (fuel rod) and FA (fuel assembly) growth inspections were conducted for assemblies after 4 cycles (~ 47.5 GWd/MTU). In January 2016, visual inspections and length measurements were done on fifth burned (~ 51 GWd/MTU) and fourth burned (~ 44 GWd/MTU) assemblies. In June 2016, oxide measurements were conducted on fifth-burned assembly and rods were extracted. The fuel assembly was inserted back for the 6-cycle irradiation during the 2018 outage and the oxide measurements data performed on peripheral rods in August 2019 are included in the database.

In summary, oxide data of **AXIOM** clad fuel rods with **[**

][a,c] Plant T is the only commercial plant hosting **AXIOM** LTAs with **[**

][a,c]

4.2.6 Halden IFA-708/785 PWR Cladding Corrosion and Hydriding Test Program

The PWR cladding corrosion and hydriding test program IFA-708 in the Halden reactor was designed to evaluate the performance of modern commercial zirconium alloys in very aggressive conditions exceeding those currently allowable in operating PWRs, including high pH, high heat flux and high mass evaporation rates. The Westinghouse materials include **[ ]**[a,c]. The test started in July 2007 and terminated a couple of times due to rod failure events. Major modifications to the test conditions were conducted. Irradiation resumed in new test rig IFA785 in fall 2015 and stopped in 2018 due to the Halden shutdown. The test data from the Halden program was not used for **AXIOM** corrosion model development since the operating conditions were significantly different from prototypical PWR conditions. The test data were discussed in Section 5 to support the robust corrosion resistance performance of **AXIOM** cladding under abnormal chemistry conditions.

4.2.7 Plant AH Unit 1 AXIOM Cladding Creep LTR

The **AXIOM** cladding creep LTR program in Plant AH Unit 1 was implemented to study the creep behavior of **AXIOM** cladding. A total of **[ ]**[a,c] **AXIOM** rods were included in the 17 RFA XL **Optimized ZIRLO** fuel assembly that was irradiated for one (1) cycle in Plant AH Unit . The irradiation started in fall 2017. In March 2019, at the end of the first cycle, **[ ]**[a,c] **AXIOM** alloy rods were extracted and shipped to hotcell for profilometry measurement. No poolside post irradiation examination (PIE) or other hotcell examinations were conducted. The profilometry measurements from the one-cycle **AXIOM** alloy rods are included in **AXIOM** cladding creep model development.

4.2.8 Plant W Full AXIOM Cladding LTA Program

A total of eight full **AXIOM** alloy LTA was inserted into Plant W Unit 3 in fall 2017. The LTAs are the same as the remainder of the core with typical **[ ]**[a,c] fuel products, except for **AXIOM** cladding. **Optimized ZIRLO** cladding is used for the remainder of the core. After the first and second cycles of irradiation, assembly visual examinations were performed on the LTAs during the Plant W Unit 3 refueling outage. These LTAs performed as expected. No evidence of mechanical integrity or crud deposition anomalies were noted. Fuel inspections consisted of visual examinations, fuel rod growth, and peripheral rod oxide measurements are planned on selected twice-burned and thrice-burned rods.

The purpose of Plant W **AXIOM** alloy LTAs was for production demonstration and irradiation performance verification. The measurement data from Plant W LTAs are not considered for **AXIOM** cladding model developments.

5 CHARACTERIZATION OF AXIOM CLADDING BEHAVIOR

5.1 CORROSION

5.1.1 Operating PWRs

Post-irradiation examination results of **AXIOM** cladding have shown very good in-reactor corrosion performance. The **AXIOM** alloy oxide database used for the **AXIOM** cladding corrosion model development included measurements from **[**

][a,c]

The eddy current measured oxide thickness from pool-side measurements of different plants is shown in Figure 5.1-1 as a function of rod average burnup. The data indicate that oxide data for all **AXIOM** alloy rods and **Optimized ZIRLO** alloy rods are similar to those for **ZIRLO** alloy rods at low burnups of about 20-30 GWd/MTU. At higher burnups, on the other hand, the advantage of the **AXIOM** and **Optimized ZIRLO** alloys over **ZIRLO** alloy becomes significant. At high burnups of about 70 GWd/MTU, the advantage of **AXIOM** cladding over **Optimized ZIRLO** cladding becomes significant. The oxide levels for **AXIOM** alloys remain in the lower range of the **ZIRLO** oxide database. The measured maximum oxide thickness of the **AXIOM** alloys are less than 50 μm for a burnup of close to 75 GWd/MTU.

5.1.2 Demanding Conditions: Halden IFA-708/785

The main objective of Halden IFA-708/785 is to evaluate the performance of modern zirconium-based materials in aggressive conditions exceeding those currently allowable in operating PWRs including the effects of elevated pH, high power rating and significant subcooled boiling. **[**

][a,c]

The oxide thickness results for Westinghouse alloys from the Halden test program are presented in Table 5.1-1 and Figure 5.1-2. **AXIOM** alloy is noted as A1 in Halden Report (Reference 5.1). As shown, **AXIOM** cladding has better corrosion performance (less oxidation) than coresident **ZIRLO** and **Optimized ZIRLO** cladding at and above 38 MWd/kg UO_2.

5.1.3 Corrosion Model

5.1.3.1 Introduction

This section describes the **AXIOM** cladding corrosion database used for model development, the **AXIOM** cladding corrosion model, the hydrogen pickup (HPU) model, and resulting corrosion limits used for normal operation and accident evaluations.

5.1.3.2 Cladding Corrosion Database

Corrosion data has been obtained from measurements for four (4) sets of LTAs, Plant M, Plant D, Plant T and Plant B. Details on the various LTAs are summarized in Section 4.2. The data from the poolside exams was assembled into a single database. Table 5.1-2 summarizes the data sets. Figure 5.1-3 is a plot of all **AXIOM** alloy data vs. TRD (accumulated thermal reactive duty). Data from the HALDEN IFA-708/785 was not used for model development since the operating conditions were significantly different from prototypical PWR conditions.

HPU data is obtained from a hotcell of fuel rods from the Plant B LTA. That data is evaluated using a correction for hydrogen in the oxide layer consistent with the **Optimized ZIRLO** cladding corrosion model (Reference 5.2) and also without using a correction based on guidance in RG 1.236 (Reference 5.6). Details are provided in Section 5.2.

5.1.3.3 Cladding Corrosion Model

The **AXIOM** cladding corrosion model uses a new fit to the thermal reaction accumulated duty (TRD) term developed originally for the Westinghouse **ZIRLO** cladding corrosion model (Reference 5.2). The TRD term is an **[**

][a,c]

The integral form of the TRD term that was developed increases with time and temperature, thus accounting for fluctuations in conditions throughout the operating history. TRD is obtained by **[**

][a,c] The next section provides details on the **AXIOM** model development as a function of TRD.

5.1.3.4 AXIOM Corrosion Model Development

These are the steps used in determining the **AXIOM** cladding corrosion model:

1. Assemble **AXIOM** cladding corrosion database.
2. Remove data from below 20 inches.
3. Randomly assign numbers **[** **]**[a,c]
4. Split into approximately **[** **]**[a,c]
5. Determine best overall model for measured oxide to TRD for calibration data set with function that **[** **]**[a,c]
6. Determine new M-Ps.
7. Bin data by TRD.
8. For each bin determine upper bound (UB).
9. Look at UB by bins and determine overall UB function.

10. Compare UB and BE models to calibration dataset.
11. Confirm fit of UB and BE models to verification dataset.

For **AXIOM** cladding **[ ]**[a,c] between measured oxide and TRD was determined to be the best overall model. The model forms of **Optimized ZIRLO** and **AXIOM** claddings are:

[ ][a,c] Equation 5.1-1

Optimized ZIRLO cladding oxide, µm

[ ][a,c] Equation 5.1-2

AXIOM cladding oxide, µm

The fit of the model is presented as measured data vs. TRD in Figure 5.1-4. Then the data is transformed to measured – predicted (M-P). The M-P data for the calibration dataset is presented in Figure 5.1-5 and Figure 5.1-6 as M-P vs. TRD and M-P vs. axial position, respectively.

Then the same model was applied to the validation dataset. That data is presented in Figure 5.1-7 and Figure 5.1-8 as M-P vs. TRD and M-P vs. axial position, respectively.

The overall statistics for the calibration and verification datasets with the **AXIOM** cladding corrosion model are shown in Table 5.1-3 below.

It can be observed that the calibration and verification datasets result in nearly the same statistics.

5.1.3.5 Corrosion Model Uncertainties

The model uncertainties were determined as a function of predicted thickness in order to **[**

][a,c]

is defined as:

[ ][a,c] Equation 5.1-3

AXIOM cladding UB oxide, µm

The UB uncertainty oxide is also shown in Figure 5.1-4 to Figure 5.1-8 as either an UB prediction or an UB uncertainty. Note in Figure 5.1-6 and Figure 5.1-8 that the **[**

][a,c] and is

included for illustration.

Table 5.1-1 Oxide Thickness Results from Halden IFA-708/785 for AXIOM, Optimized ZIRLO and ZIRLO Cladding Materials

Full Power Days	Assembly Burnup (MWD/kg UO_2)	Oxide Thickness (µm)		
		ZIRLO	*Optimized ZIRLO*	*AXIOM*

a,c

1, 2, 3, 4 – Position 1,2,3,4 from top to bottom.

Table 5.1-2 Summary of AXIOM Cladding Corrosion Data

Plant	No. of Fuel Rods	No. of Data Points	Max Burnup, GWd/MTU	Max Number of Cycles
Plant M				
Plant D				
Plant T				
Plant B				

a,c

Table 5.1-3 Overall Statistics for the Calibration and Verification Datasets with the AXIOM Cladding Corrosion Model Data

Parameter	Data Set	
	Calibration	Verification
Avg M-P, µm	[[	]] a,c
Stdev M-P, µm		
Total Pts		
UB Uncertainty, µm *		
Pts > UB		
% Bounded		

* Calculated only for Calibration dataset

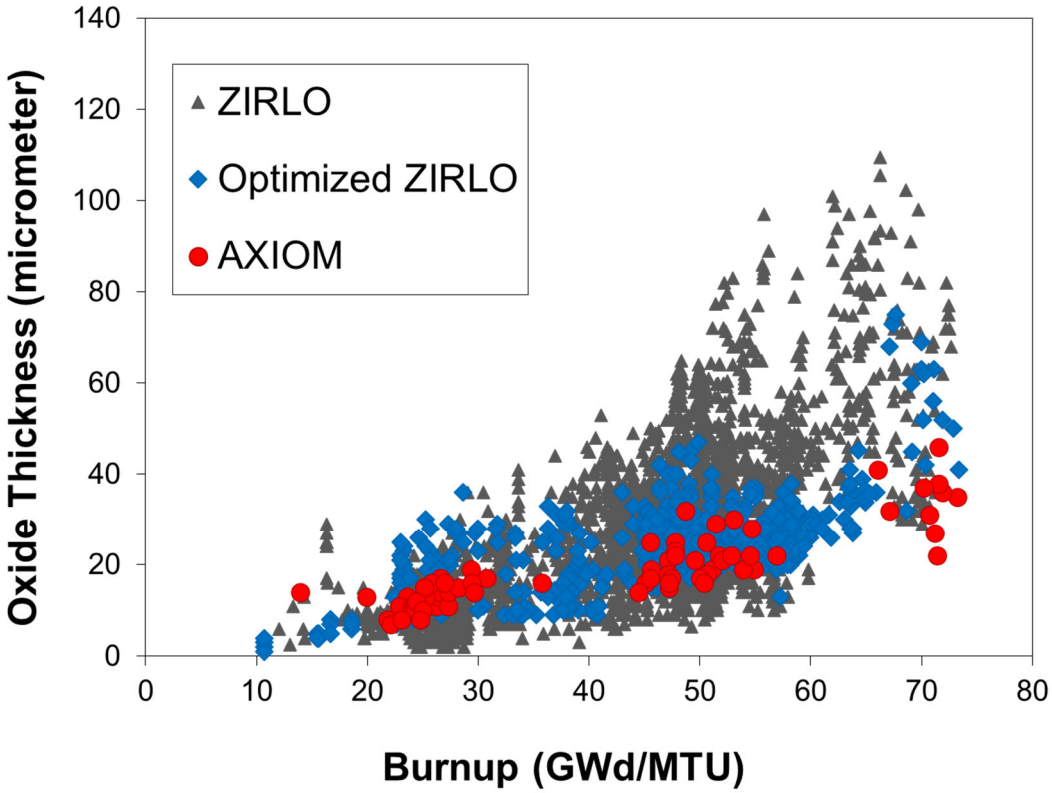

Figure 5.1-1 Rod peak oxide thickness as a function of rod average burnup

a,c

*Figure 5.1-2 Oxide thickness as a function of burnup, for **ZIRLO**, **Optimized ZIRLO**, and **AXIOM** claddings in the Halden test reactor IFA 708/785*

a,c

*Figure 5.1-3 **AXIOM** cladding measured oxide thickness versus TRD (all data)*

a,c

*Figure 5.1-4 **AXIOM** cladding measured oxide thickness versus TRD (calibration database)*

a,c

*Figure 5.1-5 **AXIOM** cladding measured – predicted (M-P) oxide thickness versus TRD (calibration database)*

a,c

*Figure 5.1-6 Calibration database measured – predicted (M-P) oxide vs. axial position using **AXIOM** cladding corrosion model and UB based on [*

]a,c

a,c

*Figure 5.1-7 **AXIOM** cladding corrosion model verification database measured – predicted (M-P) Oxide vs. TRD and UB based on [*

]a,c

a,c

*Figure 5.1-8 **AXIOM** cladding corrosion model verification database measured – predicted (M-P) oxide vs. axial position and UB based on [*

]a,c

5.2 HYDROGEN PICKUP

Hydrogen pickup in reactor for **AXIOM** cladding has been obtained from Plant B hotcell program. The rods have burnup over 70 GWd/MTU. The hydrogen content samples were selected from different elevations of the fuel rods based on the eddy current oxide traces to cover the entire range of hydrogen contents. There was a total of **[**

]a,c in developing the hydrogen pickup model for **AXIOM** cladding.

To calculate the amount of hydrogen absorbed by the metal, the hydrogen content measured from the cladding ring (including metal and oxide) was corrected by subtracting the amount of estimated hydrogen absorbed by the oxide layer. The hydrogen absorbed by the oxide was calculated based on an empirical model developed by Westinghouse based on test data which gives the amount of hydrogen in the oxide as a function of oxide thickness. The model is documented in the approved **ZIRLO** and **Optimized ZIRLO** corrosion model. (Reference 5.2). The hydrogen uptake ratio is calculated as the fraction of hydrogen absorbed by the metal relative to the amount of hydrogen generated by the waterside corrosion reaction. Figure 5.2-1 gives the calculated hydrogen content in the metal for each alloy versus the oxide thickness.

The results show that **Optimized ZIRLO** cladding has higher hydrogen uptake ratio than **AXIOM** cladding. For **AXIOM** alloy, the ratio is less than 10%. The overall maximum hydrogen content for any **AXIOM** alloy is ~ 200 ppm due to the combination of low maximum oxide thickness and low hydrogen pickup ratio.

5.2.1 Hydrogen Pickup Model

In the corrosion process the cladding reacts with the coolant in the following reaction:

$Zr + 2H_2O \rightarrow ZrO_2 + 2H_2$

An oxide layer (ZrO_2) is formed on the outside of the cladding as the cladding metal wall thickness is reduced. Of the hydrogen released from this reaction, a fraction is absorbed by both the oxide layer and in the base cladding metal. The remaining unabsorbed hydrogen goes into the coolant. Hydrogen absorbed by the base metal is in solution up to a temperature dependent solubility concentration, and hydrogen above the solubility limit precipitates out as Zr-H platelets. Approximately 125 wppm hydrogen is soluble in Zircaloy-based cladding at reactor operating temperatures. Most importantly, the hydrides formed in irradiated cladding are not uniformly distributed across the cladding wall. The hydrogen tends to accumulate near the outer cladding wall in response to the temperature gradient across the cladding. The presence and especially the distribution of hydrogen in the cladding can impact cladding properties.

While the hydrogen distribution through the cladding is an important factor with respect to the impact on cladding properties such as ductility, the overall hydrogen level can be characterized by the hydrogen absorption or hydrogen pickup (HPU), either as a fraction or a percent. The existing Westinghouse data on HPU fraction for **ZIRLO** and **Optimized ZIRLO** claddings corresponds well with the existing data for Zircaloy-4 cladding and validates that the HPU fraction is essentially the same for Zircaloy-4, **ZIRLO** and **Optimized ZIRLO** claddings.

Evaluation of the cladding hydrogen data for **AXIOM** cladding determined a lower HPU fraction of **[ ]**[a,c] for **ZIRLO** and **Optimized ZIRLO** claddings.

To determine the cladding hydrogen absorption fraction the following is performed:

1. The cladding oxide thickness is determined by eddy current (EC) or metallography.
2. The ratio of oxide to metal volume is determined for the oxide thickness.
3. A sample of the cladding is weighed.
4. The hydrogen from that sample is extracted by hot vacuum extraction (HVE) and the hydrogen volume/mass is determined.
5. The original cladding metal thickness is determined either from as-built measurements or from metallography.
6. From the oxide thickness, the loss of base metal mass to oxide is determined.
7. Based on the loss of base metal the mass of hydrogen created by the oxidation reaction is calculated.
8. The mass of hydrogen in the oxide layer is calculated and removed from the HVE hydrogen inventory. This is the metal content inventory.
9. The hydrogen absorption (HPU) fraction is calculated by dividing the metal content hydrogen inventory by the hydrogen generated.

The governing equations are presented next. The total hydrogen in a sample can be described as:

[ ]a,c

Equation 5.2-1

where:

[ ]a,c

To determine the metal hydrogen using hot vacuum extraction results for a cladding sample:

[ ]a,c

Equation 5.2-2

The formula used to account for the hydrogen concentration in the oxide layer is:

[ ]a,c

Equation 5.2-3

This is used in the **ZIRLO** and **Optimized ZIRLO** cladding corrosion models (Reference 5.2) and in PAD5 (Reference 5.3). It is based on a fit to measurements done on the hydrogen content of oxide layers. (References 5.4 and 5.5)

The remaining metal thickness is determined by:

$$t_{ZR} = t_O - \frac{t_{ox}}{O/M}$$

Equation 5.2-4

where:

t_O = Initial cladding thickness

O/M = Oxide to metal volume ratio

The oxide to metal volume ratio, *O/M*, is determined by:

[ ]^{a,c} Equation 5.2-5

The amount of hydrogen generated in the corrosion process and available for pickup in the oxide and metal is determined by the following expressions:

[ ]^{a,c} Equation 5.2-6

The fraction of the hydrogen that is generated from corrosion and deposited in the metal can be determined by:

$$H_{ZR} = Ho + F_{ZR}H_{GEN}$$ Equation 5.2-7

where:

H_{GEN} = Hydrogen generated by corrosion

H_{ZR} = Hydrogen in metal

F_{ZR} = Hydrogen pickup fraction for metal

Ho = As-built cladding hydrogen

The pickup fraction is then determined by:

[ ]^{a,c} Equation 5.2-8

This can then be inverted to determine the hydrogen based on an oxide thickness and a given as-built Hydrogen and HPU:

[ ]^{a,c} Equation 5.2-9

$H_{BE} = H_T$: Total hydrogen, ppm

h: Oxide thickness, mils

b_o: Clad wall thickness, as-fabricated, mils

The measured cladding metal hydrogen content as a function of oxide thickness is plotted in Figure 5.2-2 for the **AXIOM** cladding data.

The **AXIOM** HPU percent data as a function of oxide thickness is shown in Figure 5.2-3. The **AXIOM** HPU percent based on this data is **[ ]**[a,c].

To provide input to reactivity initiated accident such as the rod ejection accident (REA), the HPU was also calculated based on the requirements in RG 1.236 (Reference 5.6). Following the requirement that oxide correction not be used in evaluating HPU, the total hydrogen H_T can be used in place of hydrogen in metal H_{ZR} in the above equation. In that case the HPU for **AXIOM** cladding is **[ ]**[a,c].

5.2.2 Hydrogen Pickup Model Uncertainties

The HPU model uncertainties were determined as a **[**

][a,c] is defined as:

[ ]a,c Equation 5.2-10

AXIOM cladding UB hydrogen, ppm

For the REA analysis where the HBU has been calculated without oxide correction.

[ ]a,c Equation 5.2-11

AXIOM cladding UB hydrogen, ppm

The **AXIOM** cladding data is plotted as M-P vs. oxide thickness in Figure 5.2-4 and Figure 5.2-5 with and without oxide correction, respectively.

Figure 5.2-1 Calculated hydrogen content in metal as a function of oxide thickness

a,c

*Figure 5.2-2 **AXIOM** cladding metal hydrogen content vs. oxide thickness*

a,c

*Figure 5.2-3 **AXIOM** cladding HPU vs. oxide thickness, with oxide correction*

*Figure 5.2-4 **AXIOM** cladding HPU M-P vs. oxide thickness, with oxide correction*

*Figure 5.2-5 **AXIOM** cladding HPU M-P vs. oxide thickness, without oxide correction*

5.3 AXIOM CLADDING CORROSION AND HYDROGEN LIMITS FOR NORMAL OPERATION AND ACCIDENT CONDITION

The **AXIOM** cladding corrosion and HPU models are used with the fuel performance code PAD5 (Reference 5.3) to predict the cladding oxide thickness and hydrogen content. These are used to evaluate planned irradiations to compare predictions against limits or to provide input to other evaluations. Table 5.3-1 lists the applicable oxidation and hydrogen related limits for both **AXIOM** and **Optimized ZIRLO** claddings. Also listed is the type of analysis used in comparison to the limit such as best estimate (BE) and upper bound (UB).

For analyses using upper bound hydrogen the two uncertainties of corrosion and HPU are combined to obtain the UB estimate. The UB hydrogen vs. TRD is shown in Figure 5.3-1 and Figure 5.3-2. Both BE and UB curves are shown along with **AXIOM** cladding data.

For the LOCA evaluation the ductile to brittle transition (DBT) based on PQD testing is used to set ECR limits as a function of hydrogen. Since the DBT is based on **[**

][a,c]

For the REA, following RG 1.236, the total measured hydrogen inventory from both the metal and oxide are used in the HPU fraction calculation for **AXIOM** cladding. The hydrogen in the oxide layer is not removed (corrected). The **AXIOM** cladding hydrogen is calculated based on a **[**

][a,c] For comparison, **Optimized ZIRLO** cladding follows the RG 1.236 using a BE corrosion model with a 25% HPU. The excess hydrogen will be determined using the formula for terminal solid solubility for dissolution (TSSD) (Reference 5.7) for both **AXIOM** and **Optimized ZIRLO** cladding. **AXIOM** cladding and **Optimized ZIRLO** cladding PCMI enthalpy rise limits as a function of TRD are plotted in Figure 5.3-4.

Table 5.3-1 Corrosion and Oxidation Based Criteria for AXIOM Cladding Compared to Optimized ZIRLO Cladding

Parameter	Basis	**AXIOM** Value	**Optimized ZIRLO** Value
Normal Operation Conditions			
Corrosion - Oxide Thickness	BE	≤ 100 μm	≤ 100 μm
Corrosion - Cladding Hydrogen	BE	≤ [ ]^{a,c}	≤ [ ]^{a,c}
Accident Conditions			
LOCA - ECR%*	UB	[ ]^{a,c}	ECR as calculated by C-P ≤ draft RG 1.224 DBT limits based on UB H
REA – Clad Failure PCMI Enthalpy Addition	UB	[ ]^{a,c}	≤ Based on SRA limits in RG 1.236 based on BE oxide and UB HPU.
* Currently, the 10 CFR 50.46 Regulation (1988) is used to demonstrate compliance in plant licensing basis analyses that model **Optimized ZIRLO** cladding			

[ ]^{a,c}

*Figure 5.3-1 **AXIOM** cladding metal hydrogen vs. TRD, with oxide correction*

*Figure 5.3-2 **AXIOM** cladding total hydrogen vs. TRD, without oxide correction – for REA)*

*Figure 5.3-3 ECR Limits vs. TRD for **AXIOM** and **Optimized ZIRLO** cladding. **AXIOM** cladding **[ ]**^{a,c}*

*Figure 5.3-4 Enthalpy increase limit vs. TRD for **AXIOM** and **Optimized ZIRLO** cladding. **AXIOM** cladding HPU determined without oxide correction and **[***

***]**[a,c]*

5.4 FUEL ROD AXIAL GROWTH

The **AXIOM** cladding rod growth database for **AXIOM** cladding growth model is composed of measurements from **[**

][a,c] The data are summarized in Table 5.4-1**.**

The data are plotted against the **ZIRLO** and **Optimized ZIRLO** claddings single rod growth database in Figure 5.4-1. The measurements indicate that the fuel rod growth of **AXIOM** and **Optimized ZIRLO** cladding rods is similar to that of **ZIRLO** cladding rods for low to medium fast fluences up to 10×10^{21} n/cm^2 and is lower than that of **ZIRLO** cladding rods at higher fast fluences.

AXIOM cladding continues to show stable growth behavior for burnups beyond 70 GWd/MTU with no indications of instability in growth trends. The axial growth of the **AXIOM** cladding at higher fast fluences appears nearly linear as a function of fast fluence, consistently less than the behavior of both **ZIRLO** and **Optimized ZIRLO** at high fast fluences. **[**

][a,c]

5.4.1 Fuel Rod Axial Growth Model

The available rod axial growth data for **AXIOM** cladding material was used to develop a model for fractional growth as a function of fast fluence (E > 1.0 MeV) consistent with the previously licensed PAD5 fuel performance models for the **ZIRLO** and **Optimized ZIRLO** cladding materials.

The rod axial growth behavior of **AXIOM** cladding material is very similar to that of **Optimized ZIRLO** cladding material but tends to **[** **]**[a,c]. Therefore, the **AXIOM** cladding axial growth model uses **[** **]**[a,c]

[**]**[a,c]

Equation 5.4-1

[

][a,c]. For the analysis, the axial growth strain is expressed as a percent. **[**

][a,c]

The resulting **AXIOM** cladding axial rod growth model is given in the following equation (with ε_f in % and Φ in 10^{21} n/cm²):

[**]**[a,c]

Equation 5.4-2

The mean residual is **[** **]**[a,c] and the standard deviation of the residuals is **[** **]**[a,c].

The uncertainty bounds were determined using a non-parametric approach to construct one-sided 95/95 tolerance intervals. The bounds are:

[**]**[a,c]

Equation 5.4-3

Equation 5.4-4

The **AXIOM** cladding axial rod growth model is plotted with the **AXIOM** cladding axial rod growth data in Figure 5.4-2. The predicted minus measured **AXIOM** cladding growth as a function of fast fluence in Figure 5.4-3 confirms good agreement over the whole fast fluence range.

Table 5.4-1 Summary of AXIOM Cladding Growth Data

Plant	No. of Data Points	Fluence Range 10^{21} n/cm²	Burnup Range GWd/MTU	Fuel Design
Plant M	[			] **a,b,c**
Plant D Unit 1				
Plant D Unit 2				
Plant T				
Plant B				
All				

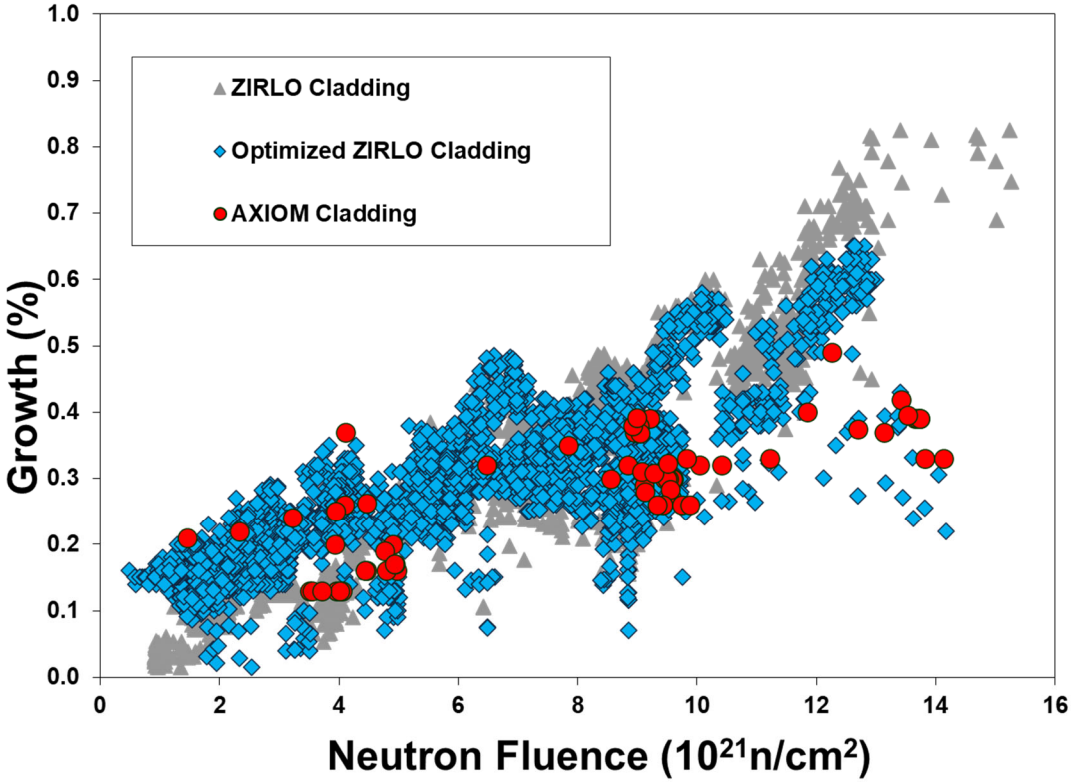

*Figure 5.4-1 Fuel rod growth data for **AXIOM**, **Optimized ZIRLO** and standard **ZIRLO** alloys as a function of fast neutron fluence*

*Figure 5.4-2 **AXIOM** cladding axial rod growth data and **AXIOM** cladding rod growth model*

a,c

*Figure 5.4-3 **AXIOM** cladding axial rod growth model measured minus predicted residual plot*

5.5 CLADDING CREEP

Based on the reduced tin content compared to **ZIRLO** and **Optimized ZIRLO** cladding, **AXIOM** alloys should have higher creep. However, the pRXA condition of **AXIOM** cladding (compared to the SRA condition for **ZIRLO** cladding) should compensate for the decrease of tin content to a certain extent as demonstrated with **Optimized ZIRLO** clad creep remaining comparable to **ZIRLO** cladding (Reference 5.8). Current data from the Plant R creep and growth program show that **AXIOM** alloy has lower creep strain than **ZIRLO** cladding.

Also, each alloy in the entire Plant R creep and growth program, including the **AXIOM** alloy indicated that the deviatoric hoop stress correlation correctly represents $\Delta D/D_o(ic)$ behavior. The deviatoric hoop stress component is the driving force for irradiation creep. Figure 5.5-1 shows the calculated irradiation creep diameter strain versus deviatoric hoop stress component for **AXIOM** alloy sample after one cycle of irradiation. The linear fit approximately passes through the point of $\Delta D/D_o(ic) = 0$ and $\sigma_\theta(deviatoric) = 0$, therefore, negative deviatoric hoop stresses result in equal and opposite (negative) diameter strains compared to positive deviatoric hoop strains.

5.5.1 Clad Creep Model

The **AXIOM** cladding creep model is based on calibration to in-reactor data. The **AXIOM** cladding creep data consisted of **[ ]**[a,c] irradiation campaigns summarized in Table 5.5-1. In-reactor fueled rods are limited to one cycle worth of data because longer operations will likely result in hard contact between the fuel and cladding and result in cladding diameter that is not purely related to the creep phenomenon. The unfueled samples in Plant R do not experience any pellet-clad contact by design. The measured in-reactor profilometry data has been **[ ]**[a,c], and **[ ]**[a,c] of the rod length have been considered. **[ ]**[a,c]

Unlike the development of the **ZIRLO** and **Optimized ZIRLO** cladding creep model, the database was not separated into calibration and validation datasets due to the limited number of data from commercial rods.

The calibration process followed can be summarized as follows:

1. Observe the trends of the creep predictions (M/P vs. fluence and M/P vs. axial elevation);
2. Eliminate or reduce any significant bias or trends in prediction against key parameters;
3. Minimize the standard deviation of M/P to the highest degree possible.

[

][a,c]

The PAD5 clad creep model functional form included in Section 5.4 of Reference 5.3 was maintained and the modifications made to the calibration coefficients were listed in Table 5.5-2.

Consistent with **ZIRLO** and **Optimized ZIRLO** cladding in PAD5, **[**

][a,c]

[

][a,c]

Figure 5.5-2 shows the BE PAD5 **AXIOM** creep down predictions vs. measurements for **[**

][a,c] Figure 5.5-3 and Figure 5.5-4 show that the **AXIOM** cladding creep model does not have biased trends associated with the amount of creep strain, fluence or axial temperature variation. As noted above and shown in Figure 5.5-3, creep data for unfueled samples is available for fluences greater than **[**

][a,c] Figure 5.5-4 also includes the unfueled samples and fueled samples. The unfueled samples have arbitrarily been included in the figure at the lowest elevation with the

results representing the middle of the sample. Overall, the creep model predicts the data well without any biases based on fluence or temperature.

To quantify the uncertainty in the creep model the **[**

][a,c] for **ZIRLO** and **Optimized ZIRLO** cladding material in PAD5 (in the response to RAI-9i of LTR-NRC-16-16 section of Reference 5.3). For comparison, the current licensed **ZIRLO**/**Optimized ZIRLO** cladding LB and UB values are listed in Table 5.5-3:

Table 5.5-1 Summary of AXIOM Cladding Creep LTR Campaigns

Campaign	Material	Comments
Plant R	[	] a,c
Plant AH		
Plant D		

Table 5.5-2 PAD5 AXIOM Cladding Creep Model Coefficients

Creep Model	Calibration Parameters	Values	Comments
Thermal Creep	STCAL		
	PTCAL		
	CTCAL		
	HTCAL		
	QTCAL		
	DTCAL		
Irradiation Creep	AICAL		
	DICAL		
	FICAL		
	TSATIRR		
Radial Growth	R_θ		

a,c

Table 5.5-3 Bounding PAD5 Creep Model Alloy Specific Material ACREEP

Cladding Material	LB ACREEP	UB ACREEP
ZIRLO/Optimized ZIRLO		
AXIOM		

a,c

a,c

*Figure 5.5-1 Irradiation creep diameter strain versus the corresponding deviatoric hoop stress for **AXIOM** alloy sample after 1 cycle of irradiation*

a,c

*Figure 5.5-2 **AXIOM** cladding creep-down predicted vs. measured creep-down*

[**a,c**

]

*Figure 5.5-3 **AXIOM** cladding creep-down M/P vs. fluence*

a,c

*Figure 5.5-4 **AXIOM** cladding creep-down M/P vs. axial elevation*

5.6 IRRADIATED MECHANICAL PROPERTIES

Axial tensile tests (ATT) and Ring tensile tests (RTT) were performed for high burnup **Optimized ZIRLO** cladding and **AXIOM** claddings from Plant B hotcell (Reference 5.9). The tensile test specimens, the hydrogen analysis sample, and the metallography and SEM samples have been selected to be adjacent to each other in rod axial location for verification. Tensile test samples were taken from ~118-inch elevation where the maximum oxide and hydrogen pickup were measured. Each set of samples includes two test temperatures: room temperature (RT) and high temperature at 385°C (HT). For ATT, about 3.5-inch-long pieces were cut from the fuel rod, defueled and then split axially into two equal halves. The final "dog-bone" type axial tensile test samples were machined from the cladding halves using a milling machine. For ring tensile tests, 5 mm rings were cut and machined to "dog-bone" type samples. The engineering stress-strain diagrams were based on the recorded load-displacement data.

Figure 5.6-1 and Figure 5.6-2 show the stress strain curves from axial tensile tests and ring tensile tests of **AXIOM** cladding samples in comparison to **Optimized ZIRLO** cladding samples from the same assembly. The analysis of the stress-strain curves gives the values of yield stress (YS, 0.2% offset yield stress), the ultimate tensile stress (UTS), the necking strain (the plastic strain measured from the point of maximum load to the specimen fracture point) and the total plastic strain (plastic strain at specimen fracture point). Figure 5.6-1 and Figure 5.6-2 show that the mechanical properties of irradiated **AXIOM** and **Optimized ZIRLO** claddings are comparable. The significant ductility improvement exhibited by **Optimized ZIRLO** cladding over **ZIRLO** and Zircaloy-4 claddings is also present for **AXIOM** cladding. The results of axial tensile tests at 385°C for **Optimized ZIRLO** and **AXIOM** cladding specimens show the total plastic strain

in the range of 6.3% to 10.5%. For comparison, the results of axial tensile tests at 350°C show that the **ZIRLO** cladding specimen (with a burnup level over 70 GWd/MTU) has a total plastic strain range of 1.3 to 6.8% and the Zircaloy-4 specimen (with a burnup level of about 55 GWd/MTU) has a total plastic strain range of 0.1 to 1.9% (Reference 5.10). All **Optimized ZIRLO** and **AXIOM** cladding specimens tested at high temperature fractured in a ductile fashion with fracture surfaces at 45° to the loading direction. Both **AXIOM** and **Optimized ZIRLO** claddings show significantly higher necking strain compared to **ZIRLO** cladding specimens for the high temperature tensile test (350°C for the **ZIRLO** cladding specimen (Reference 5.10) and 385°C for the **Optimized ZIRLO** and **AXIOM** cladding specimens). Higher necking strain is associated with higher resistance to crack propagation. Based on the axial tensile tests at high temperature, the necking strain ranges from 0% to 5% for **ZIRLO** cladding specimens, and from 4% to 8.7% for **Optimized ZIRLO** and **AXIOM** cladding specimens.

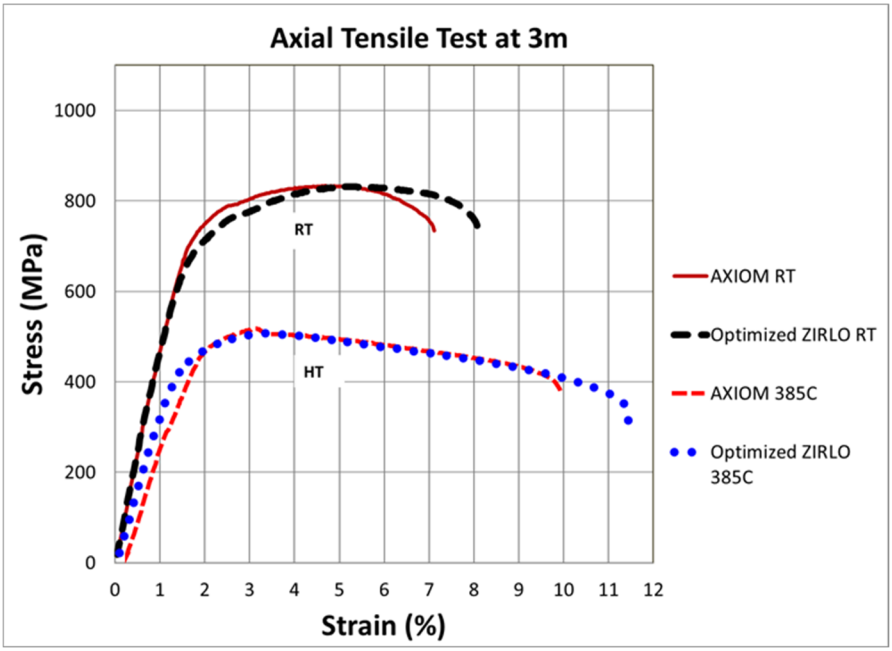

*Figure 5.6-1 Stress-strain curves of irradiated **AXIOM** and **Optimized ZIRLO** cladding: axial tensile tests*

a,c

*Figure 5.6-2 Stress-strain curves of irradiated **AXIOM** and **Optimized ZIRLO** cladding: ring tensile tests*

5.7 CHAPTER 5 REFERENCES

5.1 HWR-1240, OECD Halden Reactor Project, "Results from the second interim inspection of the PWR cladding corrosion test IFA-785," January 2019.

5.2 WCAP-12610-P-A & CENPD-404-P-A, Addendum 2-A, "Westinghouse Clad Corrosion Model for **ZIRLO** and **Optimized ZIRLO**," October 2013.

5.3 WCAP-17642-P-A, Revision 1, "Westinghouse Performance Analysis and Design Model (PAD5)," November 2017.

5.4 Hermann, Wiese, Buhner, Steinemann, and Bart, "Hydrogen Distribution Between Fuel Cladding Metal and Overlying Corrosion Layers," in proceedings of the 2000 International Topical Meeting on Light Water Reactor Fuel Performance, Park City, Utah, April 10-13, 2000

5.5 Kammenzind, B. F., Franklin, D. G., Peters, H. R., and Duffin, W. J., "Hydrogen Pickup and Redistribution in Alpha-Annealed Zircaloy-4," ASTM STP 1295, Zirconium in the Nuclear Industry: Eleventh International Symposium, pg. 338.

5.6 U. S. NRC Regulatory Guide 1.236, Revision 0, "Pressurized-Water Reactor Control Rod Ejection and Boiling-Water Reactor Control Rod Drop Accidents," June 2020 (ADAMS ML20055F490).

5.7 Kearns, J. J., "Terminal Solubility and Partitioning of Hydrogen in the Alpha Phase of Zirconium, Zircaloy-2 and Zircaloy-4," Journal of Nuclear Materials, Vol. 22, pp. 292-30, 1967.

5.8 WCAP-12610-P-A & CENPD-404-P-A, Addendum 1-A, "**Optimized ZIRLO™**," July 2006.

5.9 WAAP-9742, "Advantages Gained by **Optimized ZIRLO™** and **AXIOM®** PWR Cladding Materials," Top Fuel 2016, Boise, ID, Paper 17707, September 11-15, 2016.

5.10 Garde, A. and Mitchell, D., "Comparison of Ductility of Irradiated **ZIRLO®** and Zircaloy 4," in proceedings of Top Fuel 2012, Manchester, UK, Paper A0149, September 2-6, 2012.

6 LICENSING CRITERIA ASSESSMENT

6.1 STEADY STATE AND AOO ANALYSES (THERMO-MECHANICAL EVALUATION)

PAD5 (Reference 6.1) is the primary Westinghouse fuel rod design (FRD) tool. It incorporates all relevant fuel performance phenomena, including fuel thermal conductivity degradation with burnup and enhanced fission gas bubble swelling at high burnup, as an integrated set of interrelated performance models. Using appropriate input describing fuel rod design and operating conditions, PAD5 calculates key fuel performance parameters such as cladding stress, strain, oxidation and hydriding, fuel temperature and volume changes, and rod internal pressure.

6.1.1 Fuel Performance Models and Methods

The primary objectives of the fuel design and safety analyses are to provide assurance that:

1. The fuel system is not damaged as a result of normal operation and anticipated operational occurrences;
2. Fuel system damage is never so severe as to preclude control rod insertion when required;
3. The number of fuel rod failures is not underestimated for postulated accidents; and
4. Core coolability is always maintained.

As discussed in previous sections of this topical report, material property (Sections 3 and 5.6) and new model (Sections 5.1 through 5.5) behavior has been identified for **AXIOM** cladding. The following provides the summary of the required PAD5 code modifications to implement the new **AXIOM** cladding material properties and models:

- Material Properties (Sections 3 and 5.6)
  - Density
  - Thermal Conductivity
  - Yield Strength (Unirradiated and Irradiated)
  - Ultimate Tensile Strength (Unirradiated and Irradiated)
- Models (Sections 5.1 through 5.5)
  - Clad Corrosion
  - Hydrogen Pickup
  - Fuel Rod Axial Growth
  - Cladding Creep

The changes in **AXIOM** cladding behavior in comparison to other zirconium based alloys is not significant, with many of the remaining existing material properties and model functional forms remaining the same based on the equivalency defined in Sections 3 and 5. The interfaces and methodology defined in the NRC-approved PAD5 topical (Sections 7.2, 7.3, 7.4, and 7.5 of Reference 6.1) remain applicable unless specifically identified in the following fuel performance criteria discussion based on the preceding identified **AXIOM** cladding specific material and model updates. Furthermore, Section 7.3.2 of

Reference 6.1 describes the treatment of uncertainties in analyses and a method for determining applicable uncertainties.

For each fuel rod design criterion, the Design Category, Design Parameter, Design Basis, Acceptance Limit, and Design Evaluation Methodology are summarized. The definitions of these items are:

Design Category - The NRC groups acceptance criteria for design limits into three categories in the SRP (Reference 6.2 with fuel performance criteria following same format): Fuel System Damage, Fuel Rod Failure, and Fuel Coolability.

Design Parameter - The specific parameter that will be evaluated.

Design Basis - The reason that the design parameter needs to be considered in the safety evaluation.

Acceptance Limit - The acceptance limit is the value that must be demonstrated to be satisfied to satisfy the requirements of SRP Section 4.2 to provide an acceptable margin to fuel failure.

Design Evaluation - A description of the evaluation methods used to evaluate the design or acceptance limits.

6.1.2 Fuel Rod Design Criteria

6.1.2.1 Clad Stress

Design Category - Fuel System Damage

Design Parameter - Clad Stress

Design Basis - The fuel system will not be damaged due to excessive fuel clad stress.

Acceptance Limit - The NRC-approved PAD5 topical (Reference 6.1) clad stress criteria has been updated to support the use of **AXIOM** cladding material properties identified in Section 3.3. Along with the material property changes, the **[** **]**[a,c] of **AXIOM** cladding compared to **Optimized ZIRLO** cladding material, requires the use of **[**

][a,c].

For cladding with the debris mitigating oxide coating on the bottom 6 to 7 inches of the fuel rod, the same clad stress criteria are applied as shown in Table 7.4.1-1 of Reference 6.1 with **[**

][a,c]

Design Evaluation - At the BOL condition, the **AXIOM** cladding unirradiated strength properties are **[ ]**[a,c] relative to the **ZIRLO** and **Optimized ZIRLO** cladding materials that are currently used for the Westinghouse and Combustion Engineering (CE) fuel products. As such, **[**

][a,c]

The following address the **AXIOM** cladding material BOL clad stress methodology:

- **[**
-
-
-

][a,c]

- **[**

][a,c]

EOL clad stress analyses **[**

][a,c]

The **AXIOM** BOL (FEA clad strain based) and EOL clad stress analysis limits will be confirmed to be met on a cycle-specific basis.

Table 6.1-1 BOL AXIOM Cladding Allowable Strain Corresponding to Allowable Stress Criteria

a,c

Table 6.1-2 Westinghouse Clad Stress EOL Criteria

[ ]a,c

[1] For the oxide coated cladding region, [

]a,c

Table 6.1-3 Summary of Design Loadings and Stress Classifications

Design Loading	Stress Classification
a,c	

6.1.2.2 Clad Strain

Design Category - Fuel Rod Failure / Fuel System Damage

Design Parameter - Clad Strain

Design Basis - The fuel rod will not fail due to excessive fuel clad strain.

Acceptance Limit - The design limit for the fuel rod clad strain is that the total tensile strain, elastic plus plastic, due to uniform cylindrical fuel pellet deformation during any single Condition I or II transient shall be less than 1% from the pre-transient value.

Design Evaluation - Design analyses are performed with the NRC approved fuel performance code PAD5 (Reference 6.1) to confirm that the 1% transient clad strain criterion is satisfied for the limiting rod in the core. The updated **AXIOM** cladding based fuel performance models in Sections 5.1, 5.4, and 5.5) with updated **AXIOM** cladding material properties (Sections 3 and 5.6) will assess clad strain with same approach identified to the NRC for PAD5.

6.1.2.3 Rod Internal Pressure

Design Category - Fuel System Damage

Design Parameter - Rod Internal Pressure

Design Basis - The fuel system will not be damaged due to excessive fuel rod internal pressure.

Acceptance Limit - Per Section 7.4.3 of Reference 6.1, the internal pressure of the lead fuel rod in the reactor will:

- be limited to a value below that which could cause the diametral gap to increase (cladding liftoff) due to outward cladding creep during normal (Condition I) operation;
- be limited to a value below that which could result in cladding hydride reorientation in the radial direction; and
- be limited to preclude extensive departure from nucleate boiling (DNB) propagation.

Design Evaluation - The PAD5 code (Reference 6.1) is used to calculate the rod internal pressure (RIP) in the fuel rod, with consideration of appropriate uncertainties. The rod internal pressure design limits and the associated evaluation methods are discussed in the following sections.

6.1.2.3.1 Rod Internal Pressure No Clad-Liftoff

The no clad liftoff criterion assures that the pellet-clad gap does not reopen due to the cladding creep rate exceeding the fuel swelling rate. The concern is that gap reopening will initiate a positive feedback loop,

where the increased local temperature associated with a reopened gap will result in additional thermal fission gas release, thus increasing the rod internal pressure and further increasing the creep rate such that the gap increases in size and the process accelerates.

Design Evaluation - Fuel rod internal pressure is evaluated using the NRC-approved fuel rod performance code PAD5 (Reference 6.1). **AXIOM** cladding material dependent properties, models and uncertainties will be used in the same method as approved in Reference 6.1 to assess rod internal pressure no clad liftoff criterion to confirm this criterion on a reload specific basis.

6.1.2.3.2 No Extensive DNB Propagation

Design Evaluation - DNB propagation is evaluated on a mechanistic basis. The mechanistic approach requires rod internal pressure, the high temperature creep model and the cladding burst model. The rod internal pressure will be calculated using PAD5 with appropriate model and property changes for **AXIOM** cladding. As described in Section 3.7 the high temperature creep model is unaffected by **AXIOM** cladding. A new burst model has been developed for LOCA analyses and described in Section 6.2.1.2.2. Methods and limits described in Section 7.4.3.2 of Reference 6.1 continue to be applicable to this criterion and will be used to confirm it on a reload specific basis.

6.1.2.3.3 Rod Internal Pressure Clad Hydride Reorientation

Hydride reorientation occurs when hydride precipitates formed during reactor operation reorient from the circumferential to the radial direction. It is a precipitation driven process that occurs when fuel cladding is cooled under a tensile stress from a temperature where hydrides are dissolved. The formation of radial hydrides can reduce the cladding ductility and increase the potential for brittle failure due to subsequent fuel rod handling.

Testing of **AXIOM** cladding indicated a slight **[**

][a,c]. For **AXIOM** cladding the test was conducted with the following conditions: **[**

][a,c]. As noted in Section 3.10, external investigations into this phenomenon have been conducted on Zircaloy-4, Zircaloy-2 and **ZIRLO** cladding materials. These investigations found that the critical stress for hydride reorientation of **ZIRLO** cladding is about **[** **]**[a,c] in both the unirradiated and irradiated conditions. Westinghouse further expanded conclusions to **Optimized ZIRLO** cladding material comparing the hydride reorientation behavior to **ZIRLO** cladding material at a condition above the **ZIRLO** material threshold. This investigation concluded that the **[**

][a,c].

Based on the testing performed in Section 3.10, the **[**

][a,c].
Therefore, the RIP assessment identified in Section 7.4.3.3 of Reference 6.1 remains applicable for the hoop stress used for mitigating the onset of radial hydrides to preclude the ductility loss in the cladding. Table 7.4.3-3 of Reference 6.1 remains applicable for use of **AXIOM** cladding material and the minimum RIP limit for gap-reopening remains acceptable for the preclusion of ductility loss and hydride reorientation.

6.1.2.4 Fuel Clad Wear

Design Category - Fuel System Damage

Design Parameter - Cladding Wear

Design Basis - The fuel system will not be damaged due to grid to rod fretting (GTRF).

Acceptance Limit - Westinghouse uses a design **[ ]**[a,c] as a general guide in **[ ]**[a,c] including fretting wear marks.

Design Evaluation - Spacer Grid assembly springs are designed and then verified by testing to limit fuel rod clad fretting to less than **[ ]**[a,c] considering all pertinent factors such as spring relaxation due to irradiation, clad creep-down, grid growth, etc. Experience has shown that by meeting these spring requirements, excessive fretting of the fuel rod clad is prevented.

As the reactor starts operation, an oxide film forms on both the spring and rod surfaces. It is these surfaces that are subject to any potential fuel clad wearing. Both surfaces are zirconium oxide and there are no expected differences in the **AXIOM** cladding oxide characteristics. At lower TRDs the oxide thickness of **AXIOM** and **Optimized ZIRLO** claddings **[ ]**[a,c] where EOL GTRF is of greatest concern. Hence the wear rate for the **AXIOM** alloy fuel rods is expected to be comparable to the **Optimized ZIRLO** cladding material.

Post Irradiation Exams (PIEs) both in hotcell and poolside have not shown any significant cladding wear at spacer grid spring and dimple contact sites through burnups up to 75 GWd/MTU. Thus, the design criteria regarding clad fretting wear will be met for **AXIOM** alloy fuel rods to their design burnup.

6.1.2.5 Clad Fatigue

Design Category - Fuel System Damage

Design Parameter - Clad Fatigue

Design Basis - The fuel system will not be damaged due to fatigue.

Acceptance Limit - The fatigue life usage factor is limited to less than 1.0 to prevent reaching the material fatigue limit, considering a safety factor of 2 on stress amplitude or a safety factor of 20 on the number of cycles, whichever is more limiting (Reference 6.1).

Design Evaluation - Clad fatigue is evaluated using the NRC-approved fuel rod performance code PAD5 (Reference 6.1). Computer modeling of the fuel duty **[ ]**[a,c] Based on the fatigue tests (Section 3.4), the Langer O'Donnell fatigue model remains applicable for

AXIOM cladding. The Langer-O'Donnell fatigue model is used to determine the relationship between strain and fatigue cycles-to-failure.

Fatigue is driven by the accumulated effects of cyclic strains associated with daily load follow. The models in PAD5 have been shown to be adequate for the purpose of evaluating these loads. With the updated **AXIOM** cladding models, material properties, and corresponding model uncertainties the NRC approved fuel rod performance code PAD5 will be used to address the fatigue life usage on a reload specific basis.

6.1.2.6 Clad Oxidation

Design Category - Fuel System Damage

Design Parameter - Clad Oxidation

Design Basis - The fuel system will not be damaged due to excessive fuel clad oxidation.

Acceptance Limit - The predicted **[ ]**[a,c] shall be no greater than 100 microns for licensing applications. Furthermore, the maximum TRDs are restricted to numbers corresponding to a cladding corrosion amount of 100 microns for licensing applications.

Design Evaluation - Clad corrosion will be evaluated using the **AXIOM** cladding Corrosion Model (Section 5.1.3) using the methods described in the **ZIRLO** and **Optimized ZIRLO** cladding corrosion topical (Reference 6.3). The limit is confirmed on a reload specific basis.

6.1.2.7 Clad Hydrogen Pickup

Design Category - Fuel System Damage / Fuel Rod Failure

Design Parameter - Clad Hydrogen Pickup

Design Basis - The fuel system will be operated to prevent significant degradation of mechanical properties of the clad at low temperatures, as a result of hydrogen embrittlement caused by the formation of zirconium hydride platelets.

Acceptance Limit - The best estimate, **[ ]**[a,c] hydrogen pickup level in the most limiting clad axial node will be less than or equal to **[ ]**[a,c] at the end of fuel operation.

Design Evaluation - The best estimate cladding hydrogen pickup is calculated directly from the best estimate corrosion calculation results discussed in Section 6.1.2.6, using the hydrogen pickup fraction from Section 5.2.1 of **[ ]**[a,c]. The best estimate through-wall average hydrogen content in the cladding is calculated by Equation 5.2-9 using the methods described in the **ZIRLO** and **Optimized ZIRLO** cladding corrosion topical (Reference 6.3). The limit is confirmed on a reload specific basis.

6.1.2.8 Fuel Rod Axial Growth

Design Category - Fuel System Damage

Design Parameter - Fuel Rod Axial Growth

Design Basis - The fuel system will not be damaged due to excessive axial interference between the fuel rods and the fuel assembly structure.

Acceptance Limit - The fuel rods shall be designed with adequate clearance between the fuel rod and the top and bottom nozzles to accommodate the differences in the growth of fuel rods and the growth of the assembly without interference.

Design Evaluation - The PAD5 upper bound fuel rod axial growth model for **AXIOM** cladding (Section 5.4) is used in the calculation of the fuel rod shoulder gap as function of fast neutron fluence. The fuel rod growth analysis licensed with PAD5 (Reference 6.1) remains unchanged, except for the identified **AXIOM** cladding axial growth to confirm no fuel rod interference with the top and bottom nozzles can occur during planned operation up to the design rod average burnup limit.

6.1.2.9 Clad Flattening

Design Category - Fuel Rod Failure

Design Parameter - Clad Flattening

Design Basis - Fuel rod failures will not occur due to clad flattening.

Acceptance Limit - The fuel rod design shall preclude clad flattening during projected exposure.

Design Evaluation - Westinghouse fabricated fuel is sufficiently stable with respect to fuel densification such that the axial column gaps that can form as a result of fuel densification are too small to allow clad flattening to occur and that axial column gaps that could occur are sufficiently small that a densification power spike factor of 1.0 is appropriate (Reference 6.4). The conclusion that the clad flattening criterion is generically satisfied is applied to new fuel designs for which the **[**

][a,c]. With the updated clad creep properties for **AXIOM** cladding, the pellet to clad gap closure is **[** **]**[a,c] and the previous conclusions of Reference 6.4 remains applicable for the densification power spike factor of 1.0 with **AXIOM** cladding.

6.1.2.10 Clad Free Standing

Design Category - Fuel System Damage

Design Parameter - Clad Free Standing

Design Basis - The fuel system will not be damaged due to excessive fuel clad stress.

Acceptance Limit - The cladding shall be short-term free standing at beginning of life, at power, and during hot hydrostatic testing.

Design Evaluation – Consistent with the licensing of PAD5, the **AXIOM** cladding **[**

][a,c]

6.1.2.11 Fuel Pellet Overheating (Power-to-Melt)

Design Category - Fuel Rod Failure

Design Parameter - Fuel Pellet Overheating

Design Basis - The fuel rods will not fail due to fuel centerline melting for Condition I and Condition II events.

Acceptance Limit - The fuel rod centerline temperature shall not exceed the fuel melt temperature during Condition I and II operation, accounting for degradation of the melt temperature due to burnup and the addition of integral burnable absorbers.

Design Evaluation - The NRC-approved fuel performance code PAD5 (Reference 6.1) is used to evaluate fuel rod centerline temperatures. The PAD5 fuel temperature model incorporates the effects of fuel thermal conductivity degradation with burnup and will include the updated **AXIOM** cladding fuel performance models to continue to assess the centerline temperature to preclude the fuel pellet overheating (power to melt) criterion.

6.1.2.12 Pellet-Clad Interaction

Design Category - Fuel Rod Failure

Design Parameter - Clad strain and fuel pellet overheating

Design Basis - The fuel rod will not fail due to pellet clad interaction.

Acceptance Limit - The NRC SRP does not require a specific design criterion for PCI. Two related criteria, the one percent clad strain criterion (Section 6.1.2.2) and the fuel overheating (no centerline fuel melt) criterion (Section 6.1.2.11), must be met.

Design Evaluation - Per Section 7.4.11 of Reference 6.1, the fuel rod will not fail due to pellet-clad interaction. There is no specific design criterion for PCI so long as the clad strain and fuel overheating limits are met. PAD5 will be used to confirm the clad strain and fuel overheating limits are met for **AXIOM** cladding, so no additional PCI calculations are required.

6.1.2.13 Interface to Safety Analysis

The PAD5 code is used to generate fuel temperature, rod internal pressure, core stored energy and additional fuel and cladding parameter inputs for LOCA and Non-LOCA safety analyses. These results are used to define conditions used to initialize the transient safety analysis codes. The model and material properties changes required for **AXIOM** cladding have a minor effect on fuel temperatures and rod internal pressures provided for safety analyses. In general, lower temperatures are expected for **AXIOM** alloy fuel at higher burnups due to a reduced corrosion thickness. Minor temperature increases are expected prior to gap closure due to a decreased primary creep rate in **AXIOM** cladding. Rod internal pressure (RIP) is expected to be decreased throughout life due to the combination of creep and corrosion behavior. The minor quantitative prediction changes related to **AXIOM** cladding model updates do not change the conservative methods outlined in Section 7.5 of Reference 6.1, and therefore those methods will continue to be used with **AXIOM** cladding.

6.2 SAFETY ANALYSES

6.2.1 LOCA

Design basis loss-of-coolant accident (LOCA) analyses seek to demonstrate that the emergency core cooling system (ECCS) meets the requirements of 10 CFR 50.46. Introduction of **AXIOM** cladding to the fuel design does not affect the overall goal of the LOCA analysis but does introduce potentially different physical effects that can change the results. In this section, the phenomenon identification and ranking table (PIRT) from the **FULL SPECTRUM™** Loss-of-Coolant Accident (**FSLOCA™**) Evaluation Model (EM) are reviewed, and the **AXIOM** cladding test results with respect to both best-estimate and Appendix K LOCA methodologies are evaluated. Finally, the research findings that serve as the basis for the proposed 10 CFR 50.46c rulemaking are considered to determine applicable ECCS acceptance criteria for **AXIOM** cladding.

6.2.1.1 FULL SPECTRUM LOCA PIRT Review

As part of the development process for the **FSLOCA** EM, described in WCAP-16996-P-A, Revision 1 (Reference 6.5), a PIRT was constructed to assess the relative importance of various phenomena to both small-break LOCA (SBLOCA) and large-break LOCA (LBLOCA) results. Section 2.3.2.1 of Reference 6.5 discusses fuel-related phenomena; those are the phenomena that could be most likely affected by the introduction of **AXIOM** cladding. In addition, Section 2.3.2.2 of Reference 6.5 discusses core-related phenomena; some of which could also be affected by the introduction of **AXIOM** cladding. The potentially affected phenomena are briefly discussed below, with more specific aspects of best-estimate and Appendix K LOCA methodologies described in the following subsections.

Stored Energy

The **AXIOM** cladding normal operational corrosion varies from other zirconium-based alloys, which will lead to changes in the steady-state pellet temperatures, and thus the initial fuel stored energy.

For small breaks, the core remains covered during the early periods of the transient, and reactor trip occurs early. During this period the heat transfer is good, and there is only a small temperature difference between the fuel centerline temperature and the coolant. This removes much of the initial stored energy of the fuel. **[**

][a,c]

Clad Oxidation

The high temperature oxidation behavior of **AXIOM** cladding is **[**

][a,c] (Section 3.8). For phases of SBLOCA and LBLOCA transients **[**

][a,c] The high temperature oxidation behavior is addressed in Section 6.2.1.2.4 for the best-estimate LOCA methodologies and Section 6.2.1.3.3 for the NOTRUMP Evaluation Model (EM).

Decay Heat

Decay heat is the main driver of cladding heatup during SBLOCA transients and **[**

][a,c]

Clad Deformation (Burst Strain, Relocation)

[

][a,c]

Following burst, fuel pellet fragments can relocate into the ballooned section of the clad at the burst location, thereby increasing the local heat generation rate.

The cladding deformation behavior of **AXIOM** cladding is **[**

][a,c]

The high temperature creep behavior for **AXIOM** cladding is shown **[**

][a,c] in Sections 6.2.1.2.1 and 6.2.1.3.2, respectively.

Critical Heat Flux (CHF)

CHF was **[**

][a,c]

Post-Critical Heat Flux Heat Transfer / Steam Cooling

This phenomenon was **[**

][a,c]

Rewet / T_{min}

For SBLOCA scenarios, **[**

][a,c]

The minimum film boiling temperature results from competing effects of liquid evaporation and heat conduction from the pellet to the cladding wall surface. When the evaporation rate is high, it can prevent the liquid from making contact with the heated surface. If contact between the liquid and the wall does occur, the rate at which heat is conducted to the surface determines if the liquid is quickly thrown off the wall, or if the contact can be sustained.

[

][a,c]

Heat Transfer to a Covered Core

[

][a,c]

Radiation Heat Transfer

[

][a,c] This is assessed in Section 6.2.1.2.1 for the best-estimate LOCA methodologies and in Section 6.2.1.3.1 for the NOTRUMP EM.

6.2.1.2 Best-Estimate LOCA Evaluation Model

This section describes the aspects of the **FSLOCA** EM, described in Reference 6.5, that could be affected by **AXIOM** cladding.

6.2.1.2.1 Thermal and Mechanical Properties

The thermal properties of **ZIRLO** cladding modeled in the **FSLOCA** EM are described in Section 11.4.3 of Reference 6.5. **Optimized ZIRLO** cladding material is an improvement to the **ZIRLO** alloy and features a reduced tin content. It has been demonstrated to have equivalent material properties to **ZIRLO** alloy, for the purposes of realistic LOCA modeling (as discussed in Section 11.4.3 of Reference 6.5).

Specific Heat

The specific heat of **ZIRLO** and **Optimized ZIRLO** cladding is modeled in the **FSLOCA** EM as discussed in Section 11.4.3 of Reference 6.5. Table 11-16 of Reference 6.5 provides the values used as a function of temperature. Figure 6.2-1 compares the **FSLOCA** EM specific heat model for **ZIRLO** and **Optimized ZIRLO** cladding to the specific heat test results for **ZIRLO**, **Optimized ZIRLO**, and **AXIOM** cladding. The **FSLOCA** EM model shows **[**

][a,c]

Thermal Conductivity

Section 11.4.3 of Reference 6.5 indicates that the thermal conductivity of **ZIRLO** and **Optimized ZIRLO** cladding is modeled in the **FSLOCA** EM to be identical to that of Zircaloy-4 cladding and is given by Equation 11-152 therein. Figure 6.2-2 compares the **FSLOCA** EM thermal conductivity model for **ZIRLO** and **Optimized ZIRLO** cladding to the thermal conductivity test results for **ZIRLO**, **Optimized ZIRLO**, and **AXIOM** cladding. The **FSLOCA** EM model shows reasonable agreement with the test results for **ZIRLO**, **Optimized ZIRLO**, and **AXIOM** cladding. The variations between the model and test data are small, and LOCA transients would be insensitive to these variations in the cladding thermal conductivity, since radial temperature gradients in the cladding are of minimal importance for typical licensing-basis large-break LOCA (LBLOCA) and small-break LOCA (SBLOCA) transients. Therefore, the thermal conductivity model for **ZIRLO** and **Optimized ZIRLO** cladding in the **FSLOCA** EM can also be applied to **AXIOM** cladding.

Emissivity

Given that all Westinghouse cladding alloys have identical surface finish, the emissivity of oxidized Westinghouse fuel cladding is dominated by the zirconium oxide formed, which is unaffected by the minor differences in alloying elements (Section 3.9). **AXIOM** cladding is processed identically to the other alloys tested and has an identical surface finishing. Therefore, within the measurement uncertainty, the emissivity of oxidized **AXIOM** cladding is identical to **ZIRLO** and **Optimized ZIRLO** cladding. The emissivity for **ZIRLO** and **Optimized ZIRLO** cladding in the **FSLOCA** EM can also be applied to **AXIOM** cladding.

High Temperature Creep

The existing high temperature creep model for **ZIRLO** and **Optimized ZIRLO** cladding in the **FSLOCA** EM is based on **ZIRLO** cladding tests performed in vacuum at the Berkeley Nuclear Laboratories in the United Kingdom (Section 8.4.1 of Reference 6.5). This test facility no longer exists. Creep testing of **Optimized ZIRLO** cladding was performed by the French Commissariat a l'Energie Atomique (CEA) using the EDGAR-2 facility. These tests were performed by inductively heating individual samples of cladding to the test temperatures in steam and pressurizing with argon (Reference 6.6). **[**

][a,c] To evaluate the behavior of **AXIOM** cladding relative to the **ZIRLO** and **Optimized ZIRLO** cladding model, a limited set of high temperature biaxial creep tests were performed in vacuum (as described in Section 3.7).

The strain rate results are plotted as a function of the calculated average hoop stress in Figure 3.7-1 along with **FSLOCA** EM cladding creep model curves and the previous CEA **Optimized ZIRLO** cladding data. Comparing the strain rates between the two alloys tested side by side at identical temperature, internal pressure and time conditions shows that **[**

][a,c]

Other LOCA Models

Density, thermal expansion, Young's Modulus, and Poisson's Ratio, which are modeled in Westinghouse best-estimate LOCA methodologies, have minimal importance in typical licensing-basis LBLOCA and SBLOCA transients. These properties were measured over limited temperature ranges (which is acceptable given their minimal importance) and/or shown to be indistinguishable from Zircaloy-4, **ZIRLO** and **Optimized ZIRLO** High Performance Cladding Materials in Section 3. Given this, the current **FSLOCA** EM models for these parameters can be applied to **AXIOM** cladding.

6.2.1.2.2 Cladding Rupture Models: Burst Temperature

Section 8.4.1 of Reference 6.5 describes the cladding rupture model used for **ZIRLO** and **Optimized ZIRLO** cladding in the **FSLOCA** EM, referring to the NUREG-0630 (Reference 6.7) framework. The model, describing the burst temperature as a function of engineering hoop stress, is used to predict the

occurrence of rupture depending on local cladding temperature conditions. Section 29.4.2.1 of Reference 6.5 describes fuel rod models and their uncertainty treatment in **FSLOCA** EM analyses. The temperature at which rupture is predicted for **ZIRLO** and **Optimized ZIRLO** cladding is presented in Figure 29.4.2-1 of Reference 6.5. Figure 6.2-3 shows the result of rupture testing performed on **AXIOM** cladding (described in Section 3.6) in comparison with the existing **ZIRLO** and **Optimized ZIRLO** cladding rupture tests presented in Figure 29.4.2-1 of Reference 6.5. **[**

][a,c]

6.2.1.2.3 Cladding Rupture Models: Burst Strain

Section 8.4.1 of Reference 6.5 describes the cladding rupture model used for **ZIRLO** and **Optimized ZIRLO** cladding in the **FSLOCA** EM, with the associated burst strain model depicted in Figure 8-20 of Reference 6.5. **[**

][a,c] as described in Section 8.4.1 of Reference 6.5.

Section 29.4.2.1 of Reference 6.5 describes fuel rod models and their uncertainty treatment in **FSLOCA** EM analyses. The burst strain associated with the **ZIRLO** and **Optimized ZIRLO** cladding rupture tests is presented, and uncertainty distributions are provided in Table 29-3b of Reference 6.5. The uncertainty in the burst strain is characterized by **[**

][a,c]

<u>Nominal Burst Strain</u>

Figure 6.2-5 shows the current model used in the **FSLOCA** EM for **ZIRLO** and **Optimized ZIRLO** cladding burst strain, the historical data, and the new burst strain data for **AXIOM** cladding tests. **[**

][a,c]

[

][a,c]

Burst Strain Uncertainty Distributions

The current model used within the **FSLOCA** EM to describe the uncertainty in the burst strain for **ZIRLO** and **Optimized ZIRLO** claddings is **[**

][a,c]

[

]a,c

[ ]a,c (Equation 6.2-1)

[ ]a,c (Equation 6.2-2)

[

]a,c

[ ]a,c (Equation 6.2-3)

[

]a,c (defined in Section 29.4.2.1 of Reference 6.5).

The described approach is consistent with Section 29.4.2.1 of Reference 6.5.

6.2.1.2.4 High Temperature Oxidation

Section 8.5 of Reference 6.5 indicates that the Cathcart-Pawel model is used to calculate the oxide buildup throughout the transient and the resulting heat generation in the **FSLOCA** EM. Figure 3.8-2 compares the parabolic rate constants for the **AXIOM** cladding tests to the **ZIRLO** and **Optimized ZIRLO** cladding test results previously reported in Figure B.15-1 of Reference 6.6 as well as the Cathcart-Pawel and Baker-Just oxidation models. The results for **AXIOM** cladding show [

]a,c

Table 6.2-1 Burst Strain Distributions Used for ZIRLO and Optimized ZIRLO Cladding

[**a,c**]

Table 6.2-2 Burst Strain Distributions Used for AXIOM Cladding

a,c

a, c

*Figure 6.2-1 Comparison of specific heat test results to **FSLOCA** EM model*

[**a,c**

]

*Figure 6.2-2 Comparison of thermal conductivity test results to **FSLOCA** EM model*

a,c

*Figure 6.2-3 **ZIRLO** and **Optimized ZIRLO** historical results along with **AXIOM** cladding results*

a,c

*Figure 6.2-4 **AXIOM** cladding burst temperature model, including 5% uncertainty lines, and test data for **AXIOM** cladding*

[**a,c**

]

*Figure 6.2-5 **ZIRLO** and **Optimized ZIRLO** cladding historical burst strain data with **AXIOM** cladding data*

a,c

*Figure 6.2-6 **AXIOM** cladding burst strain data and new model for **AXIOM** cladding nominal burst strain*

[**a,c**

]

Figure 6.2-7 **[**

]a,c

[**a,c**

]

Figure 6.2-8 **[**

]

[**a,c**

]

Figure 6.2-9 **[**

]a,c

[**a,c**

]

Figure 6.2-10 **[**

]a,c

[**a,c**

]

Figure 6.2-11 **[**

]a,c

[**a,c**

]

Figure 6.2-12 **[**

]a,c

a,c

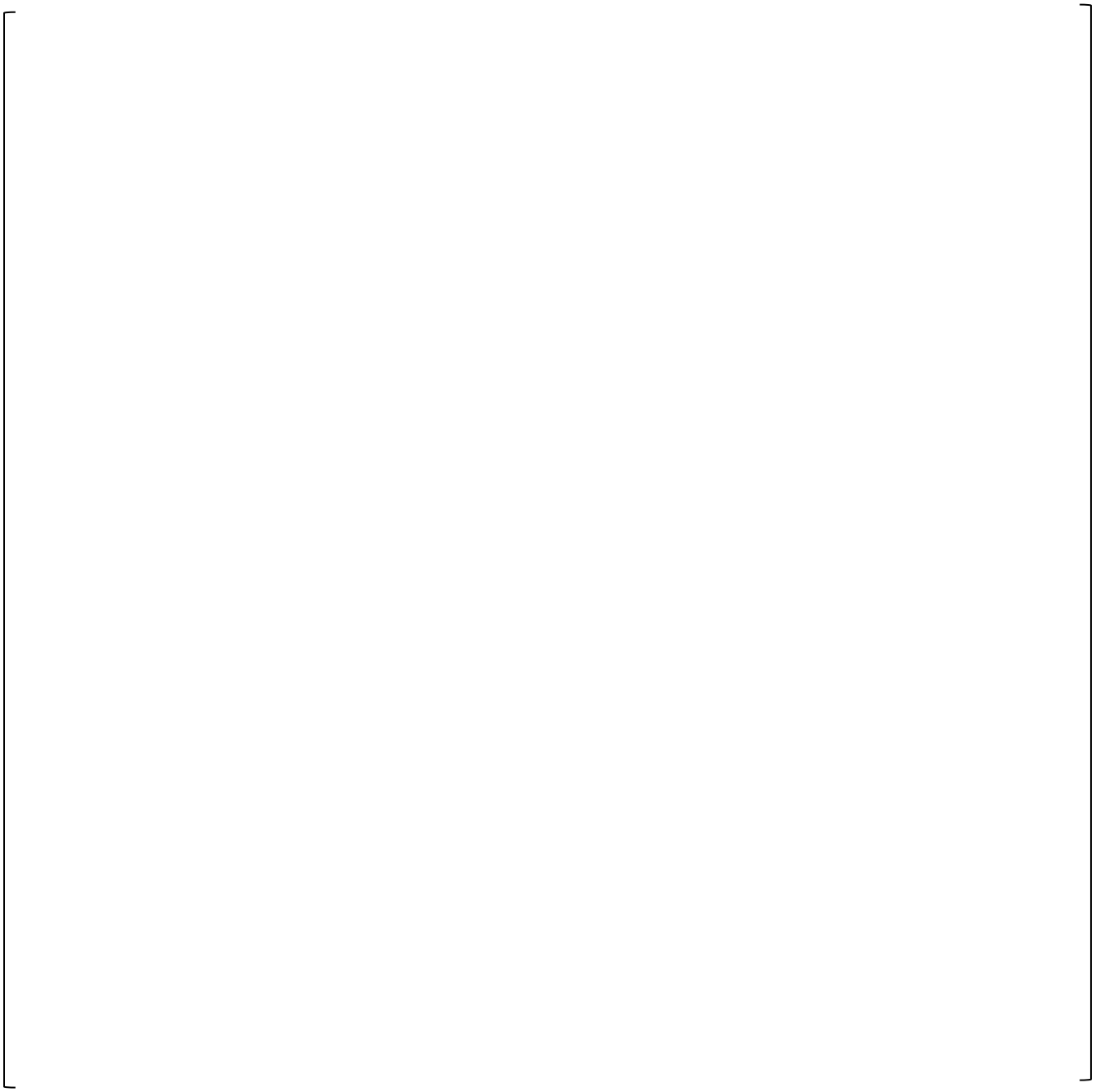

Figure 6.2-13 **[**

]

[**a,c**

]

Figure 6.2-14 **[**

]a,c

[**a,c**

]

Figure 6.2-15 **[**

]a,c

[ ]

a,c

Figure 6.2-16 [

]a,c

[**a,c**

Figure 6.2-17 **[**

]^{a,c}

6.2.1.3 NOTRUMP Evaluation Model

This section addresses the aspects of the NOTRUMP EM, described in References 6.8 and 6.9, which could be affected by **AXIOM** cladding. The models and correlations used in the NOTRUMP EM for small break LOCA analyses **[ ]**[a,c] as discussed in the following subsections.

6.2.1.3.1 Thermal and Mechanical Properties

Thermal and mechanical properties applicable to fuel rod cladding used in the NOTRUMP EM are described in Appendix T of Reference 6.9, Appendix F of Reference 6.10, and Section 4.6.1 of Reference 6.6. This section addresses the effect of **AXIOM** cladding on the relevant properties and behaviors.

Specific Heat

The NOTRUMP EM models the specific heat of **ZIRLO** and **Optimized ZIRLO** cladding materials based on **ZIRLO** cladding, as discussed in Section 4.6.1 of Reference 6.6. Figure 6.2-18 compares the NOTRUMP EM model to the test results for **ZIRLO**, **Optimized ZIRLO**, and **AXIOM** claddings. The NOTRUMP EM model shows **[**

][a,c] to **AXIOM** cladding.

Thermal Conductivity

Appendix T of Reference 6.9, Section T-4, describes the thermal conductivity for Zircaloy-4. Based on Appendix F of Reference 6.10 and Section 4.6.1 of Reference 6.6, no adjustments were made to the model to accommodate **ZIRLO** and **Optimized ZIRLO** cladding. Figure 6.2-19 compares the NOTRUMP EM model to **ZIRLO**, **Optimized ZIRLO**, and **AXIOM** claddings test data. Figure 6.2-19 **[**

][a,c] for **AXIOM** cladding.

Density

Appendix T of Reference 6.9, Section T-4, describes the temperature-dependent density of Zircaloy-4 cladding used in the NOTRUMP EM, which ranges from approximately **[**

][a,c] at 2200°F. Based on Appendix F of Reference 6.10 and Section 4.6.1 of Reference 6.6, no adjustments were made to the model to accommodate **ZIRLO** and **Optimized ZIRLO** cladding. Based on the density specified in Section 3.1.1, the room temperature density of **AXIOM** cladding is **[ ]**[a,c] Furthermore, consistent with the discussion in Section 4.6.1 of Reference 6.6, the density has minimal importance in typical licensing basis SBLOCA transients and therefore the existing NOTRUMP EM model will be used for **AXIOM** cladding.

Thermal and Elastic Expansion

The models for radial and elastic expansion of Zircaloy-4 cladding are described in Appendix T of Reference 6.9, Section T-2. Based on Appendix F of Reference 6.10 and Section 4.6.1 of Reference 6.6, no adjustments were made to these models to accommodate **ZIRLO** and **Optimized ZIRLO** cladding. Thermal and elastic expansion have minimal importance in SBLOCA transients due to the **[ ]**[a,c] Given this, and since the data in Section 3 herein indicates **[ ]**[a,c] variations in chemical compositions of the modern Westinghouse cladding alloys, the existing NOTRUMP EM models will be used for **AXIOM** cladding.

Emissivity

The emissivity of oxidized zirconium is defined by Equation T-113 of Appendix T of Reference 6.9, Section T-4. Based on Appendix F of Reference 6.10 and Section 4.6.1 of Reference 6.6, **[ ]**[a,c] As discussed in Section 3.9, given that all Westinghouse cladding alloys have identical surface finishes and that the emissivity of oxidized fuel cladding is dominated by the zirconium oxide formed, which is unaffected by the minor differences in alloying elements, the existing NOTRUMP EM emissivity values will be used for **AXIOM** cladding.

6.2.1.3.2 High Temperature Creep

Appendix F of Reference 6.10 describes the high temperature creep model **[ ]**[a,c] Figure 3.7-1 compares the creep rates of **AXIOM** and **Optimized ZIRLO** cladding to previous test results and **[ ]**[a,c] for **AXIOM** cladding.

6.2.1.3.3 High Temperature Oxidation

10 CFR 50 Appendix K Section I.A.5 requires using the Baker-Just equation to calculate the rate of energy release, hydrogen generation, and cladding oxidation from the metal-water reaction and to calculate the reaction rate on the inside of the cladding after rupture. Appendix T of Reference 6.9, Section T-1, describes the use of the Baker-Just equation in the NOTRUMP EM, and Appendix F of Reference 6.10 and Section 4.6.1 of Reference 6.6 confirm that the continued use of Baker-Just is conservative for **ZIRLO** and **Optimized ZIRLO** cladding, respectively. The parabolic oxidation rates of **AXIOM** cladding as a function of temperature are listed in Table 3.8-2 and compared to the Baker-Just and Cathcart-Pawel correlations and previously reported **ZIRLO** and **Optimized ZIRLO** cladding oxidation rates in Figure 3.8-2. The **AXIOM** cladding results show **[ ]**[a,c] for **AXIOM** cladding.

6.2.1.3.4 Clad Swelling and Rupture

Appendix F of Reference 6.10 describes the clad swelling and rupture models used for **ZIRLO** cladding in the NOTRUMP EM. Per Section 4.6.1 of Reference 6.6, **[ ]**[a,c] Based on Figure 3.6-1, which shows the comparison of **ZIRLO, Optimized ZIRLO**, and **AXIOM** cladding burst strain vs. burst temperature results, it is concluded that the **AXIOM** data is **[ ]**[a,c] Figure 3.6-2 shows the burst temperature vs. burst pressure results for **AXIOM** cladding along with **ZIRLO** and **Optimized ZIRLO** cladding results. Section 3.6 concludes the **AXIOM** cladding results **[ ]**[a,c] for **AXIOM** cladding.

[**a,c**

]

Figure 6.2-18 Comparison of specific heat test results to NOTRUMP EM model

[ ]

a,c

Figure 6.2-19 Comparison of thermal conductivity test results to NOTRUMP EM model

6.2.1.4 Consideration of 10 CFR 50.46 with Respect to AXIOM Cladding

Design basis LOCA analyses seek to demonstrate that the ECCS meets the requirements of 10 CFR 50.46. The NRC has initiated the formal process to revise the ECCS acceptance criteria in 10 CFR 50.46 via issuance of proposed rulemaking, and has published a proposed rule (Reference 6.11). The research findings that serve as the basis for the proposed rulemaking are considered to determine applicable ECCS acceptance criteria for **AXIOM** cladding.

Peak Cladding Temperature and Maximum Hydrogen Generation

The draft 10 CFR 50.46c (g)(1)(i) criterion to limit the maximum cladding temperature to 2200°F (1204°C) remains unchanged from the current 10 CFR 50.46 (b)(1) requirement, and the draft 10 CFR 50.46c (g)(1)(iv) criterion to limit the maximum hydrogen generation to 1% of the amount generated from the full reaction of metal surrounding the fuel remains unchanged from the current 10 CFR 50.46 (b)(3) requirement. As such, the Westinghouse approach used to satisfy the maximum cladding temperature criterion defined in 10 CFR 50.46 (b)(1) and maximum hydrogen generation 10 CFR 50.46 (b)(3) are unaffected by the research findings that serve as the basis for the proposed rulemaking and these criteria will be applicable to **AXIOM** cladding.

Cladding Embrittlement

Research into the mechanisms by which zirconium-based cladding alloys can become brittle following LOCA scenarios is summarized in Section 1.4 of NUREG/CR-6967 (Reference 6.12). The loss of ductility is related, in part, to the presence of hydrogen in the cladding, which promotes the absorption and diffusion of oxygen into the base metal under high-temperature LOCA conditions, causing beta-layer embrittlement. Sources of oxygen during the LOCA transient include water and steam outside of the cladding, fuel pellets inside the cladding where the pellets and the cladding have come into contact, and steam that enters the cladding through a rupture.

[

][a,c]

In the context of the 10 CFR 50.46 (b)(2) maximum local oxidation (MLO) criterion of 17% and NRC Information Notice 98-29 (Reference 6.15), Westinghouse LOCA methodologies demonstrate that the sum of the pre-accident oxidation and LOCA transient oxidation remain below 17%. **[**

][a,c]

[

]a,c

Breakaway Oxidation

The topic of breakaway oxidation is discussed in NUREG/CR-6967 (Reference 6.12), with further discussion in Section C.2 of draft RG 1.224 (Reference 6.13). If the total time spent above the temperature at which the cladding has been shown to be susceptible to breakaway oxidation is less than the breakaway time, then breakaway oxidation should not occur. In Section C.2.B of draft RG 1.224, it is stated that "time spent in steam at less than or equal to 800°C (1,472°F) was benign with regard to breakaway oxidation." Westinghouse has performed testing conforming to US NRC guidance in draft RG 1.222 (Reference 6.16) with **AXIOM** cladding. The results of the testing for breakaway time are discussed in Section 3.12.

[

]a,c

Long-Term Core Cooling

The draft 10 CFR 50.46c (g)(1)(v) criterion, which requires demonstration that effective core cooling is maintained for the long-term period required to remove decay heat, remains unchanged from the current 10 CFR 50.46 (b)(5) requirement. As such, the Westinghouse approach used to satisfy the long-term

cooling criterion defined in 10 CFR 50.46 (b)(5) is unaffected by the research findings that serve as the basis for the proposed rulemaking and this criterion remains applicable to **AXIOM** cladding.

[**a,c**

Figure 6.2-20 [

]a,c

6.2.2 Non-LOCA Transient Analyses

This section discusses the effect of the **AXIOM** fuel cladding on the non-loss-of-coolant-accident (non-LOCA) safety analyses for both Westinghouse and CE designed PWR plants.

6.2.2.1 Non-LOCA Analysis Methods and Computer Codes

An evaluation of the non-LOCA safety analysis methods and computer codes has been conducted relative to the impact of **AXIOM** fuel cladding, as compared to current cladding alloys (Zircaloy-4, **ZIRLO**, and **Optimized ZIRLO** claddings).

The material and thermal properties for **AXIOM** cladding are discussed in Section 3 herein. Generally, there are only insignificant or minor differences such that the current parameters used in the non-LOCA analysis models and codes for the **ZIRLO** and **Optimized ZIRLO** alloys will remain valid for **AXIOM** cladding. Any adjustments to code inputs or built-in code values necessary to model certain **AXIOM** cladding properties will be made within the underlying approved non-LOCA analysis methods.

The non-LOCA safety analyses use inputs and models for fuel-related parameters based on the nuclear design, thermal-hydraulic design, and fuel rod design. As described in Section 6.3, the use of **AXIOM** cladding will have a negligible impact on the nuclear design. Therefore, there are no changes to key parameters such as reactivity feedback coefficients and weighting, peaking factors, neutronics cross sections, pellet power distributions, power shapes, decay heat, and fission energy deposition fractions. As described in Section 6.4, there are no changes to thermal-hydraulic design considerations for **AXIOM** cladding. Core thermal limits and DNB correlations and methods remain valid. Heat transfer coefficients used in non-LOCA safety analyses remain valid. Only small changes to fuel temperature vs. rod power profiles are calculated for fuel with **AXIOM** alloy cladding compared to the existing cladding alloys (Section 6.1.2.13). These changes can be modeled via code inputs and will have at most only minor impacts on the transient results for affected events. These minor impacts will be accommodated, either via available margin to limits or by offsetting changes to other inputs within the approved non-LOCA analysis methods.

6.2.2.2 Non-LOCA Acceptance Criteria

With respect to the impact of a change of fuel product, the following two categories of non-LOCA event analyses need to be considered:

1) analyses of events that are dependent upon core average effects
2) analyses of events for which local effects in the fuel rods are addressed

For the first category of analyses, several non-LOCA events are analyzed to address gross core or plant criteria, such as no return to criticality (no loss of shutdown margin), maintaining margin to the hot leg saturation temperature, not exceeding the pressure limits of the RCS and main steam system, and not filling the pressurizer water-solid. All these criteria were established independent of the details of the fuel cladding material, and therefore remain applicable for implementation of **AXIOM** fuel cladding material.

For the second category of analyses, some non-LOCA events are analyzed to address local effects in the fuel rods. Such analyses are performed in two steps: (1) prediction of the average core response to an

initiating event, and (2) hot channel or hot spot calculations for such local effects as minimum DNBR, fuel centerline melting, fuel enthalpy (cal/g), and PCT. Based on the confirmations in Section 6.3 and Section 6.4, for **AXIOM** fuel cladding material there is no impact on the applicable limit DNBR and kW/ft acceptance criteria. The fuel enthalpy and PCT criteria are discussed in the following.

Fuel Enthalpy (cal/g)

A maximum fuel enthalpy acceptance criterion is used in the analysis of the rod ejection accident (REA) to demonstrate that core coolability is maintained. A 280 cal/g limit is specified in the rod ejection analysis guidance of RG 1.77 (Reference 6.17), but a conservative limit of 200 cal/g has been applied in Westinghouse plant rod ejection analyses that use a one-dimensional (1-D) core kinetics model. A limit of 280 cal/g or 250 cal/g has typically been applied in CE plant rod ejection analyses.

The historical tests that were used to establish fuel enthalpy limits used UO_2 fuel pellets with cladding materials available at the time. The test results showed a strong relationship between fuel failure and the hydrogen content of the cladding material. A limit of 200 cal/g is conservative with respect to the 230 cal/g limit specified for core coolability in the new rod ejection analysis guidance of RG 1.236. However, the pellet-clad mechanical interaction (PCMI) cladding failure threshold limits specified in RG 1.236 are expressed in terms of the peak radial fuel enthalpy rise (Δcal/g) versus excess cladding hydrogen content (wppm). Section 3.10.1 herein indicates the threshold may be different for fuel rods with **AXIOM** fuel cladding material compared to other fuel cladding materials. Regardless of the specific fuel cladding material used, it is anticipated that RG 1.236 limits for rod ejection core coolability and fuel and cladding failure will ultimately will be addressed as part of the implementation of the three-dimensional (3-D) rod ejection analysis methodology (Reference 6.18) for a specific plant.

Peak Cladding Temperature

For Westinghouse plants, cladding temperature calculations are performed in the analysis of locked rotor accident. The PCT acceptance criterion historically used for this event has been 2700°F. For **Optimized ZIRLO** cladding a conservatively lower value of 2375°F has been applied as the limit (Reference 6.6). These locked rotor PCT limits are used in conjunction with a maximum percentage of zirconium reacted (due to zirconium-water reaction) limit of 16% to show that cladding integrity is maintained so as to demonstrate the core will remain in place and geometrically intact with no loss of core cooling capability. As noted in Section 3.8, **AXIOM** cladding will have a similar oxidation rate as **ZIRLO** and **Optimized ZIRLO** cladding up to a PCT of 1300°C (~2375°F). Therefore, it is expected that the locked rotor PCT limit currently applied for **Optimized ZIRLO** cladding will also be used for **AXIOM** cladding, assuming confirmation from additional high temperature oxidation and ductility testing. For CE plant analyses of postulated accidents (PAs), there are no applicable fuel cladding temperature criteria.

6.2.2.3 Non-LOCA Conclusions

The computer codes and methods used in the analysis of the non-LOCA licensing basis events, and the acceptance criteria applied remain applicable for fuel rods with **AXIOM** cladding material, except that rod ejection limits relative to the new RG 1.236 guidance would be addressed via future implementation of 3-D methodology for a specific plant. Any changes to non-LOCA safety analysis results due to the use of **AXIOM** cladding will be small, such that applicable limits will continue to be met.

6.2.3 Containment Integrity Analyses

This section discusses the effect of the **AXIOM** cladding material on the containment integrity analyses. Any impact would be the result of change in the mass and energy released to containment due to a pipe rupture accident because the containment integrity analyses themselves do not model the fuel. Containment integrity analyses consider the mass and energy released to containment from a LOCA or a steamline break (SLB) event.

6.2.3.1 Short Term LOCA Mass and Energy (M&E) Releases

The short term LOCA mass and energy (M&E) releases are used to determine the maximum differential pressure for structural analyses within sub-compartments inside the containment building resulting from postulated pipe ruptures in the primary system piping. These transients are typically performed for 1 to 3 seconds in duration and are governed by the mass flux at the break location. Therefore, the parameters that influence the short term LOCA M&E releases are the break location, the corresponding temperature of the fluid in the postulated ruptured pipe, the size of the break, and the initial reactor coolant system pressure. The fuel product and specific aspects of the fuel performance do not influence the short term LOCA M&E. Therefore, any change to the fuel cladding materials would not impact the short term LOCA M&E releases used for short term sub-compartment analyses.

6.2.3.2 Long Term LOCA Mass and Energy (M&E) Releases

There are three licensed methodologies currently in use to generate the long term LOCA M&E releases used for long term containment integrity, maximum sump temperature, and equipment qualification for Westinghouse and Combustion Engineering (CE) designs. Those licensed methodologies are:

- WCAP-10325-P-A (Reference 6.19)
- WCAP-17721-P-A (Reference 6.20)
- CENPD-132P (Reference 6.21)

<u>WCAP-10325-P-A Methodology</u>

The core is modeled as an average core for the generation of the long term LOCA M&E releases. There is no hot rod or hot assembly modeled when generating long term LOCA M&E. It is conservative for the long term LOCA M&E to maximize the rate of transfer of energy from the core into the coolant and out of the break. Thus, pellet and cladding interaction and rod burst are not modeled. The specific fuel product is modeled with respect to rod inside and outside diameter, flow area through the core, proposed peaking factors, rod initial gas fractions, rod initial internal pressure, theoretical density of the pellet, the material properties of the pellet, the material properties of the cladding material, and the burnup where the highest fuel temperature during the proposed cycle would occur. These fuel performance characteristics are controlled by a parameter known as the core stored energy that is provided by the fuel rod designers (whether Westinghouse, the utility, or a competitor fuel vendor). An iterative process is used to adjust fuel temperature to arrive at the value provided for the core stored energy. An investigation into the expected differences in fuel temperatures related to **AXIOM** cladding was performed by core engineering and determined that the core stored energy would be unaffected by the transition to **AXIOM** cladding.

Information provided in Section 3 states that the **AXIOM** cladding material properties important to the long-term LOCA M&E releases can be represented by the material properties of **Optimized ZIRLO** cladding, including the theoretical density, the specific heat capacity, the thermal diffusivity, and the thermal expansion. Please note that the mechanical material properties of the cladding are not pertinent to the long term LOCA M&E releases. **[**

][a,c] Based on the information in Section 3 that the thermal material properties for the **AXIOM** cladding material can be represented by the standard Westinghouse methodology established for **Optimized ZIRLO** cladding, no changes are needed for the WCAP-10325-P-A methodology that models an average core or the current plant specific analysis of record values for a full core with **AXIOM** alloy fuel.

WCAP-17721-P-A Methodology

The methodology approved in WCAP-17721-P-A uses the WC/T (WCOBRA/TRAC) code. **[**

][a,c] Thus, the core is modeled as an average core. The data that comes from the fuel performance calculations is used as input for the generation of the LOCA mass and energy releases.

Information provided in Section 3 states that the **AXIOM** cladding material properties important to the long-term LOCA M&E releases can be represented by the material properties of **Optimized ZIRLO** cladding, including the theoretical density, the specific heat capacity, the thermal diffusivity, and the thermal expansion. Please note that the mechanical material properties of the fuel pellet are not pertinent to the long term LOCA M&E releases. **[**

][a,c] Based on the information in Section 3 that the thermal material properties for the **AXIOM** cladding material can be represented by the standard Westinghouse methodology established for **Optimized ZIRLO** cladding, no changes are needed for the WCAP-17721-P-A methodology that models an average core for a full core with **AXIOM** alloy fuel.

CENPD-132 Methodology

The CE methodology is documented in CENPD-132. The CEFLASH-4A computer code is used for the blowdown portion of the transient for both the ECCS and LOCA M&E calculations. This code and methodology are based on a hot rod model. Nominal, cold conditions are the foundation for the fuel dimensions. The fuel temperatures that are used are based on a bounding fuel centerline temperature versus linear heat rate over the entire fuel cycle. The decay heat generated by the core is included in the total energy released to the containment in order to maximize the long-term containment pressure and temperature response. The fuel material properties are also an input into the code. Based on the information in Section 3 that the thermal material properties for the **AXIOM** cladding material can be represented by the standard Westinghouse methodology established for **Optimized ZIRLO** cladding, **[**

][a,c] no methodology changes will be needed for a full core with **AXIOM** alloy fuel.

6.2.3.3 Short-Term Steamline Break M&E Releases

The short-term SLB M&E releases are used to determine the short-term pressure increase transients for structural analyses within subcompartments inside or outside the containment building resulting from postulated secondary-side pipe ruptures. These transients are typically performed for 1 to 10 seconds in duration and are governed by the mass flux at the break location. Therefore, the parameters that influence the short-term SLB M&E releases are the break location corresponding to the initial secondary system pressure, temperature and quality of the fluid in the postulated ruptured pipe, and the size of the break. The fuel product and specific aspects of the fuel performance do not influence the short-term SLB M&E releases. Therefore, any change to the fuel cladding materials do not impact the short-term SLB M&E releases used for short-term subcompartment analyses.

6.2.3.4 Long-Term Steamline Break M&E Releases

The long-term SLB M&E releases analyses use methods and models similar to those discussed for the non-LOCA analyses in Section 6.2.2 and remain valid for the **AXIOM** cladding. The **AXIOM** cladding material properties important to the long-term SLB M&E releases are equivalent to **Optimized ZIRLO** cladding.

There are three licensed methodologies currently in use to calculate the long-term SLB M&E releases used for long-term pressure and temperature responses inside containment and long-term temperature response within compartments (steam tunnels or main steam valve vaults) outside containment. The SLB methodologies utilize the following codes to calculate the long-term M&E releases:

- WCAP-8822-S1-P-A (References 6.22 through 6.24)
- WCAP-14882-P-A (Reference 6.25)
- CESSAR Appendix 6B (Reference 6.26)

<u>WCAP-8822-S1-P-A and WCAP-14882-P-A Methodologies</u>

The long-term SLB M&E releases safety analyses licensed codes and methods are not tied directly to any specific fuel design. Therefore, the safety analyses of the long-term SLB M&E releases are not specifically dependent on the materials that comprise the fuel cladding. The SLB safety analyses assume bounding reactivity feedback modeling within the licensed computer models to conservatively bound plant operation at the end of core life. Related to the effect of the **AXIOM** alloy fuel on the long-term SLB M&E releases safety analyses,

- there are no changes required in methods to accommodate the **AXIOM** cladding,
- there are no changes in any of the acceptance criteria due to the **AXIOM** cladding,
- there are no licensing or other documentation requiring possible revision and/or NRC approval for the **AXIOM** clad fuel, and
- there are no tests or analyses required to be performed to support the **AXIOM** clad fuel.

CESSAR Appendix 6B Methodology

The heat effects in the reactor coolant system such as core stored energy, core to coolant heat transfer and decay heat tend to maintain the temperature in the reactor coolant system following a steam line break. A wide variation in these parameters, however, has little effect on the rate of energy release from the steam generators. Due to the overall conservatism in the SGNIII methodology, there will not need to be any changes to the methodology when modeling a full core with **AXIOM** alloy fuel.

6.2.3.5 Conclusions

The computer codes and methods currently used in the analyses of the LOCA and SLB M&E releases used in containment integrity analyses, and therefore the containment integrity analyses themselves, are valid for the **AXIOM** alloy fuel.

6.2.4 Radiological Consequences Analyses

Implementing **AXIOM** fuel rod cladding does not impact the models and methods used in performing offsite and control room radiological consequences analyses for accidents. The accident radiological consequences analyses do not model the cladding. While it is possible that the change in cladding material from **ZIRLO** or **Optimized ZIRLO** cladding could impact input to the accident radiological consequences analyses (such as the extent of fuel cladding damage resulting from the postulated accidents or the mass of steam released to the environment from the steam generators to remove energy stored in the fuel and reactor coolant system) this would be incorporated in a plant-specific analysis using methods consistent with the plant-specific analysis of record.

6.2.5 Fuel Assembly Seismic and LOCA Evaluation

In general, for seismic and LOCA analyses the full core fuel assembly seismic and LOCA analysis is performed to evaluate the grid impact forces against their allowable grid impact strengths. Subsequently, the fuel assembly stress analysis is performed to confirm that the guide thimble tube and fuel rod cladding stresses do not exceed their respective stress limits as well as confirm that control rod insertability is maintained.

Seismic and LOCA analysis models are established based on fuel assembly mechanical tests. The fuel rods, as the part of the fuel assembly, affect the fuel assembly dynamic behaviors and characteristics such as frequencies and modal shapes. Since the tested fuel assembly is in the elastic region, the primary effective parameter is the Young modulus. Since the **AXIOM** cladding Young's modulus is the same as **ZIRLO** and **Optimized ZIRLO** cladding per Section 3.3.1 , the fuel assembly BOL (Beginning-of-Life) and EOL (end-of-life) analysis models established based on the NRC-approved Seismic and LOCA methodologies remain applicable. The fuel assembly seismic and LOCA evaluation and the demonstration analysis have been performed for the BOL and EOL conditions. The fuel assembly designs are primarily impacted by the **[ ]**[a,c], as demonstrated by the **[ ]**[a,c] performed on **AXIOM**, **ZIRLO** and **Optimized ZIRLO** cladding. The other area of the fuel assembly design that is impacted by the change from **ZIRLO** or **Optimized ZIRLO** cladding to **AXIOM** cladding is the reduction in corrosion or oxidation and a corresponding reduction in hydrogen pickup. These latter impacts are benefits with respect to the fuel assembly structural capability and with respect to fuel assembly growth considerations. An assessment of the impact of **AXIOM**

cladding on fuel assembly seismic and LOCA evaluations for the BOL and EOL conditions is provided in the following subsections.

6.2.5.1 BOL Seismic and LOCA Evaluation

For Westinghouse US plants, the evaluations for the **AXIOM** cladding **[** **]**[a,c] compared to ZIRLO and **Optimized ZIRLO** cladding were performed for the fuel assembly beginning-of-life (BOL) based on the current analysis-of-record (AOR). The BOL analysis AOR are used in addition to the evaluations in Section 6.1.2.1. The evaluation results show that the fuel rod cladding stresses for the evaluated Westinghouse US plants meet with **AXIOM** cladding lower bound allowable limits for Condition III & IV. For Condition II OBE loads, a review of the fuel rod stress limits applied in the AORs as defined in Reference 6.27 showed them to include additional conservatism than those approved by the NRC in Section 7.4.1 of the PAD5 topical report (Reference 6.1). BOL seismic and LOCA analyses for **AXIOM** cladding will utilize the fuel rod cladding stress acceptance limits for compressive loadings as defined in Table 8 of Reference 6.1. When comparing the calculated fuel rod stresses for **AXIOM** cladding for Condition II OBE events to the allowable stress limits from Reference 6.1, the results show that the example evaluations continue to meet with **AXIOM** fuel cladding lower bound allowable limits for Condition II OBE load.

For CE plants, a single fuel rod stress analysis exists. The fuel rod stress methods defined in Section 6.1.2.1 will be applied to CE plants containing **AXIOM** clad fuel rods.

6.2.5.2 EOL Seismic and LOCA Evaluation

The effect of the **AXIOM** fuel rod cladding on the Seismic and LOCA analysis results at the end of life (EOL) conditions has been performed to address Information Notice (IN) 2012-09 (US NRC, June 2012) issued by the NRC in 2012 (Reference 6.28) following the analysis methodology and process described in the Westinghouse and PWR Owners Group (PWROG) topical report (Reference 6.29).

In support of this topical report, two example seismic and LOCA analysis cases for fuel assembly designs (**[** **]**[a,c]) were evaluated for EOL conditions. The example results of the evaluation show that the grid impact forces remain below the grid impact allowable limits for both **[** **]**[a,c] fuel designs under Condition II, III and IV seismic and LOCA loadings at EOL condition.

The stress evaluations of the **[** **]**[a,c] fuel rods and thimble tubes were also performed. The stress results show that all the stresses of the fuel rod meet the **AXIOM** cladding allowable limits approved by the NRC in Section 7.4.1 of the PAD5 topical report (Reference 6.1), and the thimble tubes meet with the **ZIRLO** cladding allowable limits for both **[** **]**[a,c] designs. Therefore, it is concluded that the **[** **]**[a,c] fuel demonstration cases at EOL condition with **AXIOM** cladding meet the design criteria: Fuel rod fragmentation will not occur, coolable geometry will be maintained, and RCCA insertion will be maintained. The demonstration cases confirm that the EOL seismic and LOCA analysis method in Reference 6.29 can be applied to other Westinghouse fuel designs in support of **AXIOM** cladding implementation.

6.3 IMPACT ON NUCLEAR DESIGN REQUIREMENTS

The nuclear design methods applied to the calculation of key reload safety parameters (Reference 6.30), assumptions made to percentage of heat generated in fuel, and decay heat characteristics of the core are not impacted by the implementation of **AXIOM** cladding material. Review of a comparison of pin powers, reaction rates, and gamma maps modeled over a bounding burnup has shown negligible neutronic impact when **AXIOM** cladding is compared to **ZIRLO** and **Optimized ZIRLO** cladding materials.

In addition, Combustion Engineering methods and codes (References 6.31, 6.32 and 6.33) are not impacted by the implementation of **AXIOM** cladding material. Nodal cross section codes do contain homogenized cross sections for the clad, but the indistinguishable differences between **AXIOM** cladding and **ZIRLO** and **Optimized ZIRLO** cladding will not impact any results. The CEA (Control Element Assembly) Ejection methodology utilizes point kinetics models for neutronics that would not be impacted by **AXIOM** cladding. Fission energy disposition will not change due to the nearly indistinguishable neutronic characteristics of the cladding.

Multi-dimension rod ejection methodology (Reference 6.18) is not impacted. **AXIOM** cladding is nearly indistinguishable from **ZIRLO** and **Optimized ZIRLO** cladding neutronically and from the viewpoint of irradiation induced activity.

There will be no limitations imposed on nuclear design aspects of the core design resulting from **AXIOM** cladding material.

6.4 APPLICABILITY OF THERMAL-HYDRAULIC DESIGN METHODS

The thermal-hydraulic methods consist of a DNB correlation such as WRB-1 (Reference 6.34), WRB-2 (Reference 6.35), WRB-2M (Reference 6.36), WSSV (Reference 6.37) and WNG-1 (Reference 6.38), a thermal-hydraulic (T/H) subchannel code such as Westinghouse version of the VIPRE-01 code, referred to as the VIPRE-W code (Reference 6.39), and a statistical method for determination of a 95/95 DNB Ratio (DNBR) limit, such as the Revised Thermal Design Procedure (RTDP) (Reference 6.40) and the Westinghouse Thermal Design Procedure (Reference 6.41). Thermal-hydraulic analysis can also be performed as part of the integrated non-LOCA analysis methodology described in References 6.18 and 6.42.

Implementation of the **AXIOM** cladding material on the existing fuel designs does not require modification or update to any previously NRC-approved methods and topical reports for DNB and thermal-hydraulic analyses, such as References 6.18, and 6.34 through 6.42. The **AXIOM** cladding does not change any fuel rod geometric parameters or characteristics that could adversely affect DNB performance as compared to the **Optimized ZIRLO** cladding, and the existing DNB correlations remain applicable. The VIPRE-W code can perform steady-state and transient DNBR calculations and non-LOCA post-critical heat flux (CHF) fuel rod transient analysis. There is no change in the VIPRE-W transient modeling method as described in Reference 6.39 for its application to the **AXIOM** cladding based on its similarities with the **ZIRLO** or **Optimized ZIRLO** cladding.

The method using the VIPRE-W code for the DNB propagation evaluation, applicable to both Westinghouse and Combustion Engineering PWR plants, is described in Reference 6.43. The cladding burst model

applicable to the **AXIOM** cladding as discussed in Section 6.2.1 is input to the DNB propagation evaluation. There is no change in the evaluation method and the conditions for its application as described in Reference 6.43.

6.5 LICENSING CRITERIA CONCLUSION

As discussed in the previous sections, due to similarities in the performance between **AXIOM** cladding and other NRC-approved cladding alloys, **AXIOM** cladding can be used in place of current Westinghouse NRC-approved claddings. The new analytical methods and models defined herein are appropriate to analyze the performance of **AXIOM** cladding and the acceptance criteria are appropriate to confirm safe operation with **AXIOM** alloy fuel. From this, **AXIOM** cladding material can be fully characterized and analyzed to show that it may be safely used in commercial operating nuclear reactors within the constraints identified in Section 1.3.

6.6 CHAPTER 6 REFERENCES

6.1 WCAP-17642-P-A, Revision 1, "Westinghouse Performance Analysis and Design Model (PAD5)," November 2017.

6.2 U.S. NRC NUREG-0800, Standard Review Plan for the Review of Safety Analysis Reports for Nuclear Power Plants, Chapter 4.2, "Fuel System Design," March 2007.

6.3 WCAP 12610-P-A & CENPD-404-P-A Addendum 2-A, "Westinghouse Clad Corrosion Model for ZIRLO and Optimized ZIRLO," October 2013.

6.4 WCAP-13589-A, "Assessment of Clad Flattening and Densification Power Spike Factor Elimination in Westinghouse Nuclear Fuel," March 1995.

6.5 WCAP-16996-P-A, Revision 1, "Realistic LOCA Evaluation Methodology Applied to the Full Spectrum of Break Sizes (FULL SPECTRUM LOCA Methodology)," November 2016.

6.6 WCAP-12610-P-A & CENPD-404-P-A, Addendum 1-A, "Optimized ZIRLO™," July 2006.

6.7 U.S. NRC NUREG-0630, "Cladding Swelling and Rupture Models for LOCA Analysis," 1980.

6.8 WCAP-10054-P-A, "Westinghouse Small Break ECCS Evaluation Model Using the NOTRUMP Code," August 1985.

6.9 WCAP-10079-P-A, "NOTRUMP A Nodal Transient Small Break and General Network Code," August 1985.

6.10 WCAP-12610-P-A, "VANTAGE+ Fuel Assembly Reference Core Report," April 1995.

6.11 U. S. Nuclear Regulatory Commission, Federal Register Notice, "Performance-Based Emergency Core Cooling Systems Requirements and Related Fuel Cladding Acceptance Criteria (10 CFR Parts 50 and 52, RIN 3150-AH42)," 2016 (ADAMS ML15238B016).

6.12 U.S. NRC NUREG/CR-6967, "Cladding Embrittlement During Postulated Loss-of-Coolant Accidents," 2008.

6.13 U.S. NRC Regulatory Guide 1.224, "Establishing Analytical Limits for Zirconium-Alloy Cladding Material," (Draft), 2016 (ADAMS ML16005A133).

6.14 U.S. NRC Regulatory Guide 1.223, "Determining Post Quench Ductility." (Draft), 2016 (ADAMS ML16005A134).

6.15 U.S. NRC Information Notice 98-29, "Predicted Increase in Fuel Rod Cladding Oxidation," 1998.

6.16 U.S. NRC Regulatory Guide 1.222, "Measuring Breakaway Oxidation Behavior." (Draft), 2016 (ADAMS ML16005A135).

6.17 U.S. NRC Regulatory Guide 1.77, "Assumptions Used for Evaluating a Control Rod Ejection Accident for Pressurized Water Reactors," May 1974.

6.18 WCAP-15806-P-A, "Westinghouse Control Rod Ejection Accident Analysis Methodology Using Multi-Dimensional Kinetics," November 2003.

6.19 WCAP-10325-P-A, "Westinghouse LOCA Mass and Energy Release Model for Containment Design March 1979 Version," May 1983.

6.20 WCAP-17721-P-A, "Westinghouse Containment Analysis Methodology – PWR LOCA Mass and Energy Release Calculation Methodology," September 2015.

6.21 CENPD-132P, "Calculative Methods for the C-E Large Break LOCA Evaluation Model," August 1974.

6.22 WCAP-8822, "Mass and Energy Release Following a Steam Line Rupture," September 1976.

6.23 Letter from NRC (Cecil O. Thomas) to Westinghouse (E. P. Rahe, Jr.), "Acceptance for Referencing of Licensing Topical Report WCAP-8821 (P) / 8859 (NP), 'TRANFLO Steam Generator Code Description', and WCAP-8822 (P) / 8860 (NP), 'Mass and Energy Release Following a Steam Line Rupture'," August 1983.

6.24 WCAP-8822-S1-P-A, "Mass and Energy Releases Following a Steam Line Rupture, Supplement 1 - Calculations of Steam Superheat in Mass/Energy Releases Following a Steamline Rupture," September 1986.

6.25 WCAP-14882-P-A, "RETRAN-02 Modeling and Qualification for Westinghouse Pressurized Water Reactor Non-LOCA Safety Analyses," April 1999.

6.26 CESSAR Appendix 6B, "Description of the SGNIII Digital Computer Code Used in Developing Main Steam Line Break Mass/Energy Release Data for Containment Analysis," January 1974.

6.27 WCAP-9401-P-A, "Verification Testing and Analyses of the 17×17 Optimized Fuel Assembly," August 1981.

6.28 U.S. NRC Information Notice 2012-09, "Irradiation Effects on Fuel Assembly Spacer Grid Crush Strength," June 28, 2012.

6.29 PWROG-16043, "PWROG Program to Address U. S. Nuclear Regulatory Commission Information Notice 2012-09: 'Irradiation Effects on Fuel Assembly Spacer Grid Crush Strength' for Westinghouse and CE PWR Fuel Designs," January 2017.

6.30 WCAP-9272-P-A, "Westinghouse Reload Safety Evaluation Methodology," July 1985.

6.31 CENPD-188-A, "HERMITE – A Multi-Dimensional Space-Time Kinetics Code for PWR Transients," July 1976.

6.32 CENPD-190-A, "C-E Method for Control Element Assembly Ejection Analysis," January 1976.

6.33 CENPD-282-P-A, "Technical Manual for the CENTS Code," December 1992.

6.34 WCAP-8762-P-A, "New Westinghouse Correlation WRB-1 for Predicting Critical Heat Flux in Rod Bundles with Mixing Vane Grids," July 1984.

6.35 WCAP-10444-P-A, "Reference Core Report VANTAGE 5 Fuel Assembly," September 1985.

6.36 WCAP-15025-P-A, "Modified WRB-2 Correlation, WRB-2M, for Predicting Critical Heat Flux in 17×17 Rod Bundles with Modified LPD Mixing Vane Grids," April 1999.

6.37 WCAP-16523-P-A, "Westinghouse Correlations WSSV and WSSV-T for Predicting Critical Heat Flux in Rod Bundles with Side-Supported Mixing Vanes," August 2007.

6.38 WCAP-16766-P-A, "Westinghouse Next Generation Correlation (WNG-1) for Predicting Critical Heat Flux in Rod Bundles with Split Vane Mixing Grids," February 2010.

6.39 WCAP-14565-P-A, "VIPRE-01 Modeling and Qualification for Pressurized Water Reactor Non-LOCA Thermal-Hydraulic Safety Analysis," October 1999.

6.40 WCAP-11397-P-A, "Revised Thermal Design Procedure," April 1989.

6.41 WCAP-18240-P, "Westinghouse Thermal Design Procedure," August 2018.

6.42 WCAP-16259-P-A, "Westinghouse Methodology for Application of 3-D Transient Neutronics to Non-LOCA Accident Analysis," August 2006.

6.43 WCAP-8963-P-A Addendum 1-A, Revision 1-A, "Safety Analysis for the Revised Fuel Rod Internal Pressure Design Basis (Departure from Nucleate Boiling Mechanistic Propagation Methodology)," June 2006.

7 SUMMARY

AXIOM alloy has achieved significant in-reactor experience with lead rods in multiple commercial PWR plants and test reactor programs. High burnup close to 75 GWd/MTU has been achieved and PIE data are available. The **AXIOM** alloy has demonstrated better in-reactor corrosion performance compared to **ZIRLO** and **Optimized ZIRLO** alloys, especially in high duty operating environments. The **AXIOM** alloy has shown excellent in-reactor dimensional stability, less irradiation growth in the axial direction, and less creep strain in the diametral direction than **ZIRLO** and **Optimized ZIRLO** cladding.

Extensive characterization tests performed on **AXIOM** cladding have elucidated the physical, mechanical, and thermal properties, often with direct comparison to **ZIRLO** and **Optimized ZIRLO** claddings. The topical report describes in detail how the properties and performance of **AXIOM** cladding are incorporated into existing NRC-approved analytical methods for use in plant-specific safety analyses. Where differences compared to existing claddings have been identified, new models and methods have been developed so that the new cladding alloy can be appropriately analyzed to show compliance with all pertinent regulations and requirements.

AXIOM alloy is planned to be used as a fuel rod cladding material in Westinghouse and Combustion Engineering PWR production fuel assemblies. Only the cladding material is being changed and will be used with all NRC-approved cladding dimensions, fuel structures, fuel assembly components, and fuel materials. For this topical report, the **AXIOM** fuel rod cladding material will be licensed to **[**

][d,e]

The cumulative description of **AXIOM** cladding documented in this topical report demonstrate that **AXIOM** cladding may be implemented in operating commercial PWRs while ensuring safety and regulatory compliance.

8 APPENDIX

8.1 TABLES

Table 8.1-1 Thermal Diffusivity and Thermal Conductivity (Section 3.2.4)

Sample	Thickness (mm)	Bulk Density ρ (g/cm³)	Temperature T (°C)	Specific Heat Cp (J/g-K)	Diffusivity α (mm²/s)	Standard Deviation (mm²/s)	Conductivity λ (W/m-K)

b,c

Table 8.1-1 Thermal Diffusivity and Thermal Conductivity (Section 3.2.4) (Continued)

Sample	Thickness (mm)	Bulk Density ρ (g/cm³)	Temperature T (°C)	Specific Heat Cp (J/g-K)	Diffusivity α (mm²/s)	Standard Deviation (mm²/s)	Conductivity λ (W/m-K)

b,c

Table 8.1-2 Contractile Strain Ratio (CSR) for AXIOM Cladding (Section 3.3.4)

Material	CSR
AXIOM	
Average	

b,c

Table 8.1-3 Creep Properties of AXIOM and ZIRLO Cladding (Section 3.3.6)

Alloy	Lot	Hours	OD Strain (%)	Normalized Midwall Strain (%)
AXIOM				
ZIRLO				

b,c

Table 8.1-4 AXIOM Cladding Corrosion Results in 800°F Steam at 1500 psi as a Function of Exposure (Section 3.5)

Lots	Time (days) / Weight Gain (mg/dm²)

b,c

Table 8.1-5 AXIOM Cladding Corrosion Results in 680°F Pure Water at 2700 psi as a Function of Exposure (Section 3.5)

Lots	Time (days) / Weight Gain (mg/dm²)

b,c

8.2 FIGURES

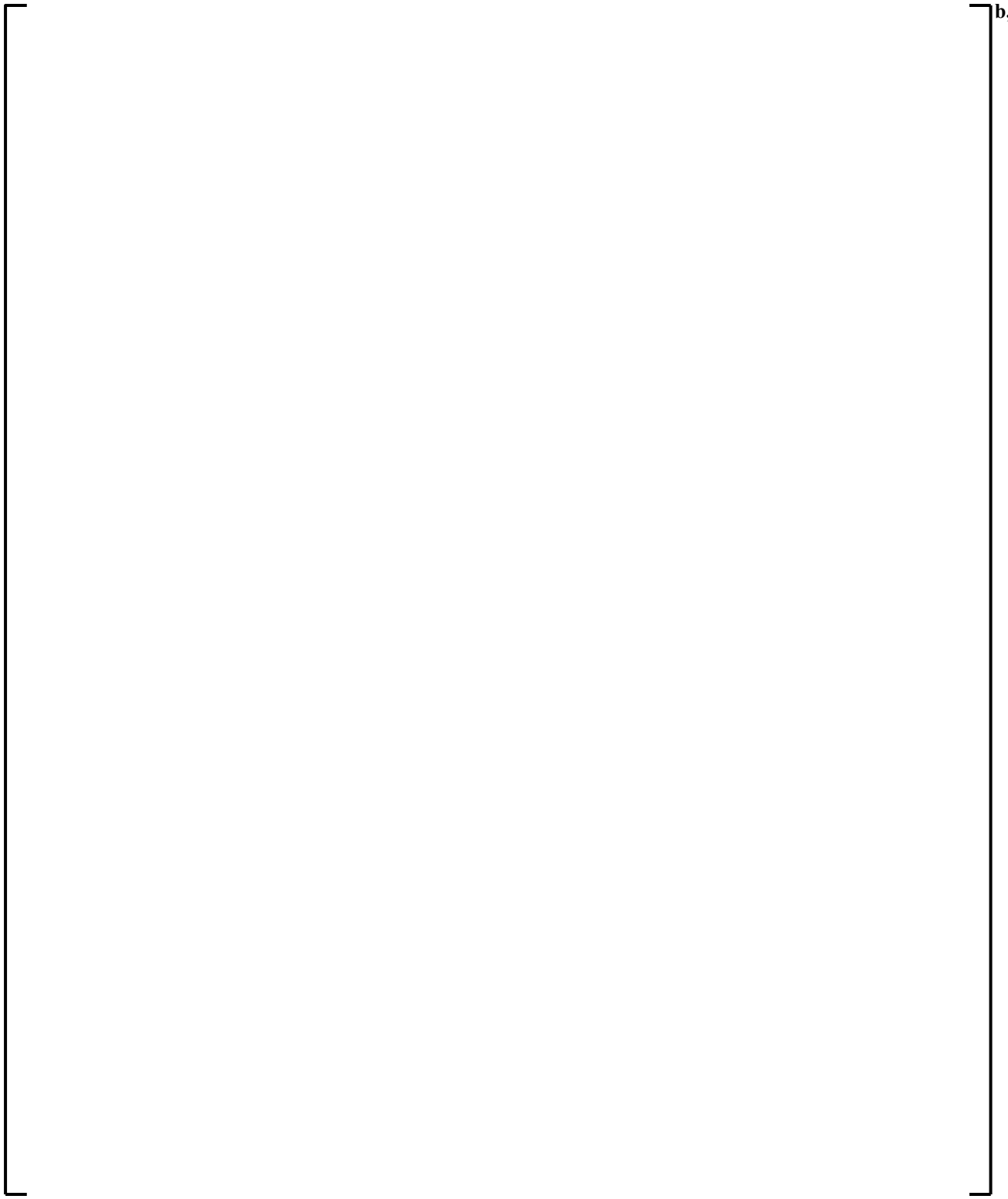

*Figure 8.2-1 Basal pole figures for **AXIOM** cladding as a function of location, a) measured and b) calculated*